INVESTIGATING THE ROLES OF CARBON METABOLIC ENZYMES FRUCTOSE 1,6-BISPHOSPHATE ALDOLASE AND MALATE SYNTHASE IN GROWTH, SURVIVAL, AND PATHOGENICITY OF *MYCOBACTERIUM TUBERCULOSIS*

A Dissertation

Presented to the Faculty of Weill Cornell Graduate School

of Medical Sciences

in Partial Fulfillment of the Requirements for the Degree of

Doctor of Philosophy

by

Susan Elizabeth Puckett

January 2015

INVESTIGATING THE ROLES OF CARBON METABOLIC ENZYMES FRUCTOSE 1,6-BISPHOSPHATE ALDOLASE AND MALATE SYNTHASE IN GROWTH, SURVIVAL, AND PATHOGENICITY OF *MYCOBACTERIUM TUBERCULOSIS*

Susan Elizabeth Puckett, Ph.D.

Cornell University 2015

Mycobacterium tuberculosis (*Mtb*) is the etiological agent of tuberculosis, a disease that has plagued mankind for millennia and remains problematic today. Over 1.3 million people died of tuberculosis in 2012, and many more remain latently infected with the potential to develop active TB. Although we have effective antibiotics, issues of drug resistance, lengthy treatment time, and drug side effects necessitate the development of novel therapies.

Mtb, like other bacterial pathogens, depends on central carbon metabolic (CCM) pathways to generate energy and biosynthetic precursors, as well as to prevent buildup of toxic metabolites. These pathways provide a reservoir of potential drug targets, and growing evidence supports a role for CCM enzymes in growth and persistence of *Mtb in vivo*. However, there remains a paucity of information about the importance, function, and redundancy of specific enzymes. Here, we focused on studying the roles of two metabolic enzymes, fructose 1,6-bisphosphate aldolase (FBA) and malate synthase (MS), for *Mtb* growth, survival, and *in vivo* pathogenicity.

Using conditional knockdown strains for FBA and MS, we found that both enzymes were essential for establishment and maintenance of infection within the mouse model. Interestingly, essentiality of both *in vitro* was dependent on the carbon source condition; FBA was essential for survival in media with single carbon sources whereas

MS was essential for survival in media with acetate or fatty acids. We also observed metabolic perturbations associated with exposure of MS and FBA knockouts to death-inducing carbon sources, suggesting that death may be induced by metabolite imbalance or toxicity. Together, these data validate MS and FBA as drug targets worth pursuing and highlight the importance of recognizing that gene essentiality can be context-dependent.

BIOGRAPHICAL SKETCH

Susan Puckett was born in Eugene, Oregon in 1986. Her fondest memories of growing up involve music (piano and clarinet), including participation in wind ensembles, concert bands, and a clarinet quartet. She attended Oregon State University (OSU) in Corvallis, Oregon from 2004-2008, graduating with a microbiology major and music minor. Her first lab experience was working through the Howard Hughes Medical Institute (HHMI) undergraduate research fellowship at AVI Biopharma (now Sarepta Therapeutics) under Dr. Bruce Geller studying bacterial resistance to antisense antibiotics. Thanks to the mentorship of Dr. Kevin Ahern at OSU, Susan pursued a summer HHMI-funded fellowship in South Africa in the lab of Professor Valerie Mizrahi. There she worked under the mentorship of Dr. Digby Warner studying rifampicin resistance of *Mycobacterium smegmatis* induced by specific growth conditions. During her time at OSU she also met her fiancé, Will Martin. Post college, she moved to New York City to become a laboratory technician at Weill Cornell Medical College in the lab of Dr. Sabine Ehrt, where she later chose to pursue her Ph.D. on carbon metabolism in *Mycobacterium tuberculosis*.

Dedicated to my dear friend,

Karena Dokken

ACKNOWLEDGEMENTS

I would not have reached this point without the support, mentorship, and encouragement from many wonderful people. This not only includes the presence of highly talented scientific mentors, but also people in my life that contribute to my state of well-being.

Thanks go to my principal investigator, Sabine Ehrt, for many things, but most for her mentorship and support over these past years. Sabine took the risk at hiring me straight out of college as a laboratory technician, and then again to support me as a graduate student in her lab. One thing I appreciated a lot was her enthusiasm during our weekly meetings, which left me more motivated than before. Thank you Sabine, for the opportunities, insight, and guidance you have provided over the years.

Thank you to the people of the Ehrt, Nathan, Ding, Rhee, and Schnappinger Labs, for being approachable, supportive, entertaining, and sources of endless knowledge. Thank you to my thesis committee Dirk Schnappinger, Kyu Rhee, and Jayanta Chaudhuri for providing valuable insight. Thank you Hyungjin Eoh and Kyu Rhee for guiding me through metabolomics experiments. I'd like to especially thank the Ehrt lab graduate students Uday Ganapathy, Weizhen Xu, Kan Lin, Ruojun Wang, and Meredith Wright for providing a great support network. Thank you fellow students in my year Lauren Dimenna, Silvia Caballero, and Helen Kang, for providing friendship and moral support. And thank you to Carolina Trujillo, Joeli Marrero, and Pradeepa Jayachandran, postdocs who were terrific mentors and friends, and who contributed to my projects. Thank you to Divya Tiwari, my postdoc neighbor for over four years in the lab who provided valuable advice and friendship. Finally, thank you to Shuang Song and Natalia Betancourt, who also helped with this work.

Thanks go to our collaborators who contributed to this work, including Mary Jackson and John Spencer at Colorado State and Jim Sacchettini, Tom Ioerger, and Inna Krieger at Texas A&M.

I must also thank Kevin Ahern and Bruce Geller at Oregon State University. Thank you Kevin, for your tireless efforts in student mentorship and teaching. Also, thanks go to Kevin for connecting me with Bruce and encouraging me to apply HHMI funding to an opportunity abroad in South Africa. Thank you Bruce for great mentorship and introducing me to the world of lab work and industry.

Thank you to Valerie Mizrahi and Digby Warner, for giving me a memorable lab and cultural experience in Johannesburg, South Africa for two months. Special thanks go to Digby for his approachability and interest in answering my questions in the lab. His passion for science has really been an inspiration. Val and Digby subsequently connected me with Sabine in New York City, for which I am very grateful.

Thank you to the National Institutes of Health for the T32 training grant (AI007621) to support my work and thank you to the Immunology and Microbial Pathogenesis program at Weill Cornell Medical College for their role in securing and distributing that funding, as well as for supporting me as a student in the program.

Finally, thank you family and friends for providing love and encouragement throughout my life. Thanks go to my parents Dave Puckett and Leonette Yee for their love and support, and for providing me with a solid foundation upon which to build. Special thanks to Karena Dokken, my friend who passed away in 2010, for believing in me and teaching me what strength really is. And thank you to Will Martin, for sharing his life with me through the good and the bad.

TABLE OF CONTENTS

LIST OF FIGURES

LIST OF TABLES

LIST OF ABBREVIATIONS

ACS	acetyl-CoA synthase
ADNaCl	growth supplement lacking oleic acid
ADP	adenosine diphosphate
AMP	adenosine monophosphate
atc	anhydrotetracycline
ATP	adenosine triphosphate
BCKADH	branched chain keto-acid dehydrogenase
BMDM	bone marrow-derived macrophages
BSA	bovine serum albumin
BSL3	biosafety level 3
CFU	colony forming unit
DHAP	dihydroxyacetone phosphate
DNA	deoxyribonucleic acid
doxy	doxycycline
DUC	dual control
EMP	Embden-Meyerhof-Parnas
FBA	fructose 1,6-bisphosphate aldolase
FBP	fructose 1,6-bisphosphate
G3P	glyceraldehyde 3-phosphate
GOGAT	glutamine oxoglutarate amidotransferase (glutamate synthase)
HIV	human immunodeficiency virus
HMP	hexose monophosphate
HOAS	2-hydroxy-3-oxoadipate synthase
ICDH	isocitrate dehydrogenase
ICL	isocitrate lyase

IFN-γ	interferon gamma
KAT	lysine acetyltransferase
KDH	α-ketoglutarate dehydrogenase
KGD	α-ketoglutarate decarboxylase
KO	knockout
KOR	α-ketoglutarate ferridoxin oxidoreductase
LC-MS	liquid chromatography mass spectrometry
MDR	multi-drug resistant
MS	malate synthase
MSA	malate synthase A (acetate-regulated)
MSG	malate synthase G (glycolate-regulated)
Mtb	*Mycobacterium tuberculosis*
NAD^+	oxidized nicotinamide adenine dinucleotide
NADH	reduced nicotinamide adenine dinucleotide
NADPH	nicotinamide adenine dinucleotide phosphate
NGMA	non-growing but metabolically active
NMR	nuclear magnetic resonance
OADC	growth supplement containing oleic acid and glucose
OD	optical density
PBS	phosphate buffered saline
PDH	pyruvate dehydrogenase
PDKA	phenyl-diketo acid
PEP	phosphoenolpyruvate
PEPCK	phosphoenolpyruvate carboxykinase
PNR/P	peroxynitrite reductase/peroxidase
PP	pentose phosphate
PTS	phosphotransferase system

TAG	triacylglygerol
TB	tuberculosis
TCA	tricarboxylic acid
VBNC	viable but non-culturable
WT	wild type

CHAPTER 1

INTRODUCTION

1.1 Tuberculosis: A global health issue, past and present

1.1.1 A brief history of tuberculosis

"To him who follows her way, Nature reveals many roads that lead in the direction of truth." ~René and Jean Dubos

Tuberculosis (TB), consumption, "white plague", and pthisis are all names for the disease caused predominately by the bacterium *Mycobacterium tuberculosis* (*Mtb*). With the limitation of having only the human species as a reservoir, *Mtb* cannot afford to kill its hosts before it has time to infect others. *Mtb* only causes active disease in 5-10% of those infected at some point in their lifetimes (Russell, 2013). Those with active TB commonly experience a lung infection, with symptoms such as a persistent cough, blood in sputum, chest pain, fatigue, fever, and weight loss. In some cases, *Mtb* can cause disease in other parts of the body such as the brain, bones, bladder, liver, or spleen. TB does not usually lead to an immediate death even in those with active disease, which allows for transmission of the bacteria via aerosolized droplets generated through coughing.

TB has been an enormous health burden to humans for millennia and is likely a product of a co-evolutionary relationship between bacterium and man. As of 2013, the oldest known human example of *Mtb* infection confirmed with DNA analysis is from the bones of a female and infant originating from Atlit-Yam, a now-submerged ancient settlement off the coast of Israel, dated 9250-8160 years ago (Anastasiou and Mitchell;

Hershkovitz et al., 2008). While *Mycobacterium bovis* from cattle has been postulated as an origin for *Mtb* during the advent of agriculture ~12,000 years ago, studies using whole genome sequencing analysis of various current *Mtb* strains support a history of *Mtb*-human co-evolution dating back to the movement of humans from Africa around 50,000-70,000 years ago (Comas et al., 2013; Hershberg et al., 2008; Russell, 2013). However, the debate is ongoing, as another study suggests a 6,000 year-old origin for *Mtb*, based on mutation-rate analysis of DNA sequences from the bones of Peruvian mummies (Bos et al., 2014). If *Mtb* is really over 50,000 years old, perhaps it is not surprising that TB remains problematic despite modern medicine, considering the time *Mtb* has had to refine its relationship with its human host.

Between the 17th and 19th centuries, approximately 1 in 5 people died of TB in North America and Europe (Comas et al., 2013). Therefore, it was of major significance in 1882 when Robert Koch meticulously demonstrated that TB is caused by a transmissible agent, christened *Mycobacterium tuberculosis* (Dubos and Dubos, 1952). For the first time, an effort could be made to directly target the cause of TB by developing treatments that could kill the bacterium. In 1943 under the direction of Selman Waksman, Albert Schatz isolated the first effective antibiotic against TB. Working as a graduate student, Schatz isolated streptomycin from a soil microbe and confirmed its efficacy against a pathogenic tuberculosis strain. Within the next two decades, the antibiotics para-amino salicyclic acid, isoniazid, pyrazinamide, and rifampicin were also introduced as TB therapies (Zumla et al., 2013). This enabled combination therapy that reduced treatment time to 6 months. Unfortunately, complete TB eradication has proved more difficult than anticipated.

1.1.2 Current state of the tuberculosis pandemic

In 2012, there were over 1.3 million deaths due to tuberculosis, putting TB among the 15 leading causes of death worldwide (World Health Organization, 2012). Out of these deaths, 320,000 were cases of human immunodeficiency virus (HIV) co-infection. HIV kills CD4+ T cells, a key component of the immune system important for containment of the infection. The World Health Organization has enacted a number of measures to improve diagnostics, health care, and treatment, which have contributed to a 45% drop in TB mortality rate from 1990-2012. The majority of TB cases are in South-east Asia, Africa, and the Western Pacific, where poverty and inadequate healthcare and diagnostics exhibit major barriers to TB eradication.

Drug-resistance has also been a major barrier to TB eradication. Current frontline treatment for tuberculosis is a lengthy 6-month course of isoniazid, rifampicin, ethambutol, and pyrazinamide, which is successful in about 85% of new TB cases. Non-compliance with the required therapy as well as improper diagnosis of drug resistance has contributed to the emergence of multi-drug resistant (MDR)-TB (Müller et al., 2013). MDR-TB is defined as a resistance to rifampicin and isoniazid and is associated with longer therapy (with other, more toxic antibiotics) and poorer patient outcomes. In 2012, roughly 170,000 people died of multi-drug resistant (MDR)-TB, making the development of novel therapies of paramount importance.

In late 2012, bedaquiline was approved by the Food and Drug Administration and became the first anti-tuberculosis drug in over 40 years to work via a novel mechanism of action (Zumla et al., 2013). Bedaquiline targets ATP synthase, an essential *Mtb* protein complex, and is now used to treat drug-resistant tuberculosis. A number of other anti-TB drugs remain in the pipeline and clinical trials (Lienhardt et al., 2012). While efforts are also ongoing to develop an effective vaccine, no attempt

has yet been successful. Novel compounds could provide alternative treatments to drugs that are no longer effective or which cause debilitating side effects, and potentially shorten the length of drug therapy. Therefore, efforts to develop new therapies remain a worthwhile investment.

1.1.3 Target-based drug development: identification of essential genes

Target-based drug design is a drug development approach in which pathways essential for viability are identified within *Mtb* prior to inhibitor testing. Once a target is identified, then high-throughput screening of compound libraries or structure-based drug design can be employed to generate compounds that inhibit the target (Payne et al., 2007). The sequencing and annotation of the complete *Mtb* genome enhanced our understanding of the potential targets in *Mtb* (Cole et al., 1998). *Mtb* has a 4.4 megabase pair genome with ~4,000 genes. Of these, ~60% were assigned a putative function (Slayden et al., 2013). In order to assess the essentiality of these genes, a genome-wide transposon mutagenesis method was developed (Griffin et al., 2011; Sassetti et al., 2003; Zhang et al., 2012b). Genes that cannot tolerate insertions are predicted essential, and the most recent approach can determine specific genomic regions that are essential, regardless whether they lie within or adjacent to a gene (Zhang et al., 2012b). However, there are caveats associated with these approaches, as mutants are always pooled together and must pass through growth stages *in vitro* that vary from the environment *in vivo*. Genetic studies involving deletion or conditional expression of specific genes are necessary to confirm whether these genes are essential and under which context. As with most research, the environment of utmost importance is the human host, in which it is not possible to study the impact of introduced *Mtb* gene mutations. Instead, the pathogenesis of *Mtb* mutants is determined using *in vitro* conditions and animal models that attempt to mimic the host

environment. Despite the limitations of these models, they contribute extensively to our understanding of *Mtb* biology.

1.2 Context of infection: *Mtb* adaptation to host environments

1.2.1 Introduction to the bug: *Mycobacterium tuberculosis*

Mtb is a rod-shaped bacterium 3-4μm in length whose structure consists of a cytoplasm encased by a complex and specialized cell envelope (Fattorini et al., 2013). In order from inside to outside, this is comprised of an inner phospholipid bilayer plasma membrane, a cell wall "core" with covalently-linked peptidoglycan-arabinogalactan-mycolic acids containing free intercalated lipids and lipoglycans, and a capsule consisting of proteins, polysaccharides, and small amounts of lipids (Hett and Rubin, 2008; Jackson, 2014; Sani et al., 2010). Detergent, such as Tween® 80 or tyloxapol, is required to prevent clumping in liquid culture and can lead to loss of the capsule layer in Mycobacterial species (Sani et al., 2010). The mycolic acids and freely-linked lipids are referred to as the outer membrane or "mycomembrane," a non-conventional bilayer. Between the outer membrane and inner membrane exists a periplasmic space. Therefore, *Mtb* shares characteristics with both Gram-positive and Gram-negative bacteria but possesses a waxy cell wall not found in either of these classes, making it uniquely resistant to certain antibiotics (Jackson, 2014). Components of this cell envelope not only protect the bacteria but also dictate the immune response of the host to *Mtb* by modulating the host response and inducing recruitment of specific macrophage populations (Cambier et al., 2014).

Mycobacterium tuberculosis shares a genus with the causative agent of leprosy, *Mycobacterium leprae*, as well as with members of the *Mycobacterium tuberculosis* complex (MTBC) such as *M. canetti*, *M. bovis*, *M. africanum*, and *M. microti*. Members of the MTBC can also cause tuberculosis, but do so much less frequently

than *Mtb*. The bacterium *M. smegmatis* is also a close relative. Unlike *Mtb*, this organism is less pathogenic and faster-growing than *Mtb* and therefore is often studied as a surrogate for *Mtb*. Also, comparisons with *Corynebacterium glutamicum*, a more distant relative, are useful as this organism's metabolism has been extensively studied and engineered for industrial production of metabolic compounds. The genome of *Mtb* is ~4,411 kilobases, while the genome of *M. smegmatis* is ~6,988 kilobases. *M. leprae* has the smallest genome of the MTBC, at ~3,268 kilobases.

Work with *Mtb* is challenging for several reasons. *Mtb* can be cultured *in vitro*, but divides very slowly in media optimized for its growth. Wild type *Mtb* has a generation time of ~24 hours and takes ~2½ weeks to form colonies on plate media. Work with pathogenic *Mtb* strains must be carried out in a biosafety level 3 (BSL3) facility, although *Mtb* DNA and protein lysates can be removed after sterilization. Options are limited for microscopy, as bacteria must be formalin-fixed prior to removal from the BSL3 facility, or the microscope must reside within the BSL3 facility. Animal models such as guinea pigs, non-human primates, rabbits, and mice have been used to mimic the course of *Mtb* infection. Mice are commonly used as they are less expensive than other models, easier to handle, and readily available, but they have significant differences compared to human infection in terms of lung lesion composition and the level of bacterial burden throughout infection.

1.2.2 Human infection with *Mtb*

Infection with *Mtb* begins with inhalation of an infectious particle, containing live bacteria. Bacteria are internalized by phagocytic cells lining the airways (Stallings and Glickman, 2010). Activation of the adaptive immune response follows trafficking of *Mtb* to the lymph nodes either by dendritic cells or entrance into the blood stream. This results in the recruitment of lymphocytes to the lung, such as CD4 T cells. These

cells secrete interferon gamma (IFNγ), a cytokine critical for macrophage activation. Activation of the adaptive immune response is required for containment and reduction of bacterial burden, but it does not eradicate all bacteria. Following initial infection, most patients enter into latent infection, in which they display no symptoms, but harbor a population of viable bacteria that for ~5-10% of people will reactivate at some point in their lifetime (Russell, 2013). At this point of active infection, bacteria may be coughed up with sputum and become airborne, ready to infect the next person.

Although *Mtb* can disseminate to regions throughout the body, it manifests primarily in the lung. *Mtb* induces the formation of granulomas, walled-off structures consisting of host cells (macrophages, surrounded by CD4 and CD8 T cells, B cells, neutrophils, epitheloid macrophages, multinucleated giant cells, fibroblasts, and dendritic cells) necrotic cell debris, cytokines, fibrosis (extracellular matrix), and bacteria (Tufariello et al., 2003). Granulomas are heterogeneous even within the same person, and may be fibrotic (consisting mainly of fibroblasts), caseous (containing a necrotic center with a cottage cheese-like consistency), or non-necrotizing (solid, consisting largely of macrophages) (Barry et al., 2009).

Mtb is an established intracellular pathogen and macrophage infection is a central component of *Mtb* pathogenesis. *Mtb* employs a wide variety of mechanisms to survive within macrophages, a cell type whose primary function is to kill invading pathogens. After phagocytosis by resting macrophages, *Mtb* exists within membrane-bound compartments called phagosomes and prevents their acidification my modulating the host response with glycolipids and secreted proteins (Russell et al., 2010). Upon IFNγ-mediated macrophage activation, *Mtb* is able to maintain intrabacterial pH despite phagosome acidification (Vandal et al., 2009). Alongside acid stress, *Mtb* must also survive exposure to reactive oxygen species, reactive

nitrogen species, nutrient limitation, and hypoxia. The mechanisms by which *Mtb* survives these stresses are the focus of active and ongoing research.

In addition to the macrophage phagosome, other host environments are habitable for *Mtb*. *Mtb* has been shown to infect cell types other than macrophages, including neutrophils and dendritic cells. There is some evidence that *Mtb* can enter the cytosol of infected cells (van der Wel et al., 2007). Extracellular survival may also be critical to *Mtb* pathogenesis. *Mtb* have been shown to form biofilm-like structures *in vitro*, which consist of clusters of bacteria held together by secreted mycolic acids (Ojha et al., 2008). In guinea pigs, bacteria have been observed by acid-fast staining in clusters around primary lesions (Orme, 2014). *Mtb* may be exposed to hypoxic stress while in areas like these, or while in the extracellular environment of the caseum. In summation, *Mtb* bacilli are exposed to a wide range of environments within a person over the course of infection, and *Mtb* must be able to survive within these environments.

1.2.3 Bacterial persistence

After establishment of infection and activation of the adaptive immune system within the host, bacterial numbers often decrease. This is termed the latent infection, in which no clinical symptoms are present. During this phase, infection is contained within granulomas, and bacteria cannot be cultivated from blood or sputum samples. Surviving *Mtb* is thought to exist in mixed populations of growing and dormant/slow-growing bacteria that are dynamic, depending on the environment (Esmail et al., 2012). This is one reason why the lengthy 6 month or longer drug therapy regimen may be necessary, as these slow-growing or dormant cells are resistant to antibiotics. The antibiotic pyrazinamide is unusual in that it is more effective against slower-growing cells than rapidly dividing cells and thus plays a role in shortening *Mtb* therapy (Zhang et al., 2012a). However, killing of a persistent population also depends on the ability

of a drug to access the target, which may differ depending on the type of granuloma and the localization of the bacteria (Fattorini et al., 2013). Furthermore, there may be subpopulations of persistent cells, each with differential susceptibility to antibiotics.

The definition of a "persister" is a bacterial cell that survives a cidal dose of antibiotics, but does not differ genetically from susceptible cells (Bigger, 1944; Girgis et al., 2012; Zhang et al., 2012a). This definition does not explain how the persister developed, nor does it define whether this persister has specific requirements for subsequent culture or is metabolically active. Further terms like "viable but non-culturable (VBNC)" or "non-growing but metabolically active (NGMA)" have been used to describe *Mtb* populations that do not grow on agar plates and are therefore non-detectable via colony-forming unit (CFU) counts, but can still "reawaken" at a later time, multiply, and cause disease. This is evidenced by the presence of a bacterial population that is not represented in CFU counts of human sputum samples (Mukamolova et al., 2010). Culture of this population is enabled by addition of supernatant of actively dividing bacteria, which contains *Mtb* resuscitation promoting factors, and perhaps other factors that stimulate bacterial growth (Mukamolova et al., 2010).

It is worth distinguishing the term of "persister" from the definition of persistence in the mouse model. In mice, bacterial burden increases for the first three weeks post-infection and then plateaus, as measured by CFU. This is termed a chronic infection, as there is little reduction in bacterial numbers for over 4 months, although a study using a clock plasmid concluded that bacteria are dividing and dying throughout this period (Gill et al., 2009). Here, this can be termed a persistent population, but the majority are not "persisters," because they are susceptible to antibiotics. The Cornell model, in which mice are infected with *Mtb* and treated with antibiotics until there are no detectable CFU, demonstrated the presence of a paucibacillary persister population

in mice. This was evidenced by the reappearance of a detectable bacterial population by CFU after the removal of antibiotics, which was exacerbated by immune suppression (McCune et al., 1966). The genes and pathways required for existence/generation of this VBNC or NGMA bacterial population remain to be determined.

How might such persister or slow-growing bacteria arise? Mycobacteria have been shown to exist in a heterogeneous population in the absence of stress. Mycobacteria divide asymmetrically, which contributes to a subpopulations of cells with differential growth-rates and susceptibility to antibiotics (Aldridge et al., 2012). Examination of single mycobacterial cells using a microfluidic device has revealed stochastic expression of enzymes such as KatG, which is critical for activation of the drug isoniazid (Wakamoto et al., 2013). Studies identifying persisters in bacterial populations did not expose the bacteria to stress prior to antibiotic treatment (Girgis et al., 2012). However, host stresses and antibiotics have been shown to induce a slow down of growth rate. *Mtb* encodes multiple stress response pathways, such as the DosR regulon, which is induced under hypoxic stress. Importantly, adaptations in carbon metabolic pathways have also been linked to establishment and maintenance of slow-growing bacterial populations (Baek et al., 2011; Eoh and Rhee, 2013; Gengenbacher et al., 2010; Rodriguez et al., 2014).

In *Mtb*, ability to slow down metabolism has been linked with drug-tolerance. Hypoxia is a stress present in the human host and is known to trigger a metabolic slow-down of *Mtb in vitro*, which is dependent on the presence of a triacylglycerol (TAG) synthase encoded by *tgs1* in *Mtb* (Baek et al., 2011). Deletion of *tgs1* or overexpression of *citA* (a gene encoding citrate synthase) increases the flux of acetate through the TCA cycle by preventing acetyl-CoA rechanneling into TAG or by

increasing the incorporation of acetyl-CoA into the TCA, respectively. These mutants also do not slow down growth in response to hypoxia or low iron stresses and are less resistant to antibiotics *in vitro* and in the mouse model (Baek et al., 2011; Deb et al., 2009). Therefore, metabolic activity of the TCA cycle may be closely linked with *Mtb* cell growth and antibiotic susceptibility. In summation, it is relevant to consider the carbon sources available to *Mtb* while in the host, whether adaptation to these carbon sources could contribute to the emergence of a latent *Mtb* population, and whether targeting metabolic pathways could be a viable strategy to kill latent bacteria.

1.2.4 Carbon source availability to *Mtb* within the host

Lipids, including fatty acids, can be used as carbon sources by *Mtb*. There is much evidence to support an abundance of lipids both within host macrophages and extracellular within the granuloma. Lipids identified within the caseum of tuberculosis granulomas include cholesterol ester, cholesterol, triacylglycerol (TAG), and lactosylceramide (Kim et al., 2010). Transcriptional profiling of caseous human lung granulomas identified upregulation of human genes involved in lipid metabolism (Kim et al., 2010). Lung surfactant is taken up my alveolar macrophages and contains fatty acids such as dipalmitoyl phosphatidylcholine (Muñoz-Elías and McKinney, 2006). Within a macrophage, lipids can be derived from the phagosomal membrane. Furthermore, the macrophages in which *Mtb* bacilli are chiefly found are abundant with lipid-rich bodies. These cells are termed foamy macrophages and are only present within tuberculous lesions. Foamy macrophages were shown to be induced by *Mtb* lipids *in vitro*, and *Mtb*-containing phagosomes within these macrophages migrated to merge with lipid bodies (Peyron et al., 2008; Russell et al., 2009). Another study showed that hypoxia also induced lipid droplet formation within human THP-1 macrophages and peripheral-blood monocyte-derived macrophages, and that *Mtb*

imported and metabolized fatty acids derived from macrophage TAG (Daniel et al., 2011).

Studies of the *Mtb* response to host and host-like environments further support a bacterial diet high in lipids. Early studies highlighted that *Mtb* harvested from human sputum samples is adapted for life on fatty acids but not carbohydrates (Segal and Bloch, 1956). *Mtb* from sputum samples was also shown to have high levels of TAG and upregulation of transcripts of the DosR regulon (Garton et al., 2008). *Mtb* has extensive duplication of genes encoding enzymes involved in β-oxidation, a major fatty acid catabolic pathway (Cole et al., 1998). *Mtb* also encodes genes for lipid transporters, including cholesterol transporters. Also, transcriptional upregulation of genes involved in fatty acid utilization pathways has been observed in *Mtb* harvested from macrophages and mice (Rohde et al., 2012; Schnappinger et al., 2003; Shi et al., 2010). Genetic studies, which will be mentioned later, highlight the importance for fatty acid metabolic pathways for establishment and maintenance of infection within mice (Marrero et al., 2010; McKinney et al., 2000; Pandey and Sassetti, 2008). Taken together, these data suggest that *Mtb* is likely to encounter and metabolize lipids within the host environment, and that lipid metabolism is important for *Mtb* virulence.

However, lipids may not be the only carbon source available for Mtb in the host. Metabolomic ^{13}C-flux spectral analysis of *Mtb*-infected human THP-1 macrophages supported a role for alanine, serine, glutamate, aspartate and CO_2 as carbon sources for *Mtb* during infection in addition to lipids. Metabolomic profiling of guinea pig lung granulomas over the course of *Mtb* infection by nuclear magnetic resonance spectroscopy (NMR) indicated an increase over time in aspartate, lactate, alanine, acetate, and glutamate, among other metabolites (Somashekar et al., 2011). Furthermore, *Mtb* lacking glucokinases, enzymes involved in utilization of

carbohydrates, were impaired in ability to persist in mice (Marrero et al., 2013). These studies suggest that *Mtb* faces a wide variety of carbon sources *in vivo*, but perhaps not simultaneously. But how does *Mtb* use these carbon sources and what is known about metabolic pathways in *Mtb*? This will be the focus of the following section.

1.3 Carbon metabolic pathways in *Mtb* and other bacteria

1.3.1 Overview of carbon metabolic pathways

All organisms on earth are "carbon-based" and require carbon metabolic pathways for growth and survival. Without them, food (in this case, a carbon-containing compound) cannot be converted into energy and building blocks for cells within the organism (Table 1.1). Carbon metabolic pathways are critical for the generation of adenosine triphosphate (ATP), a high-energy bond-containing molecule used as energy currency within the cell, as well as reduced nicotinamide adenine dinucleotide (NADH), which donates electrons into the electron transport chain to generate the proton motive force required for ATP generation. Enzymes, usually proteins, are catalysts that increase the rate of pathway reactions by lowering their activation energies. Enzymes of carbon metabolic pathways such as glycolysis and the tricarboxylic acid (TCA) cycle are conserved not only between different animal phyla, but between domains as well. The directionality of enzymatic reactions depends on the energetic favorability of the reaction or downstream reactions, their reaction mechanism, and the concentrations of substrate and product. Due to these reasons, some enzymes are unidirectional.

Mtb encodes homologs of enzymes in many of the known bacterial metabolic pathways, although many of these lack functional confirmation through biochemical, metabolomic, or gene deletion studies. This section will describe major carbon metabolic pathways known in bacteria before focusing on metabolism in *Mtb* specifically.

Table 1.1. Contributions of carbon metabolic pathways to biosynthetic precursor generation.

Metabolite precursor	Required for	Pathway
Ribose-5-phosphate	Nucleic Acids	PPP
Erythrose-4-phosphate	Amino Acids	PPP
Glucose-6-phosphate	Polysaccharides	Glycolysis/Gluconeogenesis
Fructose-6-phosphate	Cell wall peptidoglycan	Glycolysis/Gluconeogenesis
Triose-phosphate	Lipids	Glycolysis/Gluconeogenesis
3-phosphoglycerate	Amino Acids	Glycolysis/Gluconeogenesis
Phosphoenolpyruvate	Amino Acids	Glycolysis/Gluconeogenesis
Pyruvate	Amino Acids	Glycolysis/Gluconeogenesis
Acetyl-CoA	Fatty Acids	TCA cycle
α-ketoglutarate	Amino Acids	TCA cycle
Succinyl-CoA	Amino Acids	TCA cycle
Oxaloacetate	Amino Acids	TCA cycle

Glycolysis and gluconeogenesis

Glycolysis (also known as the Embden-Meyerhof-Parnas or EMP pathway) is a series of enzymatic steps that result in the formation of pyruvate from glucose (Kim, 2008). During glycolysis, two molecules of NADH and pyruvate are generated, as well as two molecules of ATP via substrate level phosphorylation for every glucose molecule. Important metabolites generated in addition to pyruvate are glucose-6-phosphate, which feeds into the pentose phosphate pathway to generate NADPH and nucleic acid precursors, and fructose-6-phosphate, which feeds into peptidoglycan synthesis. Also, triose phosphates are precursors for lipid biosynthesis, while 3-phosphoglycerate and pyruvate are precursors for amino acids. Pyruvate can also be converted to acetyl-CoA by the pyruvate dehydrogenase complex (pyruvate + coenzyme A + NAD^+ to acetyl CoA + NADH + H^+). Acetyl-CoA can then participate in the TCA cycle, fatty acid biosynthesis, or branched chain amino acid biosynthesis.

Gluconeogenesis is the series of enzymatic steps resulting in the generation of glucose-6-phosphate, glucose, or glycogen from non-carbohydrate carbon sources. Many of the enzymes that participate in glycolysis also can function in the opposite direction in gluconeogenesis. Since many steps are the reverse of glycolysis, ATP is used rather than generated for these reactions to proceed.

Enzymes that only participate in glycolysis and not gluconeogenesis are phosphofructokinase (converts fructose-6-phosphate to fructose-1,6-bisphosphate) and pyruvate kinase (phosphoenolpyruvate +ADP to pyruvate +ATP). Enzymes that participate in gluconeogenesis but not glycolysis include those involved in PEP synthesis and fructose bisphosphatase (converts fructose-1,6-bisphosphate to fructose-6-phosphate). PEP synthesis can be achieved through the action of phosphoenolpyruvate synthetase (pyruvate + ATP to PEP + AMP + P_i), pyruvate-

phosphate dikinase (pyruvate + ATP +P_i to PEP + AMP +PP_i), or phosphoenolpyruvate carboxykinase (oxaloacetate + ATP to PEP + CO_2 +ADP). Malic enzyme can generate pyruvate directly from malate (malate + NAD^+ + H^+ to pyruvate + NADH + CO_2). Oxaloacetate decarboxylase can convert oxaloacetate to pyruvate and CO_2.

To prevent futile cycling (waste of ATP due to pathways going in both directions within the same cell), many bacteria have regulatory mechanisms that drive metabolism in either the glycolytic or gluconeogenic direction. This can involve transcriptional/translational control of enzyme expression, post-translational modifications of enzymes, or allosteric regulation of enzymes by the levels of metabolites within the pathways or coenzymes such as ATP.

Pentose phosphate pathway

The pentose phosphate pathway, or hexose monophosphate (HMP) pathway, uses glucose-6-phosphate to generate NADPH and biosynthetic precursors such as ribose-5-phosphate (nucleic acid synthesis) and erythrose-4-phosphate (amino acid synthesis). NADPH can help maintain redox homeostasis by being a source of reducing power (Hasan et al., 2010). Other metabolic products include glyceraldehyde 3-phosphate and fructose-6-phosphate, which participate in glycolysis and gluconeogenesis. Therefore, the pentose phosphate pathway can act as a potential inefficient bypass of several enzymatic steps in glycolysis.

Entner-Doudoroff pathway

Some bacteria, such as *Pseudomonas* species and *E. coli*, have an Entner-Doudoroff pathway, which acts alongside or replaces glycolysis. In the ED pathway, glucose is converted into glucose-6-phosphate, which is converted into 6-phosphogluconate,

which is dehydrated to form 2-keto-3-deoxyphosphogluconate. This metabolite is split into glyceraldehyde-3-phosphate (G3P) and pyruvate. G3P can then go through the same enzymatic steps as in glycolysis to generate pyruvate. Therefore, the net gain is one ATP, one NADH, and one NADPH per glucose metabolized in this pathway.

Methylglyoxal bypass

An alternative to the glycolytic steps converting dihydroxyacetone phosphate to pyruvate is the methylglyoxyal bypass pathway. This removes the requirement for phosphate, but involves the formation of methylglyoxyal, a highly reactive compound that can damage nucleic acids and proteins. Methylglyoxyal toxicity is controlled by secretion and by glyoxylases, enzymes that converts methylglyoxal to D-lactate, which is then converted to pyruvate by lactate oxidase.

Tricarboxylic Acid cycle

The tricarboxylic acid cycle (TCA), also known as the Kreb's cycle or citric acid cycle, oxidizes the carbon from acetyl-CoA to generate CO_2, which also produces NADH, NADPH (or another NADH, depending on the type of isocitrate dehydrogenase present), and ATP. Further reactions within the TCA cycle generate $FADH_2$, and one more NADH. These cofactors can then donate electrons into the electron transport chain, resulting in the synthesis of ATP.

Because of the output of two CO_2 molecules in the TCA cycle, there is no net gain of carbon with entrance of acetyl-CoA, a two-carbon molecule. However, metabolites in the TCA cycle also are biosynthetic precursors for amino acids, so bacteria must have alternative ways of replenishing these metabolites. One way is to generate oxaloacetate from either PEP or pyruvate, with incorporation of CO_2. This is catalyzed by pyruvate carboxylase (pyruvate + HCO_3^- + ATP to oxaloacetate + ADP + P_i) or

PEP carboxylase (PEP + HCO_3^- to oxaloacetate + P_i). Phosphoenolpyruvate carboxykinase, although noted for its role in gluconeogenesis, can also convert PEP to oxaloacetate (PEP+HCO_3^-+GDP to oxaloacetate+GTP).

The TCA cycle contains one enzymatic reaction that is part of the electron transport chain, which is the conversion of succinate and FAD to fumarate and $FADH_2$ by succinate dehydrogenase. This enzyme is part of a multi-unit complex, in which at least one subunit is membrane-bound. Electrons pass directly from succinate into the electron transport chain.

Metabolites in the TCA cycle feed into amino acid biosynthesis. α-ketoglutarate contributes to glutamate, glutamine, arginine, and proline synthesis; oxaloacetate contributes to aspartate, asparagine, methionine, lysine, isoleucine, and threonine synthesis.

Glyoxylate pathway (shunt)

When bacteria grow on fatty acids, these are converted to acetyl-CoA, which cannot feed directly into PEP or pyruvate. Furthermore, the two carbons from acetyl-CoA are lost following the canonical TCA cycle. Therefore, an alternative anapleurotic pathway is required in order for carbon to be retained as biomass. This is termed the glyoxylate pathway (shunt or bypass), because glyoxylate is an intermediate. This pathway consists of two steps: the cleavage of isocitrate to glyoxylate and succinate by isocitrate lyase and the conversion of glyoxylate and acetyl-CoA to malate and CoA by malate synthase.

Methylcitrate pathway

The methylcitrate pathway is a way for bacteria to detoxify propionyl-CoA derived from odd-chain fatty acids, as well as to grow on odd-chain fatty acids. It begins with the condensation of propionyl-CoA and oxaloacetate to form methylcitrate catalyzed by methylcitrate synthase. The following steps ultimately result in the formation of pyruvate and succinate. This pathway is remarkably similar in its enzymatic steps to the TCA/glyoxylate cycle conversion of oxaloacetate and acetyl-CoA to succinate and glyoxylate.

Methylmalonyl pathway

The methylmalonyl pathway is an alternative to the methycitrate cycle as a propionyl-CoA detoxification pathway, and is also involved in lipid synthesis. The first step converts HCO_3^-, ATP, and propionyl-CoA to (S)-methylmalonyl CoA, a phosphate, and ADP with the enzyme propionyl-CoA carboxylase. This product is converted to (R)-methylmalonyl-CoA by racemase, which is then converted to succinyl-CoA and pyruvate by methylmalonyl-CoA mutase, a vitamin B12-dependent enzyme. These products can then feed into the TCA cycle and acetyl-CoA production. Methylmalonyl-CoA contributes to synthesis of methyl-branched fatty acids.

β-oxidation

β-oxidation is a series of enzymatic steps by which odd-chain (5 carbon or longer) or even-chain fatty acids (4 carbon or longer) gain CoA and are broken down and converted into acetyl-CoA, with one molecule of propionyl-CoA for odd-chain fatty acids. During this process, ATP is used while $FADH_2$ and NADH are generated. Therefore, this pathway has the potential to increase the reductive stress a cell faces, but also feeds into the TCA cycle and propionyl-CoA metabolic pathways.

1.3.2 Understanding metabolism in *Mtb*

Carbon metabolic pathways in *Mtb* are less well studied compared to those in other bacteria such as *Escherichia coli* or *Corynebacterium glutamicum*. Although these organisms, especially the more closely-related *C. glutamicum,* are useful reference points for *Mtb* metabolic pathways, research has revealed differences compared to the metabolic pathways of *Mtb*. Therefore, it is worthwhile exploring the following questions about *Mtb* specifically:

First, what pathways exist by gene annotation? What have subsequent studies on specific genes revealed about their function? Which carbon sources can *Mtb* use for growth and how does *Mtb* do this? Finally, what evidence do we have to implicate specific pathways in pathogenesis?

1.3.2.1 Gene annotation of metabolic pathways

Mtb has genes annotated to encode enzymes for glycolysis, gluconeogenesis, the pentose phosphate pathway, the TCA cycle, the methylcitrate cycle, the methylmalonyl pathway, and the glyoxylate pathway (Figure 1.1) (Cole et al., 1998). *Mtb* lacks homologs for the Entner-Doudoroff pathway. Furthermore, *Mtb* contains many gene homologs for β-oxidation enzymes, suggesting an important role for fatty acid breakdown for *Mtb* pathogenesis. However, ~40 percent of open reading frames encode hypotheticals or genes of unknown function, leaving the possibility of the presence of undiscovered metabolic enzymes (Slayden et al., 2013).

Despite the usefulness of gene annotation, genetic, metabolomics, and biochemical studies are necessary to confirm the functions of specific genes and the absence of genes with similar functions. For example, glucokinase is an enzyme that

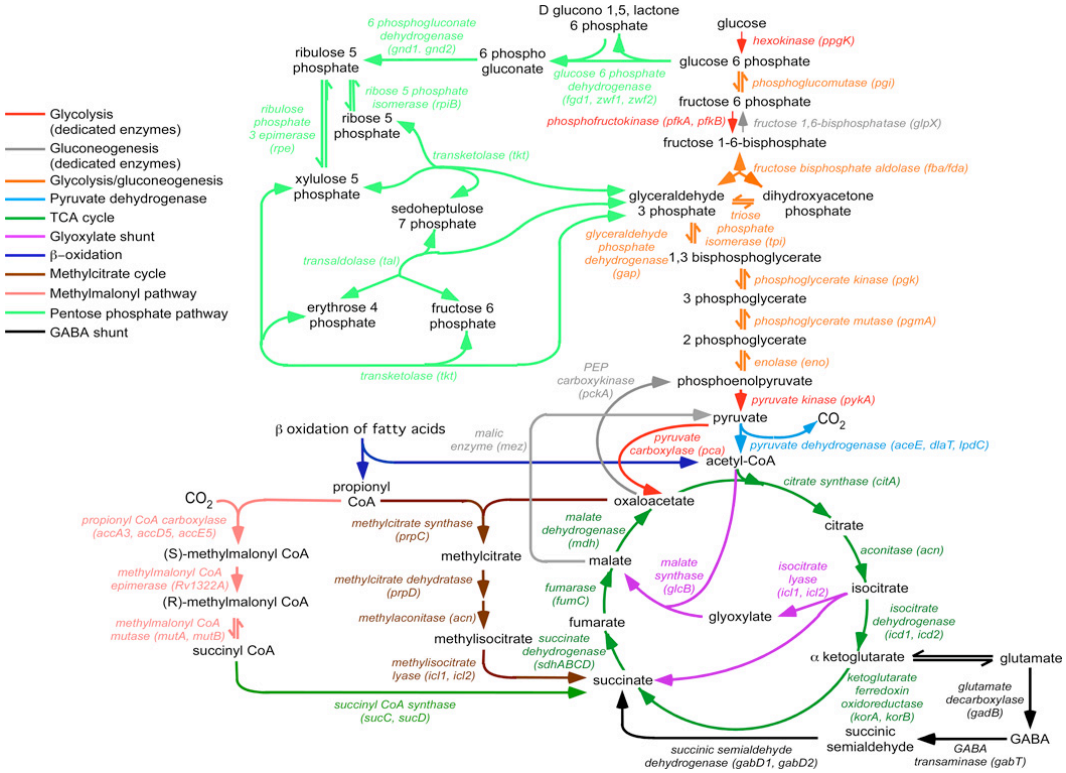

Figure 1.1. Carbon metabolic pathways in *Mtb*. (Figure from Rhee et al., 2011)

phosphorylates glucose as the first committed step of glycolysis. An *Mtb* knockout lacking the only predicted glucokinase gene *ppgK* had impaired but not abolished growth on glucose (Marrero et al., 2013). However, a double knockout lacking both *ppgK* and *rv0650* (annotated as a "possible sugar kinase") was unable to grow in glucose entirely and exhibited a persistence defect in the mouse.

Conversely, in some cases a gene has a predicted function but genetic studies fail to support it. *Mtb* encodes two predicted phosphofructokinases, *pfkA* and *pfkB*. However, knockout of *pfkA* alone was enough to abolish growth on glucose, while knockout of *pfkB* did not have an effect on growth in glucose (Phong et al., 2013). Furthermore, the *pfkB* knockout exhibited PFK activity *in vitro*, wheras the *pfkA* knockout did not. The *pfkA* knockout was not impaired in ability to infect and persist in the mouse model, suggesting that either PFK is not essential for mouse infection, that *pfkB* is active *in vivo*, or that there is an alternative gene that compensates for loss of *pfkA* that may be expressed during infection.

Another example of non-predictability in *Mtb* carbon metabolic pathways is manifest in the TCA cycle conversion of α-ketoglutarate to succinate (Figure 1.2). Metabolomics analysis has suggested a partial bifurcation of the TCA cycle, as there is lack of clear flux from α-ketoglutarate to succinate (de Carvalho et al., 2010a). However, *Mtb* expresses several enzymes that can catalyze the generation of succinate from α-ketoglutarate. The enzyme encoded by Rv1248c can act as a subunit of α-ketoglutarate dehydrogenase, as well as exhibits 2-hydroxy-3-oxoadipate synthase and thiamine diphosphate-dependent α-ketoglutarate decarboxylase activity. α-ketoglutarate dehydrogenase complex converts α-ketoglutarate to succinyl-CoA, which can then be converted to succinate via succinyl-CoA synthetase. The existence

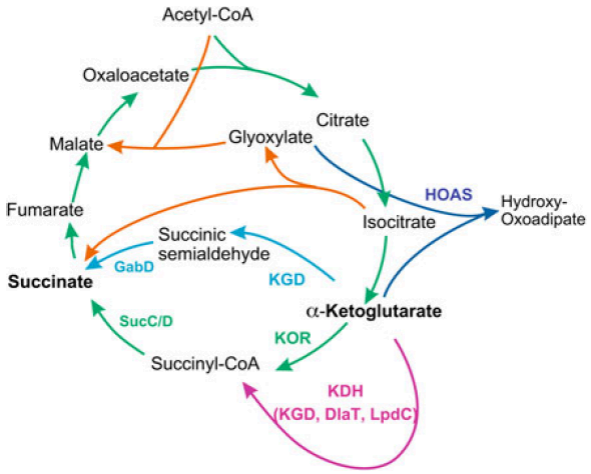

Figure 1.2. Enzymatic reactions involving α-ketoglutarate in *Mtb*. KGD, α-ketoglutarate decarboxylase; HOAS, 2-hydroxy-3-oxoadipate synthase; KOR, α-ketoglutarate ferridoxin oxidoreductase; KDH, α-ketoglutarate dehydrogenase complex. (Figure from Ehrt and Rhee, 2013)

of this enzymatic activity was thought to be absent, but has been demonstrated more recently (Tian et al., 2005; Wagner et al., 2011). 2-hydroxy-3-oxoadipate synthase (HOAS) converts α-ketoglutarate and glyoxylate to 2-hydroxy-3-oxoadipate, which can potentially detoxify glyoxylate or feed into alternative metabolic pathways (de Carvalho et al., 2010b). Thiamine diphosphate-dependent α-ketoglutarate decarboxylase catalyzes the decarboxylation of α-ketoglutarate to succinic semialdehyde, which through the actions of succinic semialdehyde dehydrogenases GabD1 and GabD2 can be converted to succinate with the concomitant production of NADPH (Tian et al., 2005). Furthermore, the existence of α-ketoglutarate ferridoxin oxidoreductase (KOR) provides an alternative pathway for conversion of α-ketoglutarate to succinyl-CoA (Baughn et al., 2009). The gene encoding a probable succinyl-CoA synthetase, *sucC*, is one of the most abundant proteins expressed in *Mtb*, suggesting that conversion of succinyl-CoA to succinate may be an important enzymatic step (Schubert et al., 2013). These studies highlight the potential for unforeseen complexity in *Mtb* metabolic pathways and the need for biochemical, metabolomic, and genetic studies to validate gene annotations.

1.3.2.2 *Mtb* uptake and metabolism of specific carbon sources

Early studies found that *Mtb* can grow on a variety of carbon substrates, as indicated by oxygen consumption (Edson, 1951). Here, entrance of specific carbon sources into the cell and their utilization are discussed.

Carbohydrates

While *M. smegmatis* expresses many putative sugar transporters, *Mtb* only expresses genes for four ABC-type transporters and one sugar permease (Niederweis, 2008). *M. smegmatis* also expresses genes for a phosphotransferase system (PTS) which is

involved in carbon catabolite repression. This is a system by which carbon source regulates activity of specific metabolic pathways, and by which an organism can preferentially use one carbon source over another. *Mtb* lacks genes for this system (Titgemeyer et al., 2007). Currently, it is known that *Mtb* can grow on glucose, but the specific transporters required for glucose entry past the inner membrane have not been elucidated. Furthermore, carbohydrates may also require a porin to traverse the outer membrane, but this has not been elucidated (Niederweis, 2008). Within the cell, glucose can be phosphorylated by glucokinases to form glucose-6-phosphate, entering into glycolysis.

Trehalose, a disaccharide, can also be used as a sole carbon source for *Mtb* growth. One of the putative sugar transporters, the ABC transporter LpqY-SugA-SugB-SugC, has been shown to act as a trehalose transporter (Kalscheuer et al., 2010). Trehalose accounts for 1.5-3% of dry weight of *M. smegmatis* cultured *in vitro* and is incorporated into mycobacterial glycolipids (Smet et al., 2000). Conversely, trehalose levels in mammals are thought to be low, because mammals express trehalase, an enzyme that hydrolyzes trehalose to glucose. Therefore, it is doubtful that trehalose coming from the host would be sufficient to support *Mtb* growth and it is more probable that trehalose is recycled by *Mtb* during host infection (Kalscheuer et al., 2010).

Glycerol and Triglycerides/Triacylglycerol (TAG)

Glycerol is 3-carbon molecule with three hydroxyl groups and is a common component of *Mtb* culture media due to its ability to enhance growth of *Mtb*. Glycerol has been shown to diffuse through lipid membranes so therefore may not require a specific transporter (Niederweis, 2008). However, the outer membrane porin protein CpnT was recently demonstrated to play a role in glycerol uptake, and deletion of the

gene encoding CpnT in *Mtb* resulted in a growth delay compared to the wild type strain in glycerol (Danilchanka et al., 2014). Glycerol is converted to glycerol-3-phosphate by glycerol kinase (*glpK*) and then dihydroxyacetone phosphate (DHAP) by glycerol-3-phosphate dehydrogenase. DHAP can enter into either glycolysis or gluconeogenesis.

Triacylglycerol (TAG) is an ester composed of glycerol and three long-chain fatty acids. *Mtb* generates TAG during exposure of *Mtb* to stress conditions such as hypoxia and low pH, and *Mtb* extracted from host lesions have been shown to contain TAG inclusion bodies (Garton et al., 2002; Sirakova et al., 2006). *Mtb* may use this intracellular TAG store as a carbon source, and also has been shown to incorporate TAG-derived carbon from the host into its own TAG (Daniel et al., 2011). *Mtb* expressed LipY, a TAG hydrolase, that could be involved in the breakdown of TAG for use as a carbon source by the bacillus (Mishra et al., 2008).

Acetate and Propionate

Acetate, a two-carbon carboxylate ion, is thought to freely permeate through bacterial membranes, and no acetate transporter has been identified in *Mtb*. *Mtb* can grow with acetate as a sole carbon source *in vitro*, which is dependent on the glyoxylate shunt to prevent loss of carbon in the form of CO_2. To enter into carbon metabolism, acetate is converted to acetyl-CoA by the enzyme acetyl-CoA synthetase (ACS), encoded by Rv3667 (Li et al., 2011). ACS is known to be inhibited by acetylation or propionylation (Noy et al., 2014). An alternative acetate incorporation pathway exists in *E. coli* and *C. glutamicum* that involves the enzymes acetate kinase and phosphotransacetylase and the intermediate metabolite acetyl-phosphate. *Mtb* encodes a homolog for acetate kinase (*ackA, rv0409*) and phosphotransacetylase (*pta*, *rv0408*). Acetate induces upregulation of *icl1,* which encodes isocitrate lyase, the first enzyme

in the glyoxylate shunt. *icl1* is repressed during growth on glucose through the activity of transcriptional repressor RamB (Micklinghoff et al., 2009).

Propionate is a three-carbon carboxylate ion. Propionate is metabolized into propionyl-CoA by ACS, which has been shown to function as a propionyl-CoA synthase (Li et al., 2011). Propionyl-CoA derived from lipids such as cholesterol or long-chain fatty acids is thought to play a critical role in *Mtb* virulence. Propionyl-CoA is required for the synthesis of cell wall lipids such as phthiocerol dimycocerosate (PDIM), which have been implicated in pathogenicity (Day et al., 2014). However, propionate and its derivatives are toxic to the cell. Three mechanisms of propionate detoxification have been proposed in *Mtb*: the methylcitrate pathway, the methylmalonyl pathway, and the incorporation of propionate into cell wall lipids(Lee et al., 2013). Indeed, increasing incorporation of propionate into TAG and PDIM through deletion of *whiB3* enhanced resistance to propionate (Singh et al., 2009).

How is propionate toxic to the cell? In *Aspergillus nidulans*, propionyl-CoA was shown to inhibit the CoA-dependent enzyme pyruvate dehydrogenase (Brock and Buckel, 2004). A similar mechanism has been proposed for *Mtb*, as addition of acetate to conditions with propionate (in the presence of glycerol) relieved propionate toxicity for a strain lacking isocitrate lyase activity (Lee et al., 2013). Also, 2-methylcitrate (a metabolite downstream of propionyl-CoA) in *Mtb* has been shown to have an inhibitory effect on fructose bisphosphatase (Eoh and Rhee, 2014). Accumulation of methylcitrate cycle intermediates has further been implicated in the disruption of membrane potential, intrabacterial pH, and NAD^+/NADH ratio in *Mtb* (Eoh and Rhee, 2014). It is possible that these mechanisms or others account for toxicity of propionate or propionate-derived metabolites within the cell.

Considering this propionate toxicity, it not surprising that *Mtb* has evolved ways of regulating propionate metabolism. Acetyltransferase (KAT) can acetylate ACS, which inactivates the enzyme, inhibiting incorporation of propionate into propionyl-CoA. Deletion of KAT enhanced susceptibility to propionate, presumably by allowing greater flux of propionate into the methylcitrate cycle (Nambi et al., 2013). In addition to regulation of ACS, *Mtb* has other mechanisms by which it responds to propionate. PrpR (encoded by *rv1129c*) is a transcription factor that is required for expression of *prpC* and *prpD*, genes encoding methylcitrate synthase and methylcitrate dehydratase, respectively (Griffin et al., 2011; Masiewicz et al., 2012). In both cholesterol and propionate, *prpC* and *prpD* are upregulated in a PrpR-dependent manner, and *Mtb* lacking *rv1129c* has growth defects in propionate or cholesterol alone. PrpR binds the promoter region of *prpC*, *prpD*, and *icl1*, which activates the transcription of these genes. PrpR also binds the promoter region of the *icl1* transcriptional regulator *ramB* and weakly interacts with the promoter region of *dnaA*, which inhibits expression of these genes (Masiewicz et al., 2014). DnaA plays a role in replication initiation, so activation of PrpR through exposure to propionate could be a mechanism by which *Mtb* slows its process of cell division (Masiewicz et al., 2014). Interestingly, expression of *prpC* and *prpD* is not upregulated in acetate-containing media, so it appears that PrpR activity is activated by propionyl-CoA-generating carbon sources (propionate and cholesterol) specifically.

Fatty acids

Mtb encodes approximately 250 genes involved in lipid metabolism, suggesting that lipids (including fatty acids) are a critical component of *Mtb*'s diet (Cole et al., 1998). Fatty acids are carboxylic acids with hydrocarbon chains. *Mtb* can use many different fatty acids as carbon sources, such as butyrate, valerate, caproate, oleic acid, and

stearate (Lee et al., 2013). Fatty acids are catabolized via β-oxidation into one or several molecules of acetyl-CoA and one molecule of propionyl-CoA (for odd-chain fatty acids). Fatty acids may diffuse freely through membranes or they may have specific transporters; the mechanisms of uptake for most fatty acids are unknown.

A fatty acid present in standard *Mtb* culture media is oleic acid. Oleic acid is an 18-carbon long monounsaturated fatty acid that enhances growth of WT *Mtb*. WT *Mtb* growing on media with low quantities of oleic acid (0.006%) forms colonies on plates more quickly and also increases in density more quickly in liquid media. As with other fatty acids, the mechanism of oleic acid uptake is unknown but may involve a transporter or permeation through mycobacterial membranes.

Cholesterol

Cholesterol is a complex lipid that is a major component of animal cell membranes and is likely catabolized by *Mtb* during infection. *Mtb* encodes multiple genes involved in cholesterol transport and catabolism, many included in the "Cho" region of the genome that comprises 83 genes, spanning from Rv3492c to Rv3574 (Van der Geize et al., 2007; Nesbitt et al., 2010). Additional genes also participate in cholesterol utilization, as a transposon mutagenesis screen identified 96 genes predicted to be required for growth on cholesterol, some outside of the Cho region (Griffin et al., 2011). *Mtb* can grow on cholesterol as a carbon source *in vitro*, which is metabolized via a complex series of steps into a mixture of propionyl-CoA, acetyl-CoA, and pyruvate (Griffin et al., 2012; Wipperman et al., 2014). Metabolism of cholesterol is dependent on the methyl-citrate pathway in the absence of a functional methylmalonyl pathway, likely due to the need for propionate detoxification (Griffin et al., 2012).

Amino Acids

Amino acid synthesis and degradation pathways are closely connected to carbon metabolic pathways in *Mtb*. For example, alanine, leucine and valine can contribute to pyruvate synthesis; aspartate, asparagine, methionine, lysine, isoleucine, and threonine are connected to oxaloacetate synthesis; and glutamate, glutamine, arginine, and proline contribute to α-ketoglutarate synthesis (Kim, 2008). Several transporters have been identified as playing a role with uptake of amino acids, which are also important for nitrogen metabolism (Gouzy et al., 2014). For example, AnsP1 is involved in uptake of aspartate, which in the presence of another carbon source (such as glycerol) can incorporate into TCA cycle metabolites (Gouzy et al., 2013). Asparagine has also been demonstrated to be used as a carbon source by *Mtb* (Lyon et al., 1969).

Glutamate can be converted to α-ketoglutarate through the action of glutamate dehydrogenase. α-ketoglutarate is at the branch point of carbon and nitrogen metabolism, and its fate is controlled by the regulator GarA. GarA inhibits both glutamate dehydrogenase and α-ketoglutarate dehydrogenase only in its non-phosphorylated form. Unphosphorylated GarA also activates glutamate synthase (also known as glutamine oxoglutarate amidotransferase or GOGAT). This promotes use of α-ketoglutarate for glutamate synthesis. While phosphorylated, GarA does not inhibit these enzymes, and α-ketoglutarate contributes to the TCA cycle (Ventura et al., 2013).

Multiple carbon sources

Mtb differs from bacteria such as *E. coli* in that it lacks homologs for carbon catabolite repression pathways and has the ability to utilize two carbon sources feeding into opposing pathways to enhance its growth (de Carvalho et al., 2010a; Görke and Stülke, 2008). This simultaneous utilization of carbon sources is referred to as co-catabolism.

This seemingly contradicts the concept of metabolic regulatory mechanisms being in place to prevent waste of energy through futile cycling. An explanation for how *Mtb* prevents futile cycling has been suggested with metabolomics labeling experiments revealing a compartmentalization of *Mtb* metabolic pathways (de Carvalho et al., 2010a). For example, in the case of two carbon sources glucose and acetate, glucose primarily contributes to glycolytic intermediates, whereas acetate feeds into the TCA cycle. Whether this compartmentalization involves segregation of metabolic enzymes into separate intracellular compartments or into enzyme complexes remains to be determined. Also, whether *Mtb* requires the ability to co-catabolize carbon within the host environment remains to be determined.

No or low carbon

There may be times in which *Mtb* encounters a lack of carbon sources or inability to generate amino acids it needs. The stringent response is a metabolic slow-down that requires the enzyme RelA to generate the alarmone (p)ppGpp (hyperphosphorylated guanosine nucleotides) which inhibits RNA polymerase function (Klinkenberg et al., 2010). The activity of RelA is regulated by the concentration of amino acids present in the cell. RelA deletion impairs *Mtb* virulence in mouse and guinea pig models, suggesting a role for the stringent response *in vivo* (Klinkenberg et al., 2010; Primm et al., 2000). However, it is unclear whether complete deprivation of carbon sources *in vivo* would be required to activate this response, or if lack of other nutrients could also trigger this response.

Carbon dioxide

Carbon dioxide (CO_2) can be converted by carbonic anhydrases (of which *Mtb* encodes three) to bicarbonate (HCO_3), which can be used as a substrate for

anapleurotic reactions from glycolysis to the TCA cycle, and for condensation with propionyl-CoA in the methylmalonyl pathway (Beste et al., 2011). Therefore, CO_2 is not sufficient on its own to support growth as a carbon source, but can supplement growth in the presence of other carbon sources. Evidence for this includes incorporation of labeled sodium bicarbonate into metabolites of the TCA cycle (Beste et al., 2011, 2013).

1.3.2.3 Genetic knockout studies identify essential pathways

Genetic studies involving mouse infections with *Mtb* knockout or knockdown strains have bolstered our understanding of the importance of carbon metabolic pathways in *Mtb in vivo*. The importance of fatty acid metabolic pathways during infection was first established in a landmark paper by McKinney et. al in 2000, which showed that deletion of one of the genes encoding the glyoxylate shunt enzyme isocitrate lyase impaired *Mtb* persistence in the mouse model (McKinney et al., 2000). Subsequent studies demonstrated that depletion of both isocitrate lyase genes rendered *Mtb* unable to establish or maintain infection in mice (Blumenthal et al., 2010; Munoz-Elias and McKinney, 2005). Interestingly, activated macrophages have been shown to produce the ICL inhibitor itaconic acid as an antibacterial response, supporting an important role for the glyoxylate shunt during infection (Michelucci et al., 2013). However, ICL also has an alternative function as a methylisocitrate lyase, which is involved in the methylcitrate cycle, a propionate detoxification pathway. Mutations in the methylcitrate cycle genes *prpDC* (encoding for methylcitrate synthase and methylcitrate dehydrogenase) did not result in a mouse phenotype but did impair growth of *Mtb* in murine macrophages *ex vivo* (Muñoz-Elías et al., 2006).

The importance of gluconeogenesis during mouse infection was demonstrated by the deletion or depletion of phosphoenolpyruvate carboxykinase (PEPCK), the first

committed step of gluconeogenesis (Marrero et al., 2010). *Mtb* lacking *pckA*, the gene encoding PEPCK, had difficulty establishing infection in mice and was impaired for growth with acetate or valerate as a single carbon source. Furthermore, depletion of *pckA* after establishment of infection resulted in a reduction of bacterial burden. Interestingly, the *pckA* knockout did not die during any *in vitro* condition tested, including low pH, oxidative stress, nitric oxide, or starvation. The mechanism of death *in vivo* therefore remains to be elucidated.

Glycolysis may also contribute to virulence during infection. Import of trehalose, a carbon source feeding into glycolysis, was required for establishment of infection in mice (Kalscheuer et al., 2010). Glucose phosphorylation, the first step in glycolysis catalyzed by the proteins encoded by *ppgK* and *rv0650*, was essential for persistence of infection (Marrero et al., 2013). Also, triose phosphate isomerase (encoded by *tpi*), an enzyme downstream of glucose phosphorylation in glycolysis, was required for *Mtb* growth and survival in glycerol, and establishment of infection in mice (Trujillo et al., 2014). However, *tpi* also participates in gluconeogenesis. Trehalose can also contribute to glycolipid formation. Also, knockout of the only phosphofructokinase gene exhibiting enzymatic activity (*pfkA*) did not impair *Mtb*'s ability to establish or maintain infection *in vivo* (Phong et al., 2013). Therefore, there is evidence supporting a role for glycolysis during infection, although it is not as substantial as that for gluconeogenesis.

Another gene involved in carbon metabolic pathways that was essential in the mouse model is *lpdC*, which encodes lipoamide dehydrogenase (Lpd) (Venugopal et al., 2011). Lpd participates in four enzyme complexes: pyruvate dehydrogenase (PDH), branched chain ketoacid dehydrogenase (BCKADH), peroxynitrite reductase/peroxidase (PNR/P), and α-ketoglutarate dehydrogenase (KGD). This is in

contrast to Dlat, which participates in PDH, PNR/P, and KGD complexes but not BCKADH. Dlat-deficient bacteria were less severely attenuated *in vivo* compared to Lpd-deficient bacteria (Wagner et al., 2011). BCKADH likely prevents toxic buildup of branched chain ketoacids, pyruvate, or branched chain amino acids, but it could also feed into central metabolism by providing carbon from amino acid breakdown. These data show that while *Mtb* may be able to cope with loss of two steps in central carbon metabolic pathways (PDH and KGD) along with PNR/P activity, additional loss of BCKADH activity is difficult for *Mtb* to overcome.

Genetic studies are also informative about roles of particular carbon sources during infection. For example, it is unlikely that *Mtb* uses glycerol as a carbon source during infection, as an *Mtb* inhibitor that was dependent on glycerol for its inhibitory effect was ineffective at inhibiting growth of *Mtb* in the mouse model. This glycerol-induced toxicity was thought to be induced by blockage of the methylglyoxyl bypass leading to the accumulation of methylglyoxal (Pethe et al., 2010). Furthermore, a mutant deficient in *glpK*, which encodes glycerol kinase, the first step of glycerol catabolism, was not attenuated during infection (Pethe et al., 2010).

Conversely, genetic studies support a critical role for cholesterol metabolism during persistent *Mtb* infection of mice and humans. A transposon mutant screen for genes essential for growth on cholesterol identified many genes also shown to be essential within the mouse model (Griffin et al., 2011). A cholesterol ABC-type transporter encoded by the *mce4* gene cluster is required for optimal growth in cholesterol, and deletion of this transporter impaired the ability of *Mtb* to maintain infection in the mouse model (Pandey and Sassetti, 2008). Mutations in the *igr* locus, involved in cholesterol catabolism, prevent *Mtb* growth in cholesterol and render *Mtb* less able to establish infection in the mouse model (Chang et al., 2009). However, deletion of

cholesterol transporter *mce4* in addition to *igr* deletion prevented cholesterol-mediated growth inhibition and enhanced *Mtb* virulence in the mouse compared to *igr* deletion alone. This suggests that blockage of cholesterol catabolism can generate toxic byproducts, and that cholesterol is internalized and metabolized throughout infection.

Together these studies outline a critical role for lipid metabolic pathways, but do not eliminate a role for glycolysis during infection. Furthermore, they exemplify the use of genetic studies to better understand the role for carbon metabolic pathways during infection.

1.4 Thesis mission statement and aims

The goal of the work in this thesis was to evaluate potential drug targets in *Mtb* metabolism and to better understand their roles in *Mtb* pathogenesis. We focused on two key enzymes, fructose bisphosphate aldolase and malate synthase, both of interest as drug targets but lacking genetic studies. Here we describe the generation and characterization of *Mtb* mutants lacking these enzymes, investigate their roles in *Mtb* growth, survival, and pathogenesis, and contribute to our understanding of the importance and function of carbon metabolic pathways in *Mtb*.

REFERENCES

Aldridge, B.B., Fernandez-Suarez, M., Heller, D., Ambravaneswaran, V., Irimia, D., Toner, M., and Fortune, S.M. (2012). Asymmetry and Aging of Mycobacterial Cells Lead to Variable Growth and Antibiotic Susceptibility. Science *335*, 100–104.

Anastasiou, E., and Mitchell, P.D. Palaeopathology and genes: Investigating the genetics of infectious diseases in excavated human skeletal remains and mummies from past populations. Gene.

Baek, S.-H., Li, A.H., and Sassetti, C.M. (2011). Metabolic Regulation of Mycobacterial Growth and Antibiotic Sensitivity. PLoS Biol *9*, e1001065.

Barry, C.E., Boshoff, H., Dartois, V., Dick, T., Ehrt, S., Flynn, J., Schnappinger, D., Wilkinson, R.J., and Young, D. (2009). The spectrum of latent tuberculosis: rethinking the goals of prophylaxis. Nat. Rev. Microbiol. *7*, 845–855.

Baughn, A.D., Garforth, S.J., Vilchèze, C., and Jacobs, W.R., Jr. (2009). An Anaerobic-Type α-Ketoglutarate Ferredoxin Oxidoreductase Completes the Oxidative Tricarboxylic Acid Cycle of Mycobacterium tuberculosis. PLoS Pathog *5*, e1000662.

Beste, D.J.V., Bonde, B., Hawkins, N., Ward, J.L., Beale, M.H., Noack, S., Nöh, K., Kruger, N.J., Ratcliffe, R.G., and McFadden, J. (2011). ^{13}C metabolic flux analysis identifies an unusual route for pyruvate dissimilation in mycobacteria which requires isocitrate lyase and carbon dioxide fixation. PLoS Pathog. *7*, e1002091.

Beste, D.J.V., Nöh, K., Niedenführ, S., Mendum, T.A., Hawkins, N.D., Ward, J.L., Beale, M.H., Wiechert, W., and McFadden, J. (2013). 13C-flux spectral analysis of host-pathogen metabolism reveals a mixed diet for intracellular Mycobacterium tuberculosis. Chem. Biol. *20*, 1012–1021.

Beste, D.J.V., Nöh, K., Niedenführ, S., Mendum, T.A., Hawkins, N.D., Ward, J.L., Beale, M.H., Wiechert, W., and McFadden, J. 13C-Flux Spectral Analysis of Host-Pathogen Metabolism Reveals a Mixed Diet for Intracellular Mycobacterium tuberculosis. Chem. Biol.

Bigger, J. (1944). Treatment of staphylococcal infections with penicillin by intermittent sterilisation. The Lancet *244*, 497–500.

Blumenthal, A., Trujillo, C., Ehrt, S., and Schnappinger, D. (2010). Simultaneous Analysis of Multiple Mycobacterium tuberculosis Knockdown Mutants In Vitro and In Vivo. PLoS ONE *5*.

Bos, K.I., Harkins, K.M., Herbig, A., Coscolla, M., Weber, N., Comas, I., Forrest, S.A., Bryant, J.M., Harris, S.R., Schuenemann, V.J., et al. (2014). Pre-Columbian

mycobacterial genomes reveal seals as a source of New World human tuberculosis. Nature *advance online publication*.

Brock, M., and Buckel, W. (2004). On the mechanism of action of the antifungal agent propionate. Eur. J. Biochem. *271*, 3227–3241.

Cambier, C.J., Takaki, K.K., Larson, R.P., Hernandez, R.E., Tobin, D.M., Urdahl, K.B., Cosma, C.L., and Ramakrishnan, L. (2014). Mycobacteria manipulate macrophage recruitment through coordinated use of membrane lipids. Nature *505*, 218–222.

De Carvalho, L.P.S., Fischer, S.M., Marrero, J., Nathan, C., Ehrt, S., and Rhee, K.Y. (2010a). Metabolomics of Mycobacterium tuberculosis reveals compartmentalized co-catabolism of carbon substrates. Chem. Biol. *17*, 1122–1131.

De Carvalho, L.P.S., Zhao, H., Dickinson, C.E., Arango, N.M., Lima, C.D., Fischer, S.M., Ouerfelli, O., Nathan, C., and Rhee, K.Y. (2010b). Activity-based metabolomic profiling of enzymatic function: Identification of Rv1248c as a mycobacterial 2-hydroxy-3-oxoadipate synthase. Chem. Biol. *17*, 323–332.

Chang, J.C., Miner, M.D., Pandey, A.K., Gill, W.P., Harik, N.S., Sassetti, C.M., and Sherman, D.R. (2009). igr Genes and Mycobacterium tuberculosis Cholesterol Metabolism. J. Bacteriol. *191*, 5232–5239.

Cole, S.T., Brosch, R., Parkhill, J., Garnier, T., Churcher, C., Harris, D., Gordon, S.V., Eiglmeier, K., Gas, S., Barry, C.E., et al. (1998). Deciphering the biology of Mycobacterium tuberculosis from the complete genome sequence. Nature *393*, 537–544.

Comas, I., Coscolla, M., Luo, T., Borrell, S., Holt, K.E., Kato-Maeda, M., Parkhill, J., Malla, B., Berg, S., Thwaites, G., et al. (2013). Out-of-Africa migration and Neolithic coexpansion of Mycobacterium tuberculosis with modern humans. Nat. Genet. *45*, 1176–1182.

Daniel, J., Maamar, H., Deb, C., Sirakova, T.D., and Kolattukudy, P.E. (2011). Mycobacterium tuberculosis Uses Host Triacylglycerol to Accumulate Lipid Droplets and Acquires a Dormancy-Like Phenotype in Lipid-Loaded Macrophages. PLoS Pathog *7*, e1002093.

Danilchanka, O., Sun, J., Pavlenok, M., Maueroder, C., Speer, A., Siroy, A., Marrero, J., Trujillo, C., Mayhew, D.L., Doornbos, K.S., et al. (2014). An outer membrane channel protein of Mycobacterium tuberculosis with exotoxin activity. Proc. Natl. Acad. Sci. U. S. A. *111*, 6750–6755.

Day, T.A., Mittler, J.E., Nixon, M.R., Thompson, C., Miner, M.D., Hickey, M.J., Liao, R.P., Pang, J., Shayakhmetov, D., and Sherman, D.R. (2014). Mycobacterium

tuberculosis strains lacking the surface lipid phthiocerol dimycocerosate are susceptible to killing by an early innate host response. Infect. Immun. IAI.01340–13.

Deb, C., Lee, C.-M., Dubey, V.S., Daniel, J., Abomoelak, B., Sirakova, T.D., Pawar, S., Rogers, L., and Kolattukudy, P.E. (2009). A Novel In Vitro Multiple-Stress Dormancy Model for Mycobacterium tuberculosis Generates a Lipid-Loaded, Drug-Tolerant, Dormant Pathogen. PLoS ONE *4*.

Dubos, R.J., and Dubos, J. (1952). The White Plague: Tuberculosis, Man, and Society (Rutgers University Press).

Edson, N.L. (1951). The intermediary metabolism of the mycobacteria. Bacteriol. Rev. *15*, 147–182.

Ehrt, S., and Rhee, K. (2013). Mycobacterium Tuberculosis Metabolism and Host Interaction: Mysteries and Paradoxes. In Pathogenesis of Mycobacterium Tuberculosis and Its Interaction with the Host Organism, J. Pieters, and J.D. McKinney, eds. (Springer Berlin Heidelberg), pp. 163–188.

Eoh, H., and Rhee, K.Y. (2013). Multifunctional essentiality of succinate metabolism in adaptation to hypoxia in Mycobacterium tuberculosis. Proc. Natl. Acad. Sci. U. S. A. *110*, 6554–6559.

Eoh, H., and Rhee, K.Y. (2014). Methylcitrate cycle defines the bactericidal essentiality of isocitrate lyase for survival of Mycobacterium tuberculosis on fatty acids. Proc. Natl. Acad. Sci. U. S. A. *111*, 4976–4981.

Esmail, H., Barry, C.E., and Wilkinson, R.J. (2012). Understanding latent tuberculosis: the key to improved diagnostic and novel treatment strategies. Drug Discov. Today *17*, 514–521.

Fattorini, L., Piccaro, G., Mustazzolu, A., and Giannoni, F. (2013). Targeting Dormant Bacilli to Fight Tuberculosis. Mediterr. J. Hematol. Infect. Dis. *5*.

Garton, N.J., Christensen, H., Minnikin, D.E., Adegbola, R.A., and Barer, M.R. (2002). Intracellular lipophilic inclusions of mycobacteria in vitro and in sputum. Microbiology *148*, 2951–2958.

Garton, N.J., Waddell, S.J., Sherratt, A.L., Lee, S.-M., Smith, R.J., Senner, C., Hinds, J., Rajakumar, K., Adegbola, R.A., Besra, G.S., et al. (2008). Cytological and Transcript Analyses Reveal Fat and Lazy Persister-Like Bacilli in Tuberculous Sputum. PLoS Med. *5*.

Van der Geize, R., Yam, K., Heuser, T., Wilbrink, M.H., Hara, H., Anderton, M.C., Sim, E., Dijkhuizen, L., Davies, J.E., Mohn, W.W., et al. (2007). A gene cluster encoding cholesterol catabolism in a soil actinomycete provides insight into

Mycobacterium tuberculosis survival in macrophages. Proc. Natl. Acad. Sci. U. S. A. *104*, 1947–1952.

Gengenbacher, M., Rao, S.P.S., Pethe, K., and Dick, T. (2010). Nutrient-starved, non-replicating Mycobacterium tuberculosis requires respiration, ATP synthase and isocitrate lyase for maintenance of ATP homeostasis and viability. Microbiology *156*, 81–87.

Gill, W.P., Harik, N.S., Whiddon, M.R., Liao, R.P., Mittler, J.E., and Sherman, D.R. (2009). A replication clock for Mycobacterium tuberculosis. Nat. Med. *15*, 211–214.

Girgis, H.S., Harris, K., and Tavazoie, S. (2012). Large mutational target size for rapid emergence of bacterial persistence. Proc. Natl. Acad. Sci. U. S. A. *109*, 12740–12745.

Görke, B., and Stülke, J. (2008). Carbon catabolite repression in bacteria: many ways to make the most out of nutrients. Nat. Rev. Microbiol. *6*, 613–624.

Gouzy, A., Larrouy-Maumus, G., Wu, T.-D., Peixoto, A., Levillain, F., Lugo-Villarino, G., Gerquin-Kern, J.-L., de Carvalho, L.P.S., Poquet, Y., and Neyrolles, O. (2013). Mycobacterium tuberculosis nitrogen assimilation and host colonization require aspartate. Nat. Chem. Biol. *9*.

Gouzy, A., Poquet, Y., and Neyrolles, O. (2014). Nitrogen metabolism in Mycobacterium tuberculosis physiology and virulence. Nat. Rev. Microbiol. *advance online publication*.

Griffin, J.E., Gawronski, J.D., DeJesus, M.A., Ioerger, T.R., Akerley, B.J., and Sassetti, C.M. (2011). High-Resolution Phenotypic Profiling Defines Genes Essential for Mycobacterial Growth and Cholesterol Catabolism. PLoS Pathog. *7*.

Griffin, J.E., Pandey, A.K., Gilmore, S.A., Mizrahi, V., Mckinney, J.D., Bertozzi, C.R., and Sassetti, C.M. (2012). Cholesterol Catabolism by Mycobacterium tuberculosis Requires Transcriptional and Metabolic Adaptations. Chem. Biol. *19*, 218–227.

Hasan, M.R., Rahman, M., Jaques, S., Purwantini, E., and Daniels, L. (2010). Glucose 6-Phosphate Accumulation in Mycobacteria Implications for a Novel F420-Dependent Anti-oxidant Defense System. J. Biol. Chem. *285*, 19135–19144.

Hershberg, R., Lipatov, M., Small, P.M., Sheffer, H., Niemann, S., Homolka, S., Roach, J.C., Kremer, K., Petrov, D.A., Feldman, M.W., et al. (2008). High Functional Diversity in Mycobacterium tuberculosis Driven by Genetic Drift and Human Demography. PLoS Biol *6*, e311.

Hershkovitz, I., Donoghue, H.D., Minnikin, D.E., Besra, G.S., Lee, O.Y.-C., Gernaey, A.M., Galili, E., Eshed, V., Greenblatt, C.L., Lemma, E., et al. (2008). Detection and

Molecular Characterization of 9000-Year-Old Mycobacterium tuberculosis from a Neolithic Settlement in the Eastern Mediterranean. PLoS ONE *3*.

Hett, E.C., and Rubin, E.J. (2008). Bacterial Growth and Cell Division: a Mycobacterial Perspective. Microbiol. Mol. Biol. Rev. MMBR *72*, 126–156.

Jackson, M. (2014). The Mycobacterial Cell Envelope—Lipids. Cold Spring Harb. Perspect. Med. a021105.

Kalscheuer, R., Weinrick, B., Veeraraghavan, U., Besra, G.S., and Jacobs, W.R. (2010). Trehalose-recycling ABC transporter LpqY-SugA-SugB-SugC is essential for virulence of Mycobacterium tuberculosis. Proc. Natl. Acad. Sci. U. S. A. *107*, 21761–21766.

Kim, B.H. (2008). Bacterial Physiology and Metabolism (Cambridge New York: Cambridge University Press).

Kim, M.-J., Wainwright, H.C., Locketz, M., Bekker, L.-G., Walther, G.B., Dittrich, C., Visser, A., Wang, W., Hsu, F.-F., Wiehart, U., et al. (2010). Caseation of human tuberculosis granulomas correlates with elevated host lipid metabolism. EMBO Mol. Med. *2*, 258–274.

Klinkenberg, L.G., Lee, J.-H., Bishai, W.R., and Karakousis, P.C. (2010). The stringent response is required for full virulence of Mycobacterium tuberculosis in guinea pigs. J. Infect. Dis. *202*, 1397–1404.

Lee, W., VanderVen, B.C., Fahey, R.J., and Russell, D.G. (2013). Intracellular Mycobacterium tuberculosis Exploits Host-derived Fatty Acids to Limit Metabolic Stress. J. Biol. Chem. *288*, 6788–6800.

Li, R., Gu, J., Chen, P., Zhang, Z., Deng, J., and Zhang, X. (2011). Purification and characterization of the acetyl-CoA synthetase from Mycobacterium tuberculosis. Acta Biochim. Biophys. Sin. *43*, 891–899.

Lienhardt, C., Raviglione, M., Spigelman, M., Hafner, R., Jaramillo, E., Hoelscher, M., Zumla, A., and Gheuens, J. (2012). New Drugs for the Treatment of Tuberculosis: Needs, Challenges, Promise, and Prospects for the Future. J. Infect. Dis. *205*, S241–S249.

Lyon, R.H., Hall, W.H., and Costas-Martinez, C. (1969). Uptake and Distribution of Labeled Carbon from 14C-Asparagine by Mycobacterium tuberculosis. J. Bacteriol. *98*, 317–318.

Marrero, J., Rhee, K.Y., Schnappinger, D., Pethe, K., and Ehrt, S. (2010). Gluconeogenic carbon flow of tricarboxylic acid cycle intermediates is critical for Mycobacterium tuberculosis to establish and maintain infection. Proc. Natl. Acad. Sci. U. S. A. *107*, 9819–9824.

Marrero, J., Trujillo, C., Rhee, K.Y., and Ehrt, S. (2013). Glucose Phosphorylation Is Required for Mycobacterium tuberculosis Persistence in Mice. PLoS Pathog *9*, e1003116.

Masiewicz, P., Brzostek, A., Wolanski, M., Dziadek, J., and Zakrzewska-Czerwinska, J. (2012). A Novel Role of the PrpR as a Transcription Factor Involved in the Regulation of Methylcitrate Pathway in Mycobacterium tuberculosis. PLoS ONE *7*.

Masiewicz, P., Wolanski, M., Brzostek, A., Dziadek, J., and Zakrzewska-Czerwinska, J. (2014). Propionate represses the dnaA gene via the methylcitrate pathway-regulating transcription factor, PrpR, in Mycobacterium tuberculosis. Antonie Van Leeuwenhoek *105*, 951–959.

McCune, R.M., Feldmann, F.M., Lambert, H.P., and McDermott, W. (1966). Microbial Persistence. J. Exp. Med. *123*, 445–468.

McKinney, J.D., zu Bentrup, K.H., Muñoz-Elías, E.J., Miczak, A., Chen, B., Chan, W.-T., Swenson, D., Sacchettini, J.C., Jacobs, W.R., and Russell, D.G. (2000). Persistence of Mycobacterium tuberculosis in macrophages and mice requires the glyoxylate shunt enzyme isocitrate lyase. Nature *406*, 735–738.

Michelucci, A., Cordes, T., Ghelfi, J., Pailot, A., Reiling, N., Goldmann, O., Binz, T., Wegner, A., Tallam, A., Rausell, A., et al. (2013). Immune-responsive gene 1 protein links metabolism to immunity by catalyzing itaconic acid production. Proc. Natl. Acad. Sci. U. S. A. *110*, 7820–7825.

Micklinghoff, J.C., Breitinger, K.J., Schmidt, M., Geffers, R., Eikmanns, B.J., and Bange, F.-C. (2009). Role of the Transcriptional Regulator RamB (Rv0465c) in the Control of the Glyoxylate Cycle in Mycobacterium tuberculosis. J. Bacteriol. *191*, 7260–7269.

Mishra, K.C., de Chastellier, C., Narayana, Y., Bifani, P., Brown, A.K., Besra, G.S., Katoch, V.M., Joshi, B., Balaji, K.N., and Kremer, L. (2008). Functional role of the PE domain and immunogenicity of the Mycobacterium tuberculosis triacylglycerol hydrolase LipY. Infect. Immun. *76*, 127–140.

Mukamolova, G.V., Turapov, O., Malkin, J., Woltmann, G., and Barer, M.R. (2010). Resuscitation-promoting Factors Reveal an Occult Population of Tubercle Bacilli in Sputum. Am. J. Respir. Crit. Care Med. *181*, 174–180.

Müller, B., Borrell, S., Rose, G., and Gagneux, S. (2013). The heterogeneous evolution of multidrug-resistant Mycobacterium tuberculosis. Trends Genet. *29*, 160–169.

Munoz-Elias, E.J., and McKinney, J.D. (2005). M. tuberculosis isocitrate lyases 1 and 2 are jointly required for in vivo growth and virulence. Nat. Med. *11*, 638–644.

Muñoz-Elías, E.J., and McKinney, J.D. (2006). Carbon metabolism of intracellular bacteria. Cell. Microbiol. *8*, 10–22.

Muñoz-Elías, E.J., Upton, A.M., Cherian, J., and McKinney, J.D. (2006). Role of the methylcitrate cycle in Mycobacterium tuberculosis metabolism, intracellular growth, and virulence. Mol. Microbiol. *60*, 1109–1122.

Nambi, S., Gupta, K., Bhattacharyya, M., Ramakrishnan, P., Ravikumar, V., Siddiqui, N., Thomas, A.T., and Visweswariah, S.S. (2013). Cyclic AMP-dependent Protein Lysine Acylation in Mycobacteria Regulates Fatty Acid and Propionate Metabolism. J. Biol. Chem. *288*, 14114–14124.

Nesbitt, N.M., Yang, X., Fontan, P., Kolesnikova, I., Smith, I., Sampson, N.S., and Dubnau, E. (2010). A Thiolase of Mycobacterium tuberculosis Is Required for Virulence and Production of Androstenedione and Androstadienedione from Cholesterol. Infect. Immun. *78*, 275–282.

Niederweis, M. (2008). Nutrient acquisition by mycobacteria. Microbiology *154*, 679–692.

Noy, T., Xu, H., and Blanchard, J.S. (2014). Acetylation of acetyl-CoA synthetase from Mycobacterium tuberculosis leads to specific inactivation of the adenylation reaction. Arch. Biochem. Biophys. *550–551*, 42–49.

Ojha, A.K., Baughn, A.D., Sambandan, D., Hsu, T., Trivelli, X., Guerardel, Y., Alahari, A., Kremer, L., Jacobs, W.R., and Hatfull, G.F. (2008). Growth of Mycobacterium tuberculosis biofilms containing free mycolic acids and harbouring drug-tolerant bacteria. Mol. Microbiol. *69*, 164–174.

Orme, I.M. (2014). A new unifying theory of the pathogenesis of tuberculosis. Tuberculosis *94*, 8–14.

Pandey, A.K., and Sassetti, C.M. (2008). Mycobacterial persistence requires the utilization of host cholesterol. Proc. Natl. Acad. Sci. *105*, 4376–4380.

Payne, D.J., Gwynn, M.N., Holmes, D.J., and Pompliano, D.L. (2007). Drugs for bad bugs: confronting the challenges of antibacterial discovery. Nat. Rev. Drug Discov. *6*, 29–40.

Pethe, K., Sequeira, P.C., Agarwalla, S., Rhee, K., Kuhen, K., Phong, W.Y., Patel, V., Beer, D., Walker, J.R., Duraiswamy, J., et al. (2010). A chemical genetic screen in Mycobacterium tuberculosis identifies carbon-source-dependent growth inhibitors devoid of in vivo efficacy. Nat. Commun. *1*, 1–8.

Peyron, P., Vaubourgeix, J., Poquet, Y., Levillain, F., Botanch, C., Bardou, F., Daffé, M., Emile, J.-F., Marchou, B., Cardona, P.-J., et al. (2008). Foamy Macrophages from

Tuberculous Patients' Granulomas Constitute a Nutrient-Rich Reservoir for M. tuberculosis Persistence. PLoS Pathog *4*, e1000204.

Phong, W.Y., Lin, W., Rao, S.P.S., Dick, T., Alonso, S., and Pethe, K. (2013). Characterization of Phosphofructokinase Activity in Mycobacterium tuberculosis Reveals That a Functional Glycolytic Carbon Flow Is Necessary to Limit the Accumulation of Toxic Metabolic Intermediates under Hypoxia. PLoS ONE *8*, e56037.

Primm, T.P., Andersen, S.J., Mizrahi, V., Avarbock, D., Rubin, H., and Barry, C.E. (2000). The Stringent Response of Mycobacterium tuberculosis Is Required for Long-Term Survival. J. Bacteriol. *182*, 4889–4898.

Rhee, K.Y., de Carvalho, L.P.S., Bryk, R., Ehrt, S., Marrero, J., Park, S.W., Schnappinger, D., Venugopal, A., and Nathan, C. (2011). Central carbon metabolism in Mycobacterium tuberculosis: an unexpected frontier. Trends Microbiol. *19*, 307–314.

Rodriguez, J.G., Hernandez, A.C., Helguera-Repetto, C., Aguilar Ayala, D., Guadarrama-Medina, R., Anzola, J.M., Bustos, J.R., Zambrano, M.M., Gonzalez-y-Merchand, J., Garcia, M.J., et al. (2014). Global Adaptation to a Lipid Environment Triggers the Dormancy-Related Phenotype of Mycobacterium tuberculosis. mBio *5*.

Rohde, K.H., Veiga, D.F.T., Caldwell, S., Balazsi, G., and Russell, D.G. (2012). Linking the Transcriptional Profiles and the Physiological States of Mycobacterium tuberculosis during an Extended Intracellular Infection. PLoS Pathog. *8*.

Russell, D.G. (2013). The evolutionary pressures that have molded Mycobacterium tuberculosis into an infectious adjuvant. Curr. Opin. Microbiol. *16*, 78–84.

Russell, D.G., Cardona, P.-J., Kim, M.-J., Allain, S., and Altare, F. (2009). Foamy macrophages and the progression of the human TB granuloma. Nat. Immunol. *10*, 943–948.

Russell, D.G., VanderVen, B.C., Lee, W., Abramovitch, R.B., Kim, M., Homolka, S., Niemann, S., and Rohde, K.H. (2010). Mycobacterium tuberculosis wears what it eats. Cell Host Microbe *8*, 68–76.

Sani, M., Houben, E.N.G., Geurtsen, J., Pierson, J., de Punder, K., van Zon, M., Wever, B., Piersma, S.R., Jiménez, C.R., Daffé, M., et al. (2010). Direct Visualization by Cryo-EM of the Mycobacterial Capsular Layer: A Labile Structure Containing ESX-1-Secreted Proteins. PLoS Pathog *6*, e1000794.

Sassetti, C.M., Boyd, D.H., and Rubin, E.J. (2003). Genes required for mycobacterial growth defined by high density mutagenesis. Mol. Microbiol. *48*, 77–84.

Schnappinger, D., Ehrt, S., Voskuil, M.I., Liu, Y., Mangan, J.A., Monahan, I.M., Dolganov, G., Efron, B., Butcher, P.D., Nathan, C., et al. (2003). Transcriptional

Adaptation of Mycobacterium tuberculosis within Macrophages Insights into the Phagosomal Environment. J. Exp. Med. *198*, 693–704.

Schubert, O.T., Mouritsen, J., Ludwig, C., Rost, H.L., Rosenberger, G., Arthur, P.K., Claassen, M., Campbell, D.S., Sun, Z., Farrah, T., et al. (2013). The Mtb Proteome Library: A Resource of Assays to Quantify the Complete Proteome of Mycobacterium tuberculosis. Cell Host Microbe *13*, 602–612.

Segal, W., and Bloch, H. (1956). Biochemical differentiation of Mycobacterium tuberculosis grown in vivo and in vitro. J. Bacteriol. *72*, 132–141.

Shi, L., Sohaskey, C.D., Pfeiffer, C., Datta, P., Parks, M., McFadden, J., North, R.J., and Gennaro, M.L. (2010). Carbon flux rerouting during Mycobacterium tuberculosis growth arrest. Mol. Microbiol. *78*, 1199–1215.

Singh, A., Crossman, D.K., Mai, D., Guidry, L., Voskuil, M.I., Renfrow, M.B., and Steyn, A.J.C. (2009). Mycobacterium tuberculosis WhiB3 Maintains Redox Homeostasis by Regulating Virulence Lipid Anabolism to Modulate Macrophage Response. PLoS Pathog *5*, e1000545.

Sirakova, T.D., Dubey, V.S., Deb, C., Daniel, J., Korotkova, T.A., Abomoelak, B., and Kolattukudy, P.E. (2006). Identification of a diacylglycerol acyltransferase gene involved in accumulation of triacylglycerol in Mycobacterium tuberculosis under stress. Microbiol. Read. Engl. *152*, 2717–2725.

Slayden, R.A., Jackson, M., Zucker, J., Ramirez, M.V., Dawson, C.C., Crew, R., Sampson, N.S., Thomas, S.T., Jamshidi, N., Sisk, P., et al. (2013). Updating and curating metabolic pathways of TB. Tuberculosis *93*, 47–59.

Smet, K.A.L.D., Weston, A., Brown, I.N., Young, D.B., and Robertson, B.D. (2000). Three pathways for trehalose biosynthesis in mycobacteria. Microbiology *146*, 199–208.

Somashekar, B.S., Amin, A.G., Rithner, C.D., Troudt, J., Basaraba, R., Izzo, A., Crick, D.C., and Chatterjee, D. (2011). Metabolic profiling of lung granuloma in Mycobacterium tuberculosis infected guinea pigs: ex vivo 1H magic angle spinning NMR studies. J. Proteome Res. *10*, 4186–4195.

Stallings, C.L., and Glickman, M.S. (2010). Is Mycobacterium tuberculosis stressed out? A critical assessment of the genetic evidence. Microbes Infect. Inst. Pasteur *12*, 1091–1101.

Tian, J., Bryk, R., Itoh, M., Suematsu, M., and Nathan, C. (2005). Variant tricarboxylic acid cycle in Mycobacterium tuberculosis: identification of alpha-ketoglutarate decarboxylase. Proc. Natl. Acad. Sci. U. S. A. *102*, 10670–10675.

Titgemeyer, F., Amon, J., Parche, S., Mahfoud, M., Bail, J., Schlicht, M., Rehm, N., Hillmann, D., Stephan, J., Walter, B., et al. (2007). A Genomic View of Sugar Transport in Mycobacterium smegmatis and Mycobacterium tuberculosis. J. Bacteriol. *189*, 5903–5915.

Trujillo, C., Blumenthal, A., Marrero, J., Rhee, K.Y., Schnappinger, D., and Ehrt, S. (2014). Triosephosphate Isomerase Is Dispensable In Vitro yet Essential for Mycobacterium tuberculosis To Establish Infection. mBio *5*.

Tufariello, J.M., Chan, J., and Flynn, J.L. (2003). Latent tuberculosis: mechanisms of host and bacillus that contribute to persistent infection. Lancet Infect. Dis. *3*, 578–590.

Vandal, O.H., Roberts, J.A., Odaira, T., Schnappinger, D., Nathan, C.F., and Ehrt, S. (2009). Acid-Susceptible Mutants of Mycobacterium tuberculosis Share Hypersusceptibility to Cell Wall and Oxidative Stress and to the Host Environment. J. Bacteriol. *191*, 625–631.

Ventura, M., Rieck, B., Boldrin, F., Degiacomi, G., Bellinzoni, M., Barilone, N., Alzaidi, F., Alzari, P.M., Manganelli, R., and O'Hare, H.M. (2013). GarA is an essential regulator of metabolism in Mycobacterium tuberculosis. Mol. Microbiol. *90*, 356–366.

Venugopal, A., Bryk, R., Shi, S., Rhee, K., Rath, P., Schnappinger, D., Ehrt, S., and Nathan, C. (2011). Virulence of Mycobacterium tuberculosis depends on lipoamide dehydrogenase, a member of three multi-enzyme complexes. Cell Host Microbe *9*, 21–31.

Wagner, T., Bellinzoni, M., Wehenkel, A., O'Hare, H.M., and Alzari, P.M. (2011). Functional Plasticity and Allosteric Regulation of α-Ketoglutarate Decarboxylase in Central Mycobacterial Metabolism. Chem. Biol. *18*, 1011–1020.

Wakamoto, Y., Dhar, N., Chait, R., Schneider, K., Signorino-Gelo, F., Leibler, S., and McKinney, J.D. (2013). Dynamic Persistence of Antibiotic-Stressed Mycobacteria. Science *339*, 91–95.

World Health Organization. (2012). Global tuberculosis report 2012. Retrieved from http://apps.who.int/iris/bitstream/10665/75938/1/9789241564502_eng.pdf

Van der Wel, N., Hava, D., Houben, D., Fluitsma, D., van Zon, M., Pierson, J., Brenner, M., and Peters, P.J. (2007). M. tuberculosis and M. leprae Translocate from the Phagolysosome to the Cytosol in Myeloid Cells. Cell *129*, 1287–1298.

Wipperman, M.F., Sampson, N.S., and Thomas, S.T. (2014). Pathogen roid rage: Cholesterol utilization by Mycobacterium tuberculosis. Crit. Rev. Biochem. Mol. Biol. *49*, 269–293.

Zhang, Y., Yew, W.W., and Barer, M.R. (2012a). Targeting Persisters for Tuberculosis Control. Antimicrob. Agents Chemother. *56*, 2223–2230.

Zhang, Y.J., Ioerger, T.R., Huttenhower, C., Long, J.E., Sassetti, C.M., Sacchettini, J.C., and Rubin, E.J. (2012b). Global Assessment of Genomic Regions Required for Growth in Mycobacterium tuberculosis. PLoS Pathog. *8*.

Zumla, A., Nahid, P., and Cole, S.T. (2013). Advances in the development of new tuberculosis drugs and treatment regimens. Nat. Rev. Drug Discov. *12*, 388–404.

CHAPTER 2

THE ROLE OF FRUCTOSE 1,6-BISPHOSPHATE ALDOLASE IN PATHOGENICITY OF *MYCOBACTERIUM TUBERCULOSIS**

2.1 Introduction

Identification of enzymes essential for pathogenicity and persistence of *Mycobacterium tuberculosis* (*Mtb*) is critical for guiding the development of novel anti-tuberculosis drugs. Enzymes that are mechanistically or structurally different than their human counterparts are attractive as drug targets. We thought the carbon metabolic enzyme fructose 1,6-bisphosphate aldolase (FBA) could match these criteria. However, the importance of FBA during infection of an animal model had not been demonstrated. To investigate this, we generated an FBA conditional knockdown mutant to silence FBA during a mouse model of infection. We also characterized growth of this knockdown strain upon FBA silencing, enabling us to identify the conditions that we used to generate a strain lacking FBA. These knockdown and knockout strains allowed us to assess FBA as a drug target as well as to contribute to understanding of FBA's essentiality within the host and in specific carbon source conditions.

---

*Puckett, S., Trujillo, C., Eoh, H., Marrero, J., Spencer, J., Jackson, M., Schnappinger, D., Rhee, K., Ehrt, S. (2014). Inactivation of fructose-1,6-bisphosphate aldolase prevents optimal co-catabolism of glycolytic and gluconeogenic carbon substrates in *Mycobacterium tuberculosis*. PloS Pathog 10(5): e1004144.

2.2 Background

Fructose 1,6-bisphosphate aldolase (FBA) is a metabolic enzyme central to glycolysis and gluconeogenesis. It catalyzes the reversible conversion of fructose-1,6-bisphosphate to dihydroxyacetone-phosphate (DHAP) and glyceraldehyde 3-phosphate (G3P). This step is critical for enabling the carbon from fructose 1,6-bisphosphate to participate in an ATP-generating downstream reaction catalyzed by glyceraldehyde-3-phosphate dehydrogenase. Furthermore, this reaction prevents a potentially toxic buildup of sugar phosphates. In the reverse direction, FBA is critical for the generation of bacterial cell wall precursor fructose 6-phosphate, as well as for the generation of glucose 6-phosphate, a precursor for nucleic acid synthesis.

FBAs are found in all domains of life on earth, and FBA disruptions or inhibitions have been shown to be problematic for a variety of organisms. In *E. coli*, nickel toxicity is caused by FBA inhibition (Macomber et al., 2011). Depletion of FBA in *Candida albicans* is growth inhibitory (Rodaki et al., 2006). Mutations in human ALDOA are associated with hemolytic anemia (Kishi et al., 1987) and ALDOA is a potential marker for human squamous cell carcinoma (Du et al., 2014). This presence of FBA in humans as well as pathogens highlights the importance of designing pathogen-specific FBA inhibitors. Fortunately, this may be possible due to differences in the reaction mechanism.

FBAs are grouped into two classes based on their reaction mechanism. Class I FBAs form a Schiff base intermediate, whereas Class II FBAs lack this intermediate and instead rely on a divalent metal cation (such as Zn^{2+}) to stabilize a hydroxyenolate intermediate (Pegan et al., 2013). Plants and animals, including humans, express class I FBAs, whereas prokaryotes can express either or both Class I and Class II FBAs. It was earlier hypothesized that Class II FBAs are evolutionarily primitive because they

do not exist in humans and higher mammals, but the subsequent discovery of Class I FBAs in prokaryotes suggested otherwise (Marsh and Lebherz, 1992). It is possible that organisms lacking one of the classes have eliminated the other due to functional redundancy. However, in *E. coli*, there are both classes but only Class II is essential (Pegan et al., 2009).

In *Mtb*, there is only one annotated FBA, a Class II enzyme encoded by the gene *fba* (*rv0363c*) (Figure 2.1). Early enzymatic assays detected both Class I and Class II activity in *Mtb* lysates, which can be differentiated by the use of a metal chelator to inactivate the metal-dependent Class II activity (Bai et al., 1974). Class I activity was detected primarily in high oxygen conditions. However, in a recent study Class I activity was not detectable in any condition tested, which included cells in log or stationary phase of growth, cells in low or high oxygen conditions, and cells in media containing acetate alone vs. ADNaCl, a growth supplement containing glucose (de la Paz Santangelo et al., 2011). Interestingly, Class II FBA activity was present but did not vary widely between any of these conditions, although FBA protein was found to be upregulated in culture filtrates in hypoxic conditions (Rosenkrands et al., 2002). Furthermore, the *Mtb* Class II enzyme is expressed during guinea pig and IFNγ knockout mice infection, suggesting it has a physiologically relevant role in pathogenesis (de la Paz Santangelo et al., 2011).

Is *fba* essential in *Mtb*? There is conflicting data between recent transposon mutagenesis studies, where *fba* was predicted essential (unable to tolerate insertions) for *Mtb* growth in minimal medium but not in rich medium (Griffin et al., 2011; Zhang et al., 2012). However, attempts to make the direct knockout have failed (Pegan et al., 2009). As shown using a conditional *fba* knockdown strain, growth of a non-pathogenic H37Ra strain in single carbon sources depends on *fba*

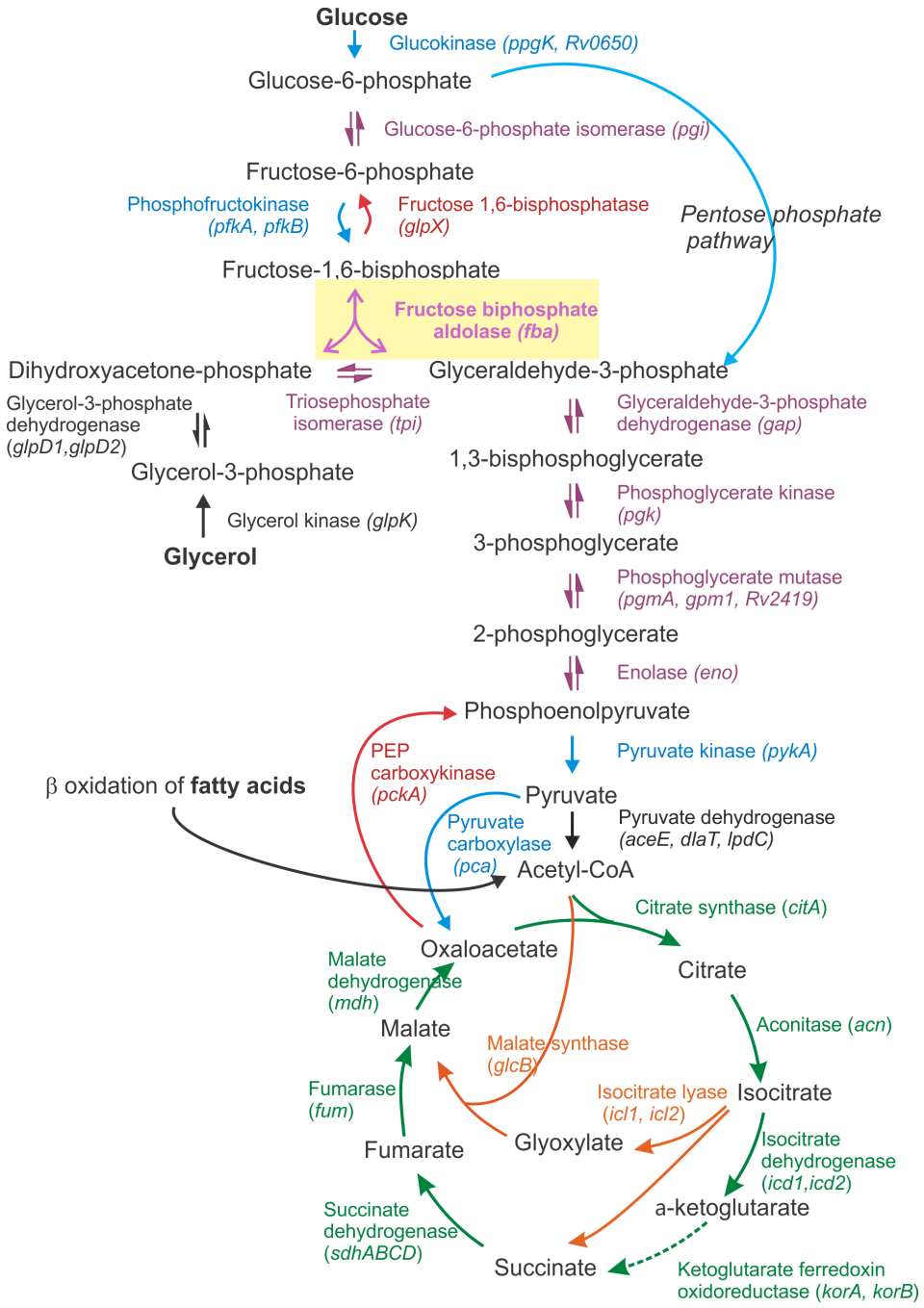

Figure 2.1. Schematic of glycolysis, gluconeogenesis, and the tricarboxylic acid (TCA) cycle in *Mtb*. Enzymes and their corresponding genes are color coded to reflect their dedicated pathways: glycolysis and pentose phosphate pathway (blue), gluconeogenesis (red), glycolysis and gluconeogenesis (purple), TCA cycle (green), and glyoxylate shunt (orange).

(de la Paz Santangelo et al., 2011). Studies like these have led to the conclusion in the literature that *Mtb* FBA is essential (Labbé et al., 2012). However, essentiality in an animal model has not been demonstrated.

Outside of its role in carbon metabolism, FBA has been shown to be secreted and may play a role in host interaction. In *Neisseria meningitidis*, FBA was shown to localize to the cytoplasm and the outer membrane and plays a role in host cell adhesion (Tunio et al., 2010). *Toxoplasma* aldolase may play a role in parasite motility and invasion, although its primary function is metabolic (Shen and Sibley, 2014). A "moon-lighting" function of FBA may also exist in *Mtb*, as FBA can bind to human plasminogen, but the importance of this function in pathogenesis is yet to be elucidated (de la Paz Santangelo et al., 2011).

FBAs, including the *Mtb* FBA, have been the focus of structural, enzymatic and drug developmental studies. The structure of the *Mtb* FBA has been solved, and FBA (344 amino acids long, 36.5 kDa as a monomer) is thought to form a tetrameric complex or "dimer of dimers" with a known tetramerization region that extends away from the rest of the protein. The importance of specific active site residues was examined and recombinant FBA with a mutation in the active site (E169A) had substantially reduced FBA activity (Pegan et al., 2013). The availability of in-depth structural knowledge has contributed to the development of Class II FBA-specific inhibitors, including substrate analogs, metal chelators and a non-competitive inhibitor (Capodagli et al., 2014; Daher et al., 2010; Fonvielle et al., 2008; Labbé et al., 2012). The FBA protein is 100% conserved across all sequenced strains of *Mtb*, including drug-resistant strains, meaning that an inhibitor effective against one *Mtb* FBA structure should be effective against others (Capodagli et al., 2014). However, only one inhibitor yet has shown to

inhibit live *Mtb in vitro* at a concentration of 0.6-1.2 mM (Capodagli et al., 2014), and none have been used in an animal model.

We aimed to assess FBA as a drug target and to understand its *in vitro* essentiality by generation and use of a conditional knockdown *fba Mtb* strain. This genetic tool allowed us to demonstrate a role for FBA in pathogenesis of *Mtb* in the mouse model but also revealed that *fba* essentiality is carbon source-dependent. Subsequent generation and characterization of an *fba* knockout strain highlighted a role for FBA in *Mtb* survival in single carbon sources, and also for co-catabolism of carbon substrates.

2.3 Results

2.3.1 FBA is required for growth in glycolytic and gluconeogenic carbon sources and for growth and persistence in mice

To investigate the role of FBA *in vitro* and *in vivo* we generated an *Mtb* strain in which expression of FBA is regulated by the recently described DUC switch (Kim et al., 2013), so that anhydrotetracycline (atc) or doxycycline (doxy) trigger transcriptional repression of the *fba* gene and simultaneous degradation of the FBA protein, as recently described. We first introduced a second copy of *fba* with a strong promoter (P_{smyc}-*fba*) via an integrative plasmid into the *Mtb* chromosome and then deleted the native copy (Ehrt et al., 2005). After confirming *fba* deletion by Southern blot (Figure 2.2A-B), we generated FBA-DUC by replacing P_{smyc}-*fba* with a DAS+4-tagged *fba* gene, whose transcription was controlled by a TetR-regulated promoter. The DAS+4-tag allowed for proteolytic inactivation of FBA. Immunoblot analysis confirmed FBA depletion upon addition of atc (Figure 2.3). Similar to previous findings with an H37Ra FBA-TetON mutant (de la Paz Santangelo et al., 2011), growth of H37Rv FBA-DUC with single carbon sources was inhibited when FBA was depleted by the addition of atc (Figure 2.4A-C). Unexpectedly, however, growth of

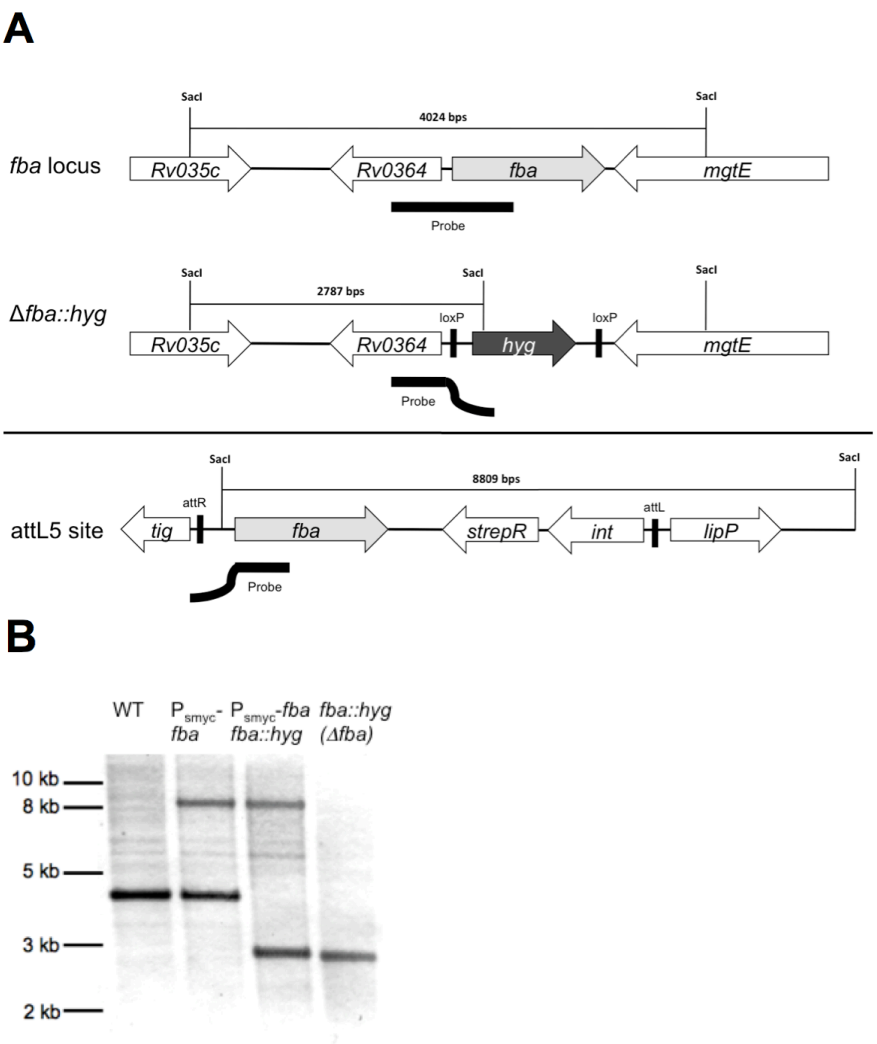

Figure 2.2. Confirmation of *fba* deletion in *fba* mutant strains. (**A**) Genomic organization and Southern blot design with (1) native *fba* locus before and after replacement with a hygromycin resistance cassette and (2) attL5 phage integration site after integration of the plasmid containing *fba* transcribed by a strong promoter (P_{smyc}-*fba*). A 1 kb probe spanning Rv0364 and *fba* detects SacI-digested DNA fragments either containing the *fba* locus or *fba* elsewhere in the genome (see supplemental for sequence). (**B**). Southern blot showing the expected band patterns for wild type (WT) and *fba* mutants. WT, with a 4024 kb band indicative of an intact native *fba* locus, was transformed with P_{smyc}-*fba,* resulting in a 8809 bp band indicative of P_{smyc}-*fba* integration at the attL5 site. Then we deleted native *fba* in this merodiploid strain by replacing it with a hygromycin resistance cassette. This mutant strain expresses *fba* at the attL5 site but not in the native locus and we observed the new expected band pattern of 2787 bps. The knockout was generated by replacement transformation, in which we selected for loss of P_{smyc}-*fba* (streptomycin sensitivity) and gain of a new plasmid (kanamycin resistance) not containing *fba*. Southern blot confirmed loss of the band indicative of *fba* at the attL5 site revealing only one band of 2787 bps. This knockout strain is referred to as *Δfba*.

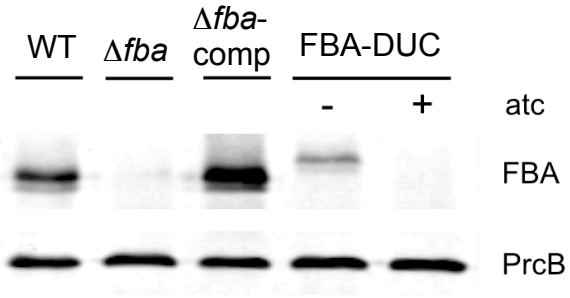

Figure 2.3. FBA expression in WT and mutants. FBA (36.5 kDa) immunoblot in protein extracts from the indicated strains grown in 7H9 media with glucose and glycerol as carbon sources. In FBA-DUC the DAS+4 tag increases FBA's molecular weight by 1.6 kDa. Anhydrotetracycline (atc) was added at 500 ng/ml. FBA antiserum was applied for one hour at a 1:3500 dilution. PrcB (30.3 kDa) served as loading control.

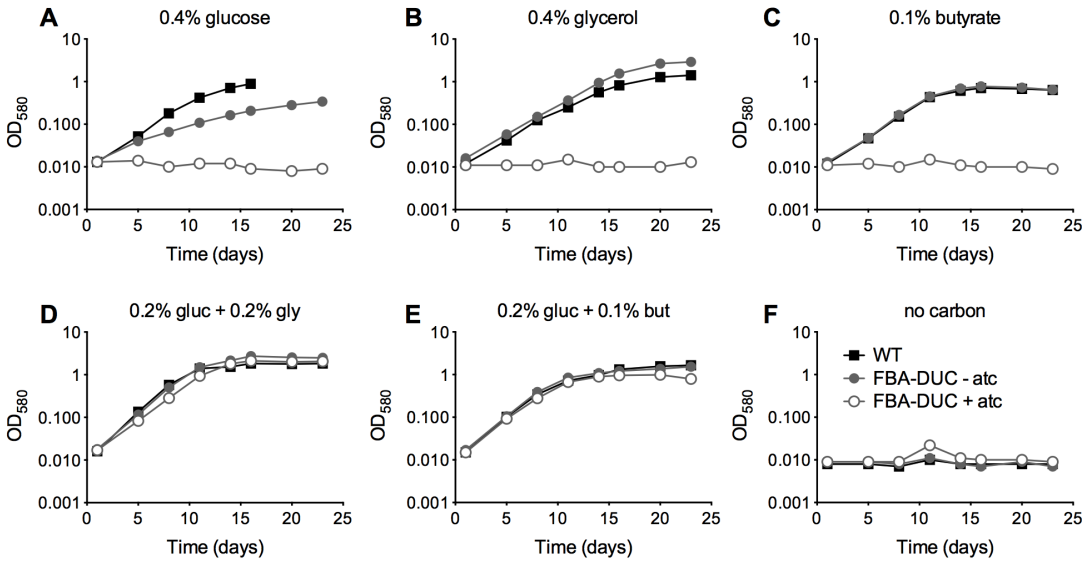

Figure 2.4. FBA depletion inhibits growth of *Mtb* in single carbon sources, but not in the presence of both a glycolytic and a gluconeogenic carbon source. Growth of WT (black squares) and FBA-DUC in the absence (grey circles) and presence (open circles) of 500 ng/ml atc in carbon defined media containing (**A**) 0.4% glucose (**B**) 0.4% glycerol (**C**) 0.1% butyrate (**D**) 0.2% glucose and 0.2% glycerol (**E**) 0.2% glucose and 0.1% butyrate or (**F**) no carbon.. Bacteria were cultured in 25 cm^2 flasks. Data are representative of at least two independent experiments.

FBA-DUC was unaffected by atc in media containing glucose and a second carbon source, such as butyrate, or glycerol (Figure 2.4D-E).

To assess if FBA is required *in vivo*, we infected mice with WT and FBA-DUC and monitored growth and survival in lungs and spleens (Figure 2.5). Mice infected with FBA-DUC were fed doxy-containing chow starting at the day of infection, on day 10, and on day 35 post-infection to determine whether FBA is required for growth and persistence of *Mtb*. FBA-DUC failed to replicate in lungs of mice fed with doxy starting on the day of infection and was undetectable by CFU determinations at day 10 post-infection (Figure 2.5A). No pathological signs of infection were observed in lungs of these mice (not shown) and no CFU were detectable in their spleens. When doxy administration was started later, CFU declined rapidly in lungs and spleens of both acutely and chronically infected mice. Decreases in CFU were accompanied by decreases in lung pathology (Figure 2.5B). In mice that did not receive doxy, FBA-DUC replicated and persisted similar to WT. Together these data establish that *Mtb* requires FBA activity for growth during acute and persistence during chronic mouse infections.

2.3.2 FBA essentiality is carbon source-dependent

Growth of FBA-DUC with atc in dual carbon source media (Figure 2.4) suggested that FBA may not be essential in all conditions and that its essentiality may be carbon source-dependent. Therefore, we next attempted to delete *fba* by replacing the integrative, plasmid containing P_{smyc}-*fba* with a plasmid that did not contain *fba*. Δ*fba* candidates grew readily on agar plates containing a carbon source combination - glucose and glycerol - that permitted growth of FBA-DUC with atc (Figure 2.6). No Δ*fba* candidates were obtained on standard *Mtb* agar plates with glycerol and Middlebrook OADC, a supplement containing oleic acid and glucose as carbon

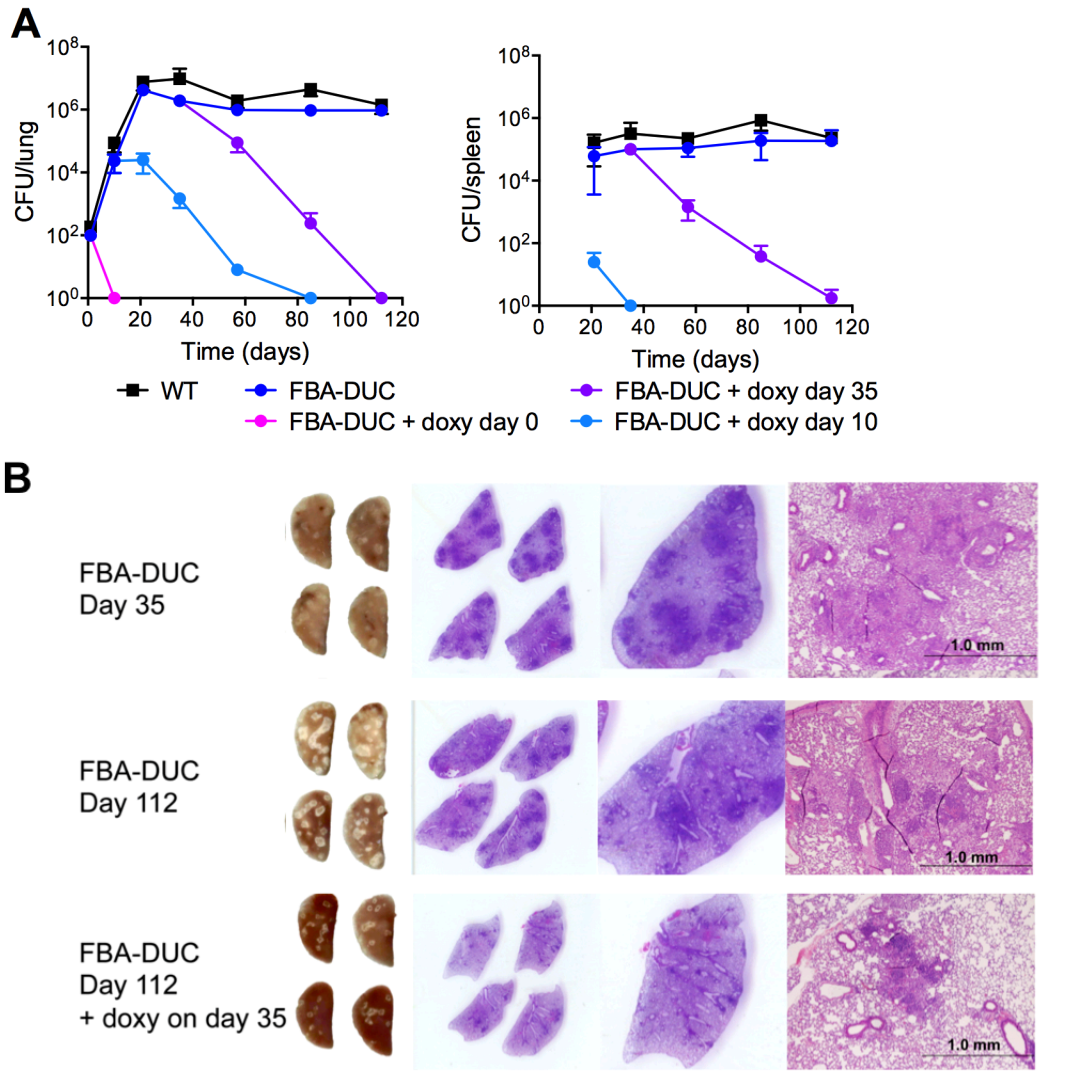

Figure 2.5. FBA is required for replication and persistence of *Mtb* in mice. (**A**) Growth and survival of WT (squares) and FBA-DUC (circles) in mouse lungs (left panel) and spleens (right panel). Mice infected with FBA-DUC received doxy-containing food from the day of infection (day 0), day 10, day 35 or not at all as indicated. CFU were not detected in spleens from mice infected with FBA-DUC and treated with doxy starting day 0. The limit of detection was 4 CFU in lungs and spleens. Data are means ± SD of four mice, except for three data points which derive from 3 and 2 mice due to the appearance of atc/doxy doxy resistant revertants in the lungs (day 57 FBA-DUC + doxy day 10, day 85 FBA-DUC + doxy day 10 and day 112 FBA-DUC + doxy day 35). (**B**) Gross pathology and H&E staining of lung sections from mice infected with FBA-DUC. Lungs were isolated at day 35 (upper panel) and day 112 (middle and lower panel) from mice not treated and administered doxy starting day 35 post infection. A second short course infection experiment reproduced the phenotype of FBA-DUC in mice not treated or treated with doxy starting on the day of infection.

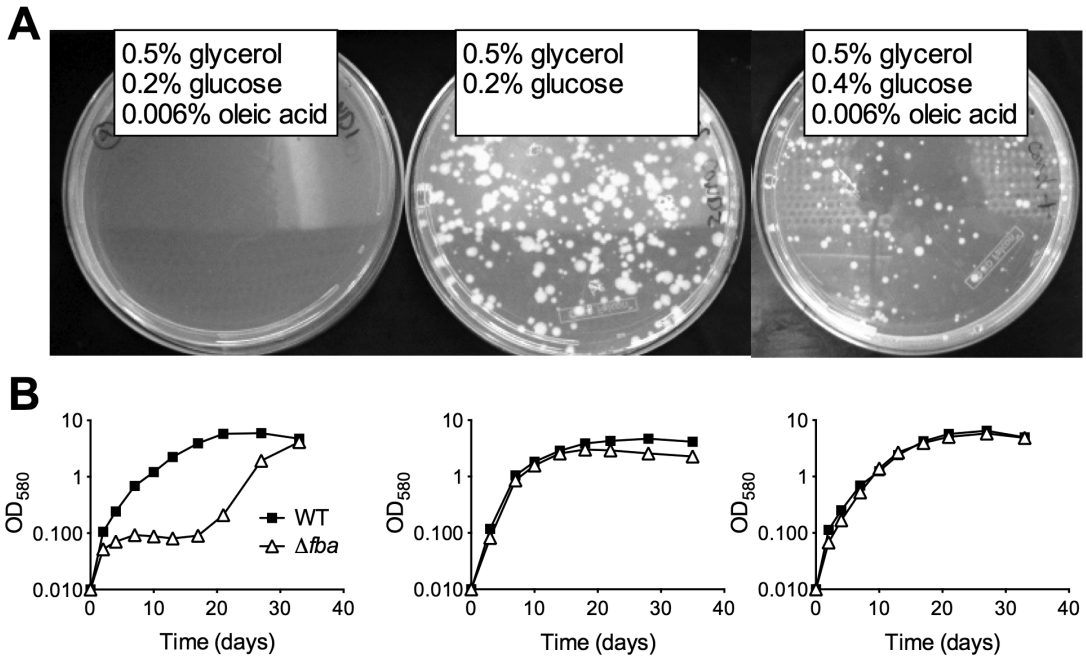

Figure 2.6. FBA essentiality is carbon source dependent. (**A**) Growth of replacement transformants of *Mtb* P_{smyc}-*fba*-*fba*::hyg with a plasmid not containing *fba* and thus resulting in Δ*fba* on agar plates containing the indicated carbon sources. (**B**) Growth of Δ*fba* in 7H9 base liquid media with identical carbon sources as in the above plate conditions.

sources. However, doubling the glucose concentration resulted in growth of colonies albeit with slower growth rate than in the absence of oleic acid (Figure 2.6A).

Southern blot and immunoblot confirmed that the Δ*fba* candidates were true knockout strains (Figure 2.2, 2.3). As observed on agar plates, growth of Δ*fba* in liquid culture was carbon source-dependent, although Δ*fba* replicated in oleic acid-containing medium following a twenty-day lag phase (Figure 2.6B). This delayed growth was not from complete *fba* suppressor mutants because these bacteria were not capable of growth with a single carbon source (Figure 2.7). Whole genome sequencing of an OADC-resistant Δ*fba* strain revealed two mutations compared to parent Δ*fba* strain: an amino acid substitution in probable heat shock protein transcriptional repressor *hrcA* (A123V) and a stop mutation in a probable membrane anchor for succinate dehydrogenase *rv0249c* (W31*). The latter caught our interest due to its role in the TCA cycle. *Mtb* encodes at least two putative succinate dehydrogenase operons, *sdhABCD* (*rv3316-rv3319*) and *rv0249c-rv0247c*. Therefore, truncation of *rv0249c* could lead to slow down, but potentially not complete blockage, of the TCA cycle. Alternatively, succinate may also buildup to a greater extent in the event of reduced succinate dehydrogenase activity. Future work involving metabolomics analysis of labeled carbon substrates could address these possibilities and examine how these changes allow for growth.

These experiments demonstrated that essentiality of FBA is conditional and suggested that *Mtb* lacking FBA (Δ*fba*) has specific carbon source requirements. Similar to the effects of conditional FBA-depletion, complete inactivation of FBA by deletion of *fba* caused a failure to replicate with a single carbon source but did not significantly affect growth with two carbon sources that enter central carbon metabolism above and below the FBA catalyzed step (Figure 2.8A). Growth of the complemented strain (Δ*fba*-

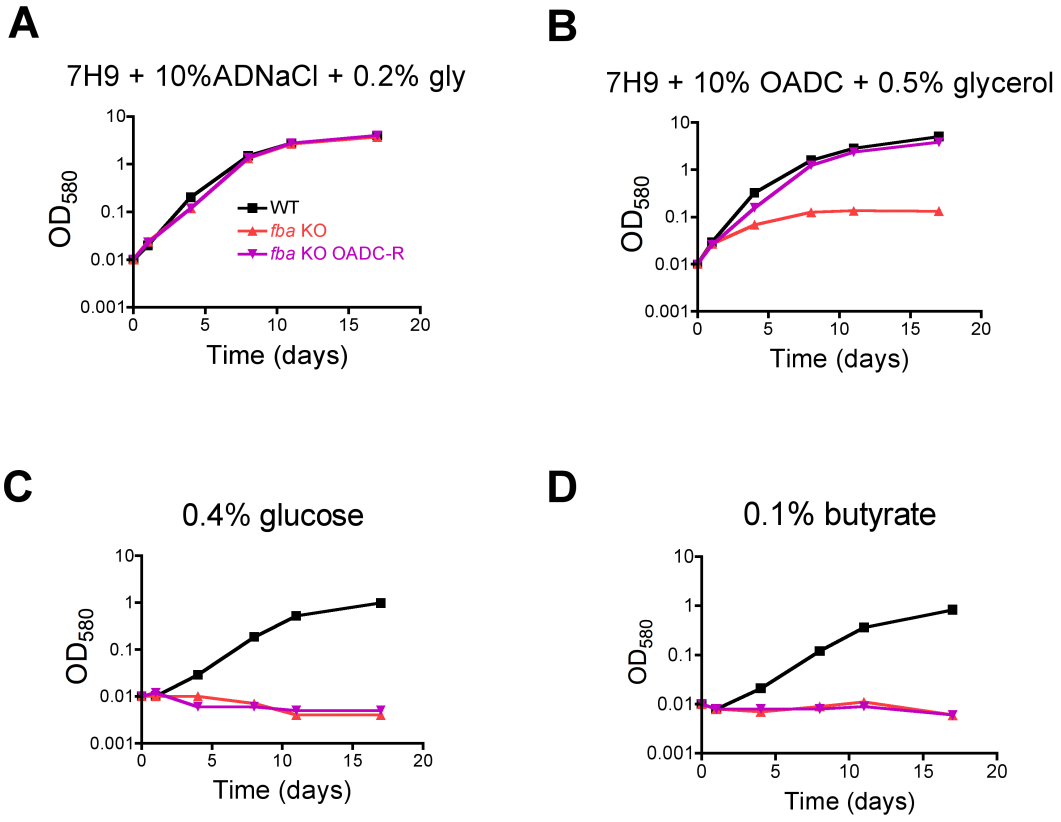

Figure 2.7. OADC-resistant *fba* KO strain does not grow in single carbon sources. Growth of the WT, Δ*fba*, and Δ*fba* OADC-resistant strains were grown in (**A**) 7H9 base media with 10% ADNaCl (made with fatty acid-free BSA) plus 0.2% glycerol, (**B**) 7H9 base media with 10% OADC (for a final of 0.006% oleic acid) and 0.5% glycerol, (**C**) carbon-defined minimal media with 0.4% glucose, or (**D**) carbon-defined minimal media with 0.1% butyrate.

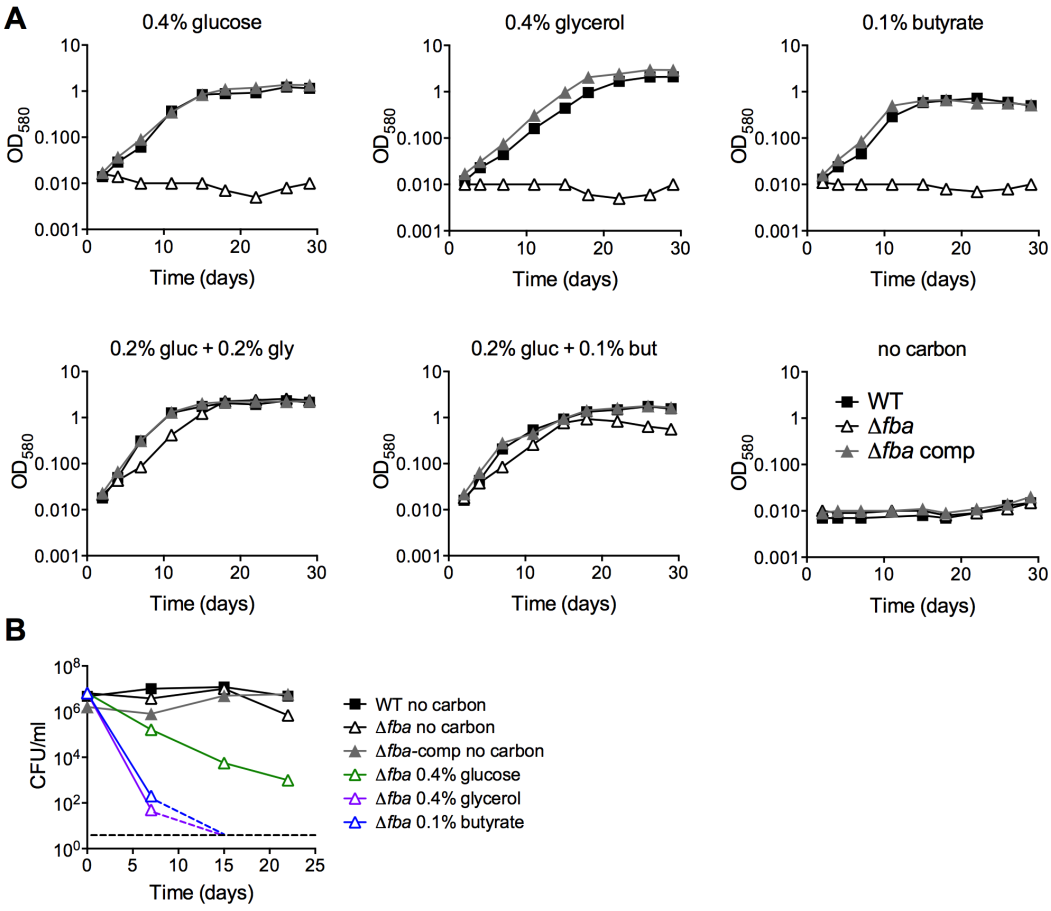

Figure 2.8. FBA is required for growth and survival in single carbon sources. (A) Growth measured by absorbance of WT (black squares), Δ*fba* (open triangles) and Δ*fba*-comp (grey triangles) in carbon-defined media containing glucose, glycerol and butyrate at the indicated concentrations. Bacteria were cultured in 25 cm^2 flasks. **(B)** Survival measured by culturing for CFU on growth-permissive agar plates of the indicated *Mtb* strains in media with single carbon sources and no carbon addition at different time points post-inoculation. Stippled lines indicate that next data point was below the limit of detection.

comp) was similar to that of WT in all conditions tested, demonstrating that the observed growth phenotypes were caused by the lack of FBA. CFU analysis of Δ*fba* in single carbon sources revealed that Δ*fba* died rapidly, with a 5 log decrease in CFU in 7 days and no detectable CFU by day 14 in media containing glycerol, butyrate, or acetate as sole carbon sources (Figure 2.8B, data not shown for acetate). Death in glucose-containing medium was slower, but also substantial. In contrast, Δ*fba* survived with only a 10-fold decrease in CFU in base media without added carbon. Thus, the presence of a single carbon source resulted in killing of Δ*fba* and the kinetics of death were dependent on the specific carbon source suggesting that the mechanism leading to death of Δ*fba* in glucose may be different from that induced by glycerol or butyrate feeding below the FBA catalyzed step.

Δ*fba* failed to replicate in resting bone marrow derived mouse macrophages (BMDM) in contrast to WT and Δ*fba*-comp (Figure 2.9A). Activation of macrophages with IFNg reduced replication of WT and Δ*fba*-comp and did not affect survival of Δ*fba*. In mice, Δ*fba* did not establish an infection and was cleared from mouse lungs by day 10 post infection (Figure 2.9B). Thus, the metabolic environment in phagosomes of macrophages *ex vivo* and in mouse lungs did not support growth of *Mtb* in the absence of FBA and resulted in killing of Δ*fba* in mice. The lack of death of Δ*fba* in isolated macrophages suggests that the intracellular environment in macrophages *ex vivo* does not exactly mimic that faced by *Mtb* in macrophages inside the lung.

2.3.3 Metabolic consequences of *fba* deletion

To better understand the impact of loss of FBA on *Mtb* metabolism we used liquid chromatography/mass spectrometry to measure metabolite levels in WT, Δ*fba*, and Δ*fba*-comp cultured on filters on top of agar plates containing 0.2% glucose, 0.2%

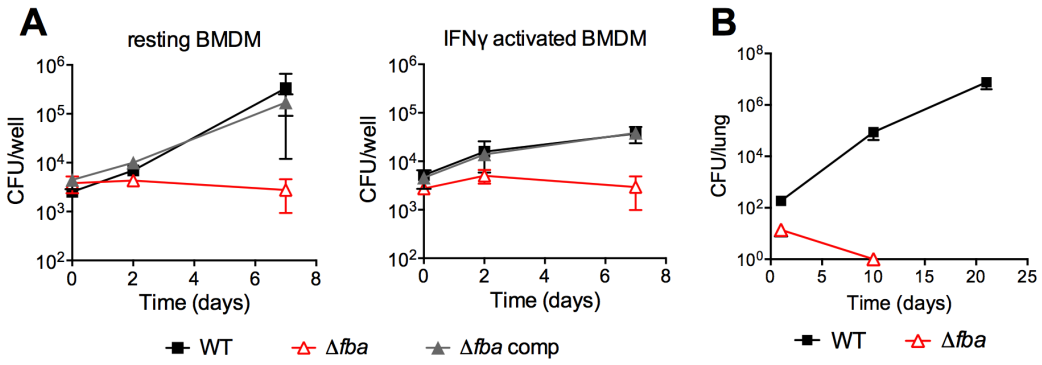

Figure 2.9. FBA is required for replication in macrophages and growth and survival in mouse lungs. (**A**) Bacterial loads in resting and IFNg activated mouse bone marrow derived macrophages (BMDM) infected with carbon-starved WT, *Δfba* and *Δfba*-comp. Data are means +/- SD of triplicate wells. **P*≤0.05; ***P*≤0.005 by Student's t-test (**B**) Growth and survival of WT and *Δfba* in mouse lungs. Data are means +/- SD from four mice. Limit of detection was 4 CFU and *Δfba* was not detectable on days 10 and 21.

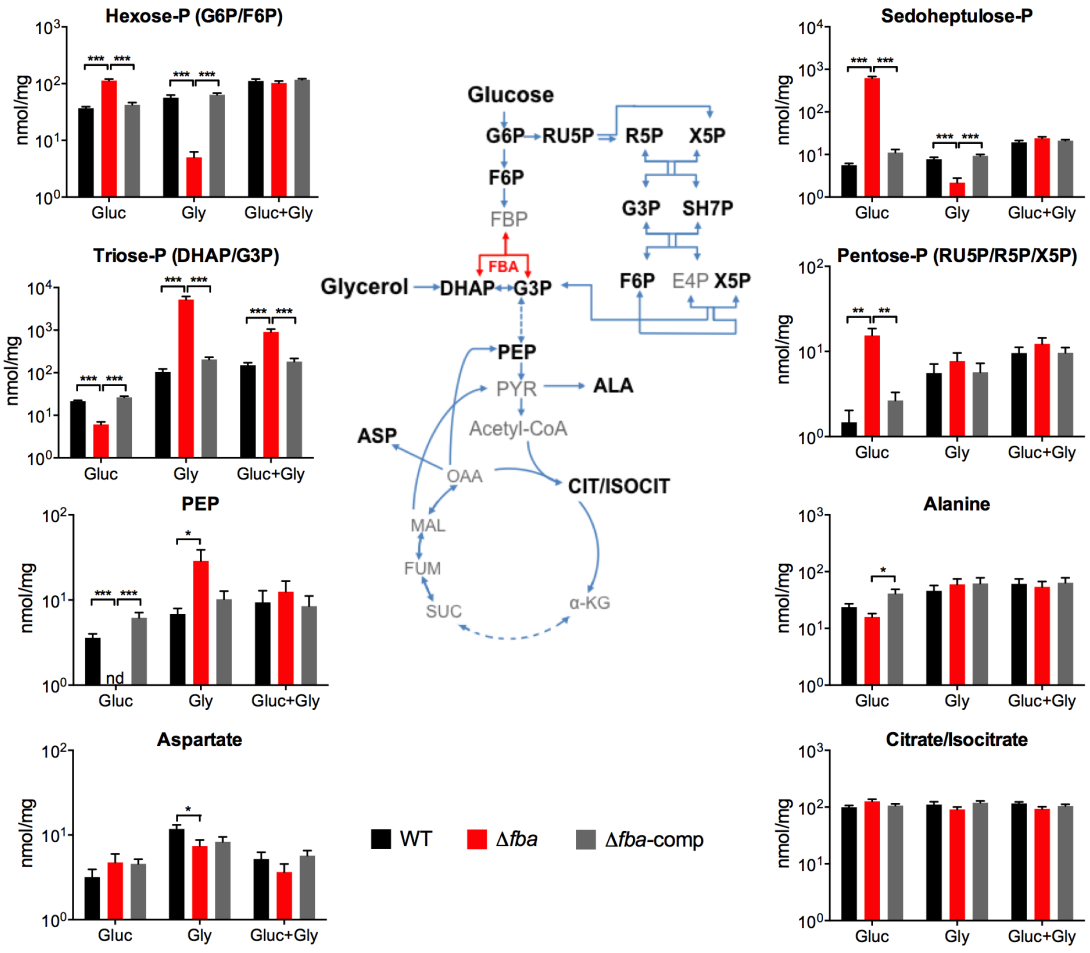

Figure 2.10. Metabolic consequences of *fba* deletion. Intrabacterial pool sizes of selected metabolites (nmol/mg protein) in the indicated *Mtb* strains after 24 hours culture on media containing either glucose (Gluc), glycerol (Gly) or a combination of both. nd = not detected. All values are means of measurements from two independent experiments, each performed with triplicate cultures ± SEM. **P*≤0.05; ***P*≤0.005; ****P*≤0.0005 by Student's t-test. ALA, alanine; α-KG, α-ketoglutarate; ASP, aspartate; CIT/ISOCIT, citrate/isocitrate; DHAP, dihydroxyacetone phosphate; E4P, erythrose 4-phosphate; FBA, fructose 1,6-bisphosphate aldolase; F6P, fructose 6-phosphate; FBP, fructose 1,6-bisphosphate; FUM, fumarate; G3P, glyceraldehyde 3-phosphate; G6P, glucose 6-phosphate; MAL, malate; OAA, oxaloacetate; PEP, phosphoenolpyruvate; PYR, pyruvate; R5P, ribose 5-phosphate; RU5P, ribulose 5-phosphate, SH7P, sedoheptulose 7-phosphate; SUC, succinate; X5P, xylulose 5-phosphate.

glycerol, or a combination of 0.2% glucose and 0.2% glycerol (Figure 2.10). Following exposure to glucose alone, Δ*fba* accumulated high levels of hexose-phosphate (P) and depleted its triose-P and phosphoenolpyruvate (PEP) pools. These metabolic changes are consistent with a defect in glucose metabolism due to the absence of FBA activity. Pentose-P and sedoheptulose-P pools were also significantly increased in Δ*fba* suggesting either increased flux through the pentose phosphate (PP) pathway or decreased metabolism of PP pathway intermediates. In contrast, exposure to glycerol as sole carbon source resulted in depletion of hexose-P and sedoheptulose-P pools while triose-P levels were increased. The presence of both glucose and glycerol reversed most metabolic changes in Δ*fba* except for the triose-P pool, which remained elevated, but not to the same extent as with glycerol as sole carbon source. These experiments demonstrate that metabolism of single carbon sources by Δ*fba* significantly altered intracellular metabolite concentrations, which was accompanied by cell death (Figure 2.8B). The buildup of PP pathway metabolites was consistent with increased flux into the PP pathway during culture on glucose; however, the PP pathway could not act as an efficient bypass to overcome loss of FBA.

2.3.4 Only a specific balance of carbon sources can compensate for lack of FBA

Growth of Δ*fba* required the presence of two carbon sources entering metabolism above and below the FBA catalyzed reaction and on agar plates was dependent on the amount of glucose in media containing glycerol and oleic acid (Figure 2.6A). We therefore sought to investigate whether FBA might regulate a specific balance of glycolytic and gluconeogenic metabolism. WT *Mtb* replicated with glucose as sole carbon source and even low concentrations of butyrate enhanced its growth as previously reported (de Carvalho et al., 2010) up to 0.4% when butyrate became toxic

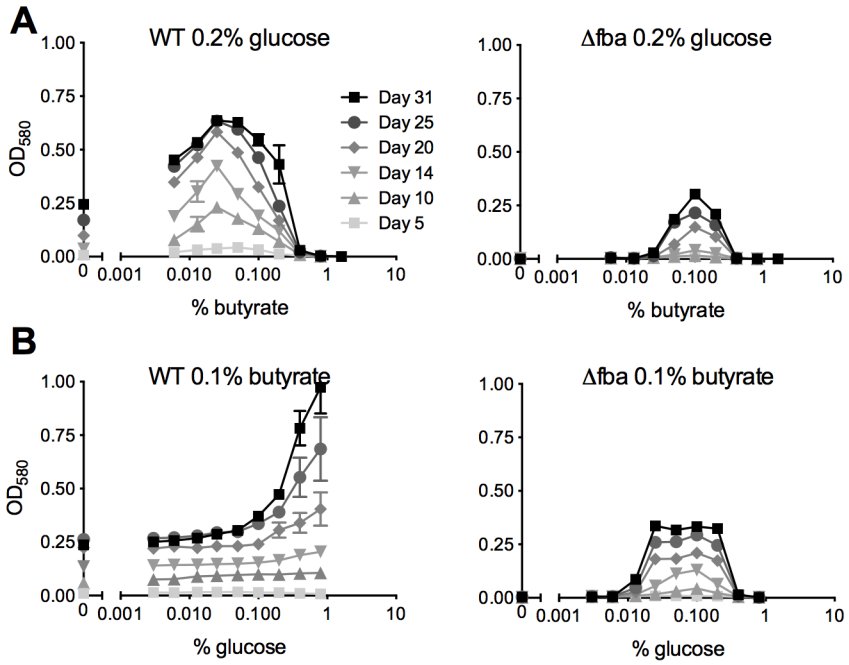

Figure 2.11. *Mtb* lacking FBA requires a balanced carbon diet for growth. Growth of WT and Δ*fba* was in media containing (**A**) 0.2% glucose with varying concentrations of butyrate and (**B**) 0.1% butyrate with varying concentrations of glucose. Bacteria were cultured in 96-well plates and absorbance was measured at the indicated time points. Data are means of triplicate cultures +/- SEM and representative of two independent experiments.

(Figure 2.11). In contrast, when provided with 0.2% glucose, Δ*fba* required at least 0.05% butyrate for growth, which was maximal with 0.1% but did not reach that of WT suggesting that *Mtb's* capacity to metabolize butyrate is limited by FBA deficiency.

With a fixed concentration of 0.1% butyrate, WT growth increased with increasing amounts of glucose (Figure 2.11B). Growth of Δ*fba,* however, plateaued with 0.025% glucose and was inhibited at concentrations above 0.2%. Inefficient glucose metabolism thus limited growth of Δ*fba* in the presence of butyrate suggesting that FBA facilitates the efficient catabolism of butyrate by driving glycolysis. Together these data imply that the efficiency of glucose metabolism determines *Mtb's* capacity to co-catabolize butyrate.

2.3.5 Vulnerability of *Mtb* to partial FBA depletion depends on the carbon source

Given the *in vivo* essentiality in acute and chronic mouse infections, our final goal was to evaluate to what degree FBA has to be depleted to result in growth inhibition and whether this is dependent on the available carbon source. FBA-DUC grew slower than WT in media with 0.4% glucose even in the absence of atc (Figure 2.4A) and in glucose FBA-DUC was more sensitive to atc-induced growth inhibition than in butyrate containing media (Figure 2.12). The reduced growth in glucose-containing, atc-free media (Figure 2.4A, 2.13A) was likely due to the low FBA amounts expressed in FBA-DUC, which were reduced by approximately 87% compared to WT even in the absence of atc (Figure 2.13B). Addition of 6.3 ng/ml atc depleted FBA by approximately 97% and abolished growth of FBA-DUC in glucose containing medium. In contrast, depletion by 87% or 97% was insufficient to reduce growth of FBA-DUC in medium with 0.1% butyrate as the sole carbon source. Addition of 25 ng/ml atc,

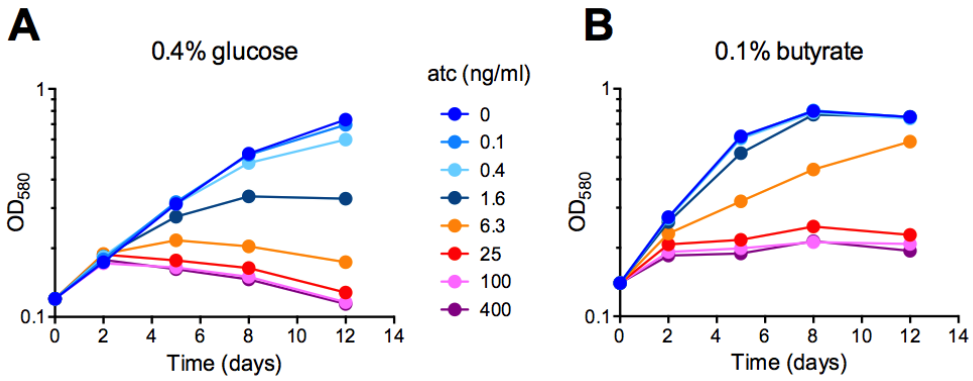

Figure 2.12. Atc-induced growth inhibition in glucose and butyrate containing media. Growth of FBA-DUC without and with indicated amounts of atc in (**A**) 0.4% glucose or (**B**) 0.1% butyrate.

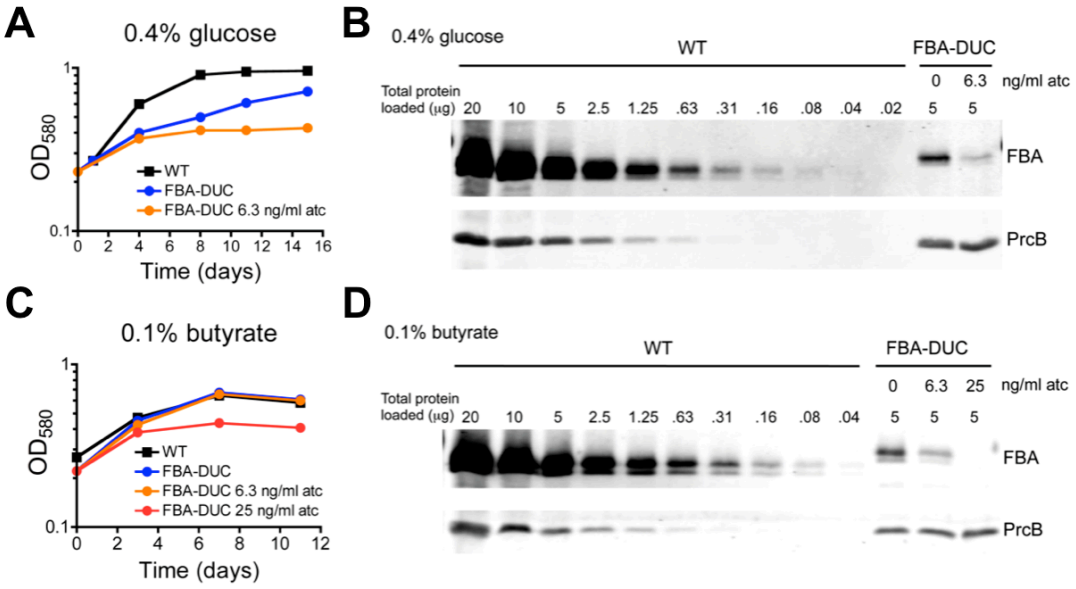

Figure 2.13. Vulnerability of *Mtb* to FBA depletion depends on the carbon source. Growth of WT and FBA-DUC without and with indicated amounts of atc in (**A**) 0.4% glucose or (**C**) 0.1% butyrate. (**B**) FBA immunoblot in protein extracts from 0.4% glucose cultures on day 15 after atc addition. (**D**) FBA immunoblot in protein extracts from 0.1% butyrate cultures on day 11 after atc addition. PrcB served as loading control.

which reduced FBA expression below the level of detection by day 11, was required to inhibit growth with butyrate. To determine whether higher FBA levels were present at earlier timepoints that still corresponded with growth inhibition, we assessed the kinetics of FBA depletion of the *fba*-DUC strain in 0.1% butyrate at various atc concentrations, in addition to both growth and survival (Figure 2.14). In this experiment, we included a day 1 timepoint and noted that survival was reduced from day 1 to 3 in the *fba*-DUC strain treated with 25 or 500 ng/ml atc. This corresponded with a reduction in FBA protein to nearly undetectable levels by day 3 for both concentrations. Therefore, FBA protein in this context is depleted by the time at which we see growth inhibition, suggesting that FBA does have to be depleted over 97% to see an effect on growth. In conclusion, *Mtb* was more sensitive to FBA depletion when grown with glucose as sole carbon source than when metabolizing butyrate emphasizing that vulnerability to depletion of an essential protein can be dependent on the growth condition.

2.4 Discussion

The experiments reported here enhance our understanding of *Mtb* carbon metabolism and are relevant to tuberculosis drug development. *Mtb fba* has previously been shown to be required for growth on standard media (Griffin et al., 2011; de la Paz Santangelo et al., 2011) and FBA inhibitors are under development (Capodagli et al., 2014; Daher et al., 2010; Fonvielle et al., 2008; Labbé et al., 2012). However, to our knowledge only one inhibitor has shown efficacy against live *Mtb*, at a concentration of 0.6-1.2 mM in 7H9-OADC broth (Capodagli et al., 2014). Furthermore, it was unknown whether FBA is essential for growth or survival of *Mtb in vivo*. Using a genetic approach we evaluated FBA as a potential drug target by assessing its essentiality for growth and persistence during mouse infections. Depletion of FBA after establishment

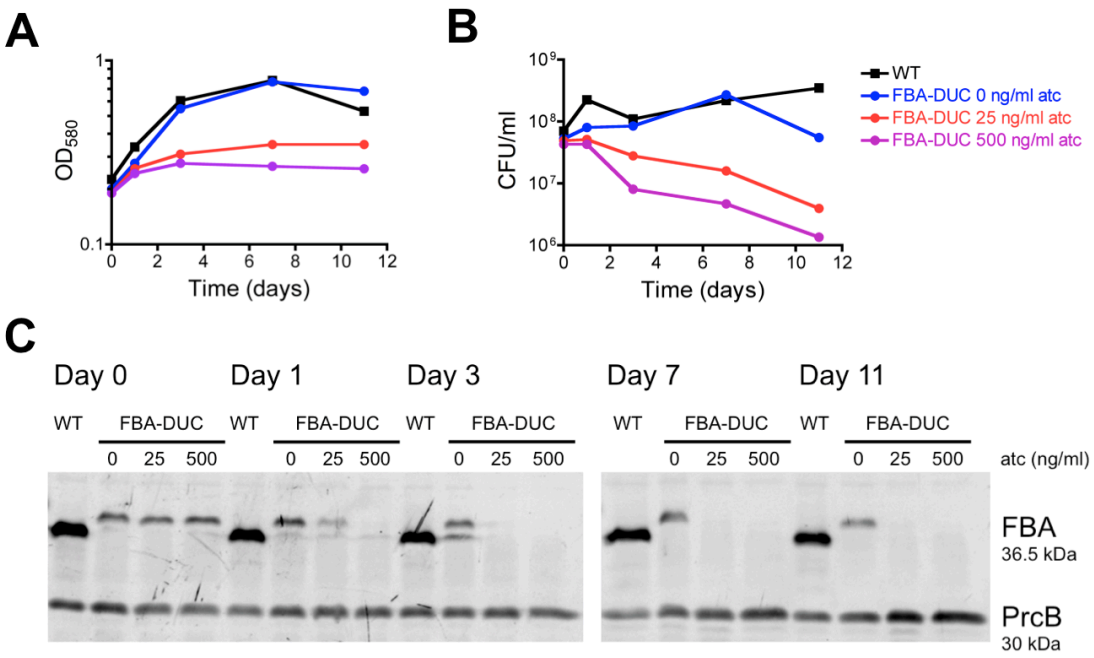

Figure 2.14. Kinetics of depletion correlated with growth and survival in 0.1% butyrate. (A) Growth and (B) survival of WT and the FBA-DUC strain upon exposure to 0, 25, or 500ng/ml atc. Time is in days after atc addition. (C) Western blot depicts FBA protein depletion over time. FBA in the FBA-DUC strain has a higher molecular weight due to the DAS tag.

of chronic infection led to complete clearance of viable *Mtb* in mouse lungs and spleens, which promotes FBA as a potential enzyme for targeting persistent bacilli.

Unexpectedly, FBA was not essential in all conditions *in vitro*, and a conditional *fba* mutant was critical to identify conditions in which Δ*fba* could be isolated. This deletion mutant was able to replicate when provided with combinations of carbon substrates entering metabolism above and below the FBA-catalyzed reaction. Thus, it will be crucial to determine the efficacy of FBA inhibitors against live *Mtb* in carbon conditions where *Mtb* is vulnerable to FBA inactivation in contrast to standard mycobacterial liquid culture medium, which contains a combination of glucose and glycerol making FBA dispensable.

Earlier studies have highlighted *Mtb's* ability to co-catabolize multiple carbon sources *in vitro* and in macrophages (Beste et al., 2011, 2013; de Carvalho et al., 2010). This is in contrast to other bacteria such as *E. coli*, which exhibits diauxic growth in the presence of multiple carbon sources resulting from their sequential metabolism (Görke and Stülke, 2008; Kovárová-Kovar and Egli, 1998). Here, we provide further evidence for *Mtb's* co-catabolism and offer insight into its metabolic regulation. Growth of WT *Mtb* on glucose and on butyrate, which requires β-oxidation for conversion into acetyl-CoA mimicking the fate of long chain fatty acids, was enhanced in a dose responsive manner by addition of the respective other carbon source. Growth of Δ*fba* only occurred with two carbon substrates, feeding into either side of the FBA reaction. Additionally, deletion of FBA rendered *Mtb* sensitive to the relative concentrations of carbon sources in the medium. In media containing glucose and butyrate, Δ*fba* was unable to efficiently utilize glucose to enhance its growth while growth of WT scaled with glucose. Metabolism of increasing amounts of butyrate was also restricted shown

by Δ*fba*'s limited growth despite the presence of 0.2% glucose. Therefore, FBA inactivation resulted in suboptimal co-catabolism of glucose and butyrate.

The mechanism of death of Δ*fba* in carbon-unbalanced media remains to be determined but may be due to buildup of FBA substrates at higher concentrations of carbon sources, as well as regulatory mechanisms allowing *Mtb* to sense carbon levels and respond accordingly. Indeed, the inability of Δ*fba* to grow on standard *Mtb* plate medium containing glucose, glycerol and oleic acid was overcome by the addition of 0.2% additional glucose, which was not required for growth in nearly identical medium lacking oleic acid. Interestingly, Δ*fba* survived much better in media containing no carbon, suggesting that death is carbon source-dependent. This is not the first example of death induced by carbon source; inhibitors were identified that only kill *Mtb* in glycerol, whose use potentially contributed to the buildup of a toxic metabolite, methylglyoxal (Pethe et al., 2010). While we did not observe an accumulation of a metabolite with the mass over charge ratio of methylglyoxyal (data not shown), this metabolite is difficult to detect, and it is possible that this or other metabolic accumulations we did observe could lead to toxicity.

Accumulation of sugar phosphates including the FBA substrate fructose-1,6-bisphosphate (FBP) has also been implicated in growth inhibition. Inactivation of FBA in *E. coli* prevented growth with glucose but not with glycerol and succinate as carbon substrates (Böck and Neidhardt, 1966a, 1966b). Suppressor mutations that prevented FBP buildup allowed for growth on glucose (Schreyer and Bock, 1973). With our metabolite extraction protocol we did not detect FBP, however other sugar phosphates including hexose-P, sedoheptulose-P and pentose-P increased dramatically in Δ*fba* cultured on glucose, while triose-P and PEP accumulated on glycerol. The accumulation of these metabolites was not observed when both glucose and glycerol

were available to Δ*fba*, except for the triose-P pools, which remained elevated but much less than in the glycerol condition. It is thus possible that the accumulation of phosphorylated metabolites is cause for the death of Δ*fba* in conditions where glycolytic and gluconeogenic carbon flow is unbalanced, such as with single carbon substrates or in mixes with an abundance of a glycolytic or gluconeogenic substrate.

To better understand the mechanism of death in single carbon sources, future work could include transcriptomics analysis to identify stress response pathways that are upregulated in response to glucose, glycerol or butyrate. Also, it may be valuable to plate dense culture of the *fba* KO onto single carbon sources, to screen for suppressor mutations. To promote the generation of mutations, a transposon mutagenesis approach may be worthwhile. This could identify pathways involved in the generation of stresses that lead to growth inhibition or death in single carbon sources.

While it is unknown whether a loss-of-function mutation could allow for growth of FBA-deficient bacteria on single carbon sources, we have isolated a strain lacking FBA that grows on OADC-containing media without the addition of extra glucose. Interestingly, this strain has a loss of function mutation in a probable succinate dehydrogenase membrane subunit, a TCA cycle enzyme complex. This mutation could cause a slow down of TCA cycle activity, leading to reduced NADH production and potentially less oxidative stress. Additionally, this mutation could increase succinate levels, which could provide protective functions for the cell as has been demonstrated for hypoxic conditions (Eoh and Rhee, 2013). Preliminary work (not shown) suggests that this mutation does not grant growth advantages in various mixtures of glucose and acetate compared to the parent knockout strain. It would be of interest in the future to define the sensitivity of Δ*fba* and Δ*fba*-OADC resistant strain to various concentrations of oleic acid, as opposed to OADC supplement.

Metabolomics experiments comparing the intracellular metabolites of Δ*fba* and Δ*fba*-OADC resistant strains in oleic acid may reveal differences in accumulation of succinate or other metabolites. However, most important is to determine whether this mutation could allow for growth of *Mtb* lacking *fba* in the mouse model.

How potent would an FBA inhibitor need to be to affect *Mtb* growth? We measured the vulnerability of *Mtb* to FBA depletion in single glycolytic and gluconeogenic carbon sources where FBA is essential. Although depleting FBA by 97% did not affect growth with butyrate as sole carbon source, it prevented growth with glucose and 87% inhibition was sufficient to reduce growth with glucose. These data reveal a differential susceptibility of *Mtb* to FBA depletion, depending on the available carbon source. Antibiotic targets vary widely in how much inhibition is required to stop replication or induce death and not all effective drug targets are highly vulnerable to inhibition (Wei et al., 2011). Specific target-drug interactions can contribute to the efficacy of a compound. We cannot predict how effectively FBA must be depleted to abolish replication *in vivo*, but the WT-like phenotype of FBA-DUC without doxy suggests that 13% of WT FBA levels are sufficient for normal growth and persistence in mice. The fast killing of *Mtb* following further FBA depletion in mouse lungs and spleens suggests that it is an effective target during acute and chronic mouse infections. During infections FBA may also have an additional, metabolism-independent function in *Mtb*'s interaction with the host as it can be secreted and bind to human plasminogen (de la Paz Santangelo et al., 2011).

The requirement of FBA for growth and persistence in mice suggests that *in vivo Mtb* either faces single carbon sources or lacks access to the growth permissive ratio of carbon sources that can compensate for the lack of FBA. This is likely due to an abundance of fatty acids and lipids which are predominant carbon sources available to

Mtb in vivo (Marrero et al., 2010; Munoz-Elias and McKinney, 2005; Pandey and Sassetti, 2008; Segal and Bloch, 1956*)*. It is unknown if FBA is essential for growth and persistence of *Mtb* in humans; experimental animal models that more closely mimic human TB pathology (Véronique Dartois, 2010) would help address this question. Given that human granulomas contain lipid-rich foamy macrophages and build up lipids in the caseum (Kim et al., 2010; Peyron et al., 2008), it is plausible that *Mtb* requires FBA also during human infection.

2.5 Materials and Methods

2.5.1 Ethics statement

Mouse studies were performed following National Institutes of Health guidelines for housing and care of laboratory animals and performed in accordance with institutional regulations after protocol review and approval by the Institutional Animal Care and Use Committee of Weill Cornell Medical College (protocol # 0601-441A, Conditional Expression of Mycobacterial Genes).

2.5.2 Strains, media and culture conditions

Mycobacterium tuberculosis (*Mtb*) H37Rv strains were grown in Middlebrook 7H9 liquid media containing 0.5% bovine serum albumin fraction V, 0.2% glucose, 0.2% glycerol, 0.085% NaCl, and 0.05% tyloxapol without shaking in 5% CO2 at 37°C. For carbon-defined growth curves, *Mtb* was cultured in Sauton's base media modified to be carbon-limited, containing 0.05% potassium phosphate monobasic, 0.05% magnesium sulfate heptahydrate, 0.2% citric acid, 0.005% ferric ammonium citrate, 0.05% ammonium sulfate, 0.0001% zinc sulfate, and 0.05% tyloxapol at pH 7.4. For solid media, Middlebrook 7H10 media with 0.5% glycerol and 10% Middlebrook OADC supplement (final concentration of 0.5% bovine serum albumin fraction V,

0.2% glucose, 0.085% NaCl, 0.006% oleic acid, 0.0003% catalase) or self-made ADNaCl (final concentration of 0.5% bovine serum albumin fraction V, 0.2% glucose, 0.085% NaCl) was used. Carbon sources glucose, glycerol, sodium acetate and butyric acid, were added at indicated concentration (%wt/vol or %vol/vol, depending on stock). When appropriate, hygromycin B (50 mg/ml), streptomycin (10 mg/ml), kanamycin (25 mg/ml), and/or zeocin (25 mg/ml) were added. Anhydrotetracycline (atc) was added at the indicated concentrations and replenished at half the initial concentration in liquid cultures every 4-5 days for growth curves but not vulnerability assays. For survival assays, bacterial culture samples were taken from growth curve cultures at the time-points indicated and plated for CFU. For metabolomic profiling, *Mtb* was seeded at OD_{580}~1 on 0.22 mM nitrocellulose filters (1ml per filter) and cultured on Middlebrook 7H10 agar medium containing 0.5% bovine serum albumin fraction V, 0.085% NaCl, 0.2% glucose, and 0.2% glycerol for 5 days. Filters were then transferred to similar plates with defined carbon sources: 0.2% glucose, 0.2% glycerol, or both together, each at 0.2%. *Mtb* was harvested 24 hours later by metabolic quenching in cold acetonitrile:methanol:H_2O (40:40:20) and mechanically lysed using a bead beater as described (de Carvalho et al., 2010; Marrero et al., 2010).

2.5.3 Generation of mutant strains

M. tuberculosis H37Rv was transformed with a plasmid expressing *fba* under the control of a strong promoter P1 (P_{smyc}) that integrates into the phage attL5 site in the *Mtb* genome (Ehrt et al., 2005). In this *fba* merodiploid strain deletion of native *fba* was achieved by allelic exchange using specialized transducing phage phAE87 as previously described (Marrero et al., 2010). After confirming removal of native *fba* by Southern blot, replacement transformations of the attL5 insets were performed to generate FBA-DUC and Δ*fba.* In FBA-DUC, *fba* contained a C-terminal DAS+4 tag

and a plasmid in the phage tweety site that allowed inducible expression of *SspB* as described (Kim et al., 2013). In Δ*fba* the attL5 site carries a kanamycin-resistant plasmid not containing *fba*. All plasmids were constructed using Gateway Cloning Technology (Invitrogen) using BP and LR recombinase reactions following the manufacturers instructions. The complemented mutant is Δ*fba* transformed with a plasmid that integrates in the attL5 site expressing *fba* from the P1 promoter.

2.5.4 Whole genome sequencing

Sequencing of *fba* KO and *fba* OADC-resistant strain DNA was performed in collaboration with Jim Sacchettini and Tom Ioerger at Texas A&M. The *fba* KO contains a deletion of *fba* as well as the following mutations compared to the WT H37Rv parent strain: Rv2226 –GC in res 373/513; Rv1968/mce3C I241I; Rv2621c V47G; Rv2934/ppsD –T in res 642/1827; and Rv3487c/lipF V15L. The *fba* OADC-resistant strain has the following mutations in addition to those found in the *fba* KO strain: Rv0249c W31* and Rv2347c/hrcA A123V.

2.5.5 Metabolomics using Liquid Chromatography-Mass Spectrometry

M. tuberculosis metabolites were separated and detected in a Agilent Accurate Mass 6220 TOF coupled to an Agilent 1200 Liquid Chromatography system using a Cogent Diamond Hydride Type C column (Microsolve Technologies) using solvents and configuration as described (Eoh and Rhee, 2013). Metabolites were quantified by standard curves generated with authentic chemicals spiked into homologous mycobacterial lysates. Quantified metabolite concentrations were normalized to bacterial biomass of individual samples determined by measuring residual protein content (BCA Protein Assay kit; Pierce).

2.5.6 Immunoblot analysis for vulnerability assay

Protein extracts were prepared from bacterial pellets from 30 ml cultures at indicated time points in specified media. Briefly, cultures were washed with phosphate buffered saline (PBS), 0.05% Tween 80 and resuspended in 1 ml PBS, 1x protease inhibitor cocktail (Roche). Cells were lysed by bead beating three times at 4500 rpm for 30 seconds with 0.1 mm Zirconia/Silica beads. Beads and cell walls were removed through centrifugation (11000 x g/ 10 min/ 4°C) and the supernatant was filtered through a 0.2 mm SpinX column (Corning). Lysate protein concentrations were determined using a DC Protein Assay Kit (Bio-Rad). For immunoblots 20-0.02 mg protein extracts were separated by SDS-PAGE, transferred to nitrocellulose membranes and probed overnight with rabbit antisera FBA (de la Paz Santangelo et al., 2011) (1:2000 dilution in 1:1 PBS/Odyssey Blocking Buffer (LI-COR Biosciences), 0.1% Tween20) or PrcB (1:18,000 dilution in 1:1 PBS/Odyssey Blocking Buffer (LI-COR Biosciences), 0.1% Tween20). As secondary antibody IRDye 680 Donkey anti-Rabbit IgG(H+L) (LI-COR Biosciences) was used. Proteins were detected using the Odyssey Infrared Imaging System (LI-COR Biosciences).

2.5.7 Mouse and macrophage infections

Female C57BL/6 mice (Jackson Laboratory) were infected by aerosol using an inhalation exposure system (Glas-Col) and early-log-phase *M. tuberculosis* cultures as single-cell suspensions in PBS to deliver 100 to 200 bacilli per mouse. Doxycycline-containing food (2000 ppm, Research Diets) was given to mice starting at the indicated time-points. Serial dilutions of lungs and spleens homogenates were cultured on 7H10 plates containing ADNaCl to determine CFU at the indicated time points.

The left lobe of each lung was fixed in 10% buffered formalin, further processed for histopathology and stained with hematoxilyn and eosin. We isolated and infected bone marrow-derived mouse macrophages as previously described (Vandal et al., 2008).

2.6 Acknowledgements

Dr. Carolina Trujillo, Dr. Hyungjin Eoh, Dr. Joeli Marrero, Dr. John Spencer, Dr. Mary Jackson, Dr. Dirk Schnappinger, and Dr. Kyu Rhee all contributed to the work in this chapter. We thank Dr. Gang Lin and Dr. Carl Nathan for PrcB-specific antiserum.

REFERENCES

Bai, N.J., Pai, M.R., Murthy, P.S., and Venkitasubramanian, T.A. (1974). Effect of oxygen tension on the aldolases of Mycobacterium tuberculosis H37Rv. FEBS Lett. *45*, 68–70.

Beste, D.J.V., Bonde, B., Hawkins, N., Ward, J.L., Beale, M.H., Noack, S., Nöh, K., Kruger, N.J., Ratcliffe, R.G., and McFadden, J. (2011). ^{13}C metabolic flux analysis identifies an unusual route for pyruvate dissimilation in mycobacteria which requires isocitrate lyase and carbon dioxide fixation. PLoS Pathog. *7*, e1002091.

Beste, D.J.V., Nöh, K., Niedenführ, S., Mendum, T.A., Hawkins, N.D., Ward, J.L., Beale, M.H., Wiechert, W., and McFadden, J. (2013). 13C-flux spectral analysis of host-pathogen metabolism reveals a mixed diet for intracellular Mycobacterium tuberculosis. Chem. Biol. *20*, 1012–1021.

Böck, A., and Neidhardt, F.C. (1966a). Isolation of a Mutant of Escherichia coli with a Temperature-sensitive Fructose-1,6-Diphosphate Aldolase Activity. J. Bacteriol. *92*, 464–469.

Böck, A., and Neidhardt, F.C. (1966b). Properties of a Mutant of Escherichia coli with a Temperature-sensitive Fructose-1,6-Diphosphate Aldolase. J. Bacteriol. *92*, 470–476.

Capodagli, G.C., Sedhom, W.G., Jackson, M., Ahrendt, K.A., and Pegan, S.D. (2014). A Noncompetitive Inhibitor for Mycobacterium tuberculosis's Class IIa Fructose 1,6-Bisphosphate Aldolase. Biochemistry (Mosc.) *53*, 202–213.

De Carvalho, L.P.S., Fischer, S.M., Marrero, J., Nathan, C., Ehrt, S., and Rhee, K.Y. (2010). Metabolomics of Mycobacterium tuberculosis reveals compartmentalized co-catabolism of carbon substrates. Chem. Biol. *17*, 1122–1131.

Daher, R., Coinçon, M., Fonvielle, M., Gest, P.M., Guerin, M.E., Jackson, M., Sygusch, J., and Therisod, M. (2010). Rational design, synthesis, and evaluation of new selective inhibitors of microbial class II (zinc dependent) fructose bis-phosphate aldolases. J. Med. Chem. *53*, 7836–7842.

Du, S., Guan, Z., Hao, L., Song, Y., Wang, L., Gong, L., Liu, L., Qi, X., Hou, Z., and Shao, S. (2014). Fructose-bisphosphate aldolase a is a potential metastasis-associated marker of lung squamous cell carcinoma and promotes lung cell tumorigenesis and migration. PloS One *9*, e85804.

Ehrt, S., Guo, X.V., Hickey, C.M., Ryou, M., Monteleone, M., Riley, L.W., and Schnappinger, D. (2005). Controlling gene expression in mycobacteria with anhydrotetracycline and Tet repressor. Nucleic Acids Res. *33*, e21–e21.

Eoh, H., and Rhee, K.Y. (2013). Multifunctional essentiality of succinate metabolism in adaptation to hypoxia in Mycobacterium tuberculosis. Proc. Natl. Acad. Sci. U. S. A. *110*, 6554–6559.

Fonvielle, M., Coinçon, M., Daher, R., Desbenoit, N., Kosieradzka, K., Barilone, N., Gicquel, B., Sygusch, J., Jackson, M., and Therisod, M. (2008). Synthesis and Biochemical Evaluation of Selective Inhibitors of Class II Fructose Bisphosphate Aldolases: Towards New Synthetic Antibiotics. Chem. – Eur. J. *14*, 8521–8529.

Görke, B., and Stülke, J. (2008). Carbon catabolite repression in bacteria: many ways to make the most out of nutrients. Nat. Rev. Microbiol. *6*, 613–624.

Griffin, J.E., Gawronski, J.D., DeJesus, M.A., Ioerger, T.R., Akerley, B.J., and Sassetti, C.M. (2011). High-Resolution Phenotypic Profiling Defines Genes Essential for Mycobacterial Growth and Cholesterol Catabolism. PLoS Pathog. *7*.

Kim, J.-H., O'Brien, K.M., Sharma, R., Boshoff, H.I.M., Rehren, G., Chakraborty, S., Wallach, J.B., Monteleone, M., Wilson, D.J., Aldrich, C.C., et al. (2013). A genetic strategy to identify targets for the development of drugs that prevent bacterial persistence. Proc. Natl. Acad. Sci. U. S. A. *110*, 19095–19100.

Kim, M.-J., Wainwright, H.C., Locketz, M., Bekker, L.-G., Walther, G.B., Dittrich, C., Visser, A., Wang, W., Hsu, F.-F., Wiehart, U., et al. (2010). Caseation of human tuberculosis granulomas correlates with elevated host lipid metabolism. EMBO Mol. Med. *2*, 258–274.

Kishi, H., Mukai, T., Hirono, A., Fujii, H., Miwa, S., and Hori, K. (1987). Human aldolase A deficiency associated with a hemolytic anemia: thermolabile aldolase due to a single base mutation. Proc. Natl. Acad. Sci. U. S. A. *84*, 8623–8627.

Kovárová-Kovar, K., and Egli, T. (1998). Growth Kinetics of Suspended Microbial Cells: From Single-Substrate-Controlled Growth to Mixed-Substrate Kinetics. Microbiol. Mol. Biol. Rev. *62*, 646–666.

Labbé, G., Krismanich, A.P., de Groot, S., Rasmusson, T., Shang, M., Brown, M.D.R., Dmitrienko, G.I., and Guillemette, J.G. (2012). Development of metal-chelating inhibitors for the Class II fructose 1,6-bisphosphate (FBP) aldolase. J. Inorg. Biochem. *112*, 49–58.

Macomber, L., Elsey, S.P., and Hausinger, R.P. (2011). Fructose-1,6-bisphosphate aldolase (class II) is the primary site of nickel toxicity in Escherichia coli. Mol. Microbiol. *82*, 1291–1300.

Marrero, J., Rhee, K.Y., Schnappinger, D., Pethe, K., and Ehrt, S. (2010). Gluconeogenic carbon flow of tricarboxylic acid cycle intermediates is critical for Mycobacterium tuberculosis to establish and maintain infection. Proc. Natl. Acad. Sci. U. S. A. *107*, 9819–9824.

Marsh, J.J., and Lebherz, H.G. (1992). Fructose-bisphosphate aldolases: an evolutionary history. Trends Biochem. Sci. *17*, 110–113.

Munoz-Elias, E.J., and McKinney, J.D. (2005). M. tuberculosis isocitrate lyases 1 and 2 are jointly required for in vivo growth and virulence. Nat. Med. *11*, 638–644.

Pandey, A.K., and Sassetti, C.M. (2008). Mycobacterial persistence requires the utilization of host cholesterol. Proc. Natl. Acad. Sci. *105*, 4376–4380.

De la Paz Santangelo, M., Gest, P.M., Guerin, M.E., Coincon, M., Pham, H., Ryan, G., Puckett, S.E., Spencer, J.S., Gonzalez-Juarrero, M., Daher, R., et al. (2011). Glycolytic and Non-glycolytic Functions of Mycobacterium tuberculosis Fructose-1,6-bisphosphate Aldolase, an Essential Enzyme Produced by Replicating and Non-replicating Bacilli. J. Biol. Chem. *286*, 40219–40231.

Pegan, S.D., Rukseree, K., Franzblau, S.G., and Mesecar, A.D. (2009). Structural basis for catalysis of a tetrameric, class IIa fructose 1,6-bisphosphate aldolase from M. tuberculosis. J. Mol. Biol. *386*, 1038–1053.

Pegan, S.D., Rukseree, K., Capodagli, G.C., Baker, E.A., Krasnykh, O., Franzblau, S.G., and Mesecar, A.D. (2013). Active site loop dynamics of a class IIa fructose 1,6-bisphosphate aldolase from Mycobacterium tuberculosis. Biochemistry (Mosc.) *52*, 912–925.

Pethe, K., Sequeira, P.C., Agarwalla, S., Rhee, K., Kuhen, K., Phong, W.Y., Patel, V., Beer, D., Walker, J.R., Duraiswamy, J., et al. (2010). A chemical genetic screen in Mycobacterium tuberculosis identifies carbon-source-dependent growth inhibitors devoid of in vivo efficacy. Nat. Commun. *1*, 1–8.

Peyron, P., Vaubourgeix, J., Poquet, Y., Levillain, F., Botanch, C., Bardou, F., Daffé, M., Emile, J.-F., Marchou, B., Cardona, P.-J., et al. (2008). Foamy Macrophages from Tuberculous Patients' Granulomas Constitute a Nutrient-Rich Reservoir for M. tuberculosis Persistence. PLoS Pathog *4*, e1000204.

Rodaki, A., Young, T., and Brown, A.J.P. (2006). Effects of Depleting the Essential Central Metabolic Enzyme Fructose-1,6-Bisphosphate Aldolase on the Growth and Viability of Candida albicans: Implications for Antifungal Drug Target Discovery. Eukaryot. Cell *5*, 1371–1377.

Rosenkrands, I., Slayden, R.A., Crawford, J., Aagaard, C., Barry III, C.E., and Andersen, P. (2002). Hypoxic Response of Mycobacterium tuberculosis Studied by Metabolic Labeling and Proteome Analysis of Cellular and Extracellular Proteins. J. Bacteriol. *184*, 3485–3491.

Schreyer, R., and Bock, A. (1973). Phenotypic Suppression of a Fructose-1, 6-Diphosphate Aldolase Mutation in Escherichia coli. J. Bacteriol. *115*, 268–276.

Segal, W., and Bloch, H. (1956). Biochemical differentiation of Mycobacterium tuberculosis grown in vivo and in vitro. J. Bacteriol. *72*, 132–141.

Shen, B., and Sibley, L.D. (2014). Toxoplasma aldolase is required for metabolism but dispensable for host-cell invasion. Proc. Natl. Acad. Sci. U. S. A. *111*, 3567–3572.

Tunio, S.A., Oldfield, N.J., Berry, A., Ala'Aldeen, D.A.A., Wooldridge, K.G., and Turner, D.P.J. (2010). The moonlighting protein fructose-1, 6-bisphosphate aldolase of Neisseria meningitidis: surface localization and role in host cell adhesion. Mol. Microbiol. *76*, 605–615.

Vandal, O.H., Pierini, L.M., Schnappinger, D., Nathan, C.F., and Ehrt, S. (2008). A membrane protein preserves intrabacterial pH in intraphagosomal Mycobacterium tuberculosis. Nat. Med. *14*, 849–854.

Véronique Dartois (2010). Immunopathology of Tuberculosis Disease across Species. In A Color Atlas of Comparative Pathology of Pulmonary Tuberculosis, (CRC Press), pp. 19–28.

Wei, J.-R., Krishnamoorthy, V., Murphy, K., Kim, J.-H., Schnappinger, D., Alber, T., Sassetti, C.M., Rhee, K.Y., and Rubin, E.J. (2011). Depletion of antibiotic targets has widely varying effects on growth. Proc. Natl. Acad. Sci. U. S. A. *108*, 4176–4181.

Zhang, Y.J., Ioerger, T.R., Huttenhower, C., Long, J.E., Sassetti, C.M., Sacchettini, J.C., and Rubin, E.J. (2012). Global Assessment of Genomic Regions Required for Growth in Mycobacterium tuberculosis. PLoS Pathog. *8*.

CHAPTER 3

THE ROLE OF MALATE SYNTHASE IN PATHOGENICITY OF *MYCOBACTERIUM TUBERCULOSIS*

3.1. Introduction

The glyoxylate shunt is an attractive pathway to target with novel anti-tuberculosis therapeutics, as it is required for *Mycobacterium tuberculosis* (*Mtb*) growth on fatty acids and is not functional in humans. Furthermore, *Mtb* deficient in isocitrate lyase (ICL), the first enzyme in the pathway, is drastically attenuated in the mouse model of infection. The interpretation of this phenotype is complicated by the fact that ICL also participates in the methylcitrate cycle, a propionyl-CoA detoxification pathway. However, the second enzyme in the glyoxylate shunt, malate synthase (MS), is not known to have a secondary metabolic function. In *Mtb*, the only known malate synthase is encoded by the gene *glcB*. Here, to evaluate malate synthase as a drug target and to enhance our understanding of the importance of the glyoxylate shunt in *Mtb* metabolism, we generated *glcB* knockdown and knockout strains to determine the requirement for malate synthase *in vitro* and in the mouse model.

3.2 Background

Malate synthase (MS) is an enzyme that converts glyoxylate and acetyl-CoA to malate and CoA. This enzymatic step is the second in the glyoxylate shunt after the conversion of isocitrate to glyoxylate and succinate by isocitrate lyase (ICL). The glyoxylate shunt is critical for growth of bacteria in fatty acid carbon sources, as it allows for retention of acetyl-CoA-derived carbon for biomass by preventing carbon

loss in the form of CO_2 following the canonical TCA cycle. The glyoxylate shunt has been implicated in the pathogenesis of several organisms, including *Candida albicans, Psuedomonas aeruginosa,* and *Rhodococcus fascians*. However, *Salmonella typhimurium, Yersinia pestis, and Aspergillus fumigatus* were unaffected in their virulence upon glyoxylate shunt disruption (Dunn et al., 2009).

Malate synthase commonly occurs in two isoforms, malate synthase A (MSA) found in plants, yeast, and prokaryotes and malate synthase G (MSG), found exclusively in prokaryotes (Lohman et al., 2008; Smith et al., 2003). The nomenclature derives from the carbon source that regulates each enzyme in *E. coli*, which contains both isoforms; MSA is regulated during growth in acetate, whereas MSG is regulated during growth on glycolate. MSGs are larger (~80kDa) than MSAs (~60kDa) and share ~65% identity within their class and ~18-20% identity with MSAs. In placental mammals, the presence of a glyoxylate pathway is doubtful, as the genetic region with malate synthase homology is a pseudogene (Kondrashov et al., 2006). Furthermore, the ICL gene is absent in animals except for nematodes, which express a fused ICL-MS gene. Therefore, it may be possible to target bacterial malate synthase without interfering with human metabolism.

Mtb expresses a single malate synthase G, an 80.4 kDa protein 741 amino acids long encoded by the gene *glcB* (*rv1837c*) (Figure 3.1). Genetic studies are lacking because multiple attempts to directly knock out *glcB* via allelic exchange were unsuccessful (Merkov, 2006). Deep-sequencing analysis assessing the ability of transposon insertions to occur within the *glcB* locus suggest that *glcB* is essential in minimal media but not in rich media (Griffin et al., 2012; Zhang et al., 2012). The crystal structure for *Mtb* MS is available, and enzymatic assays have demonstrated that the

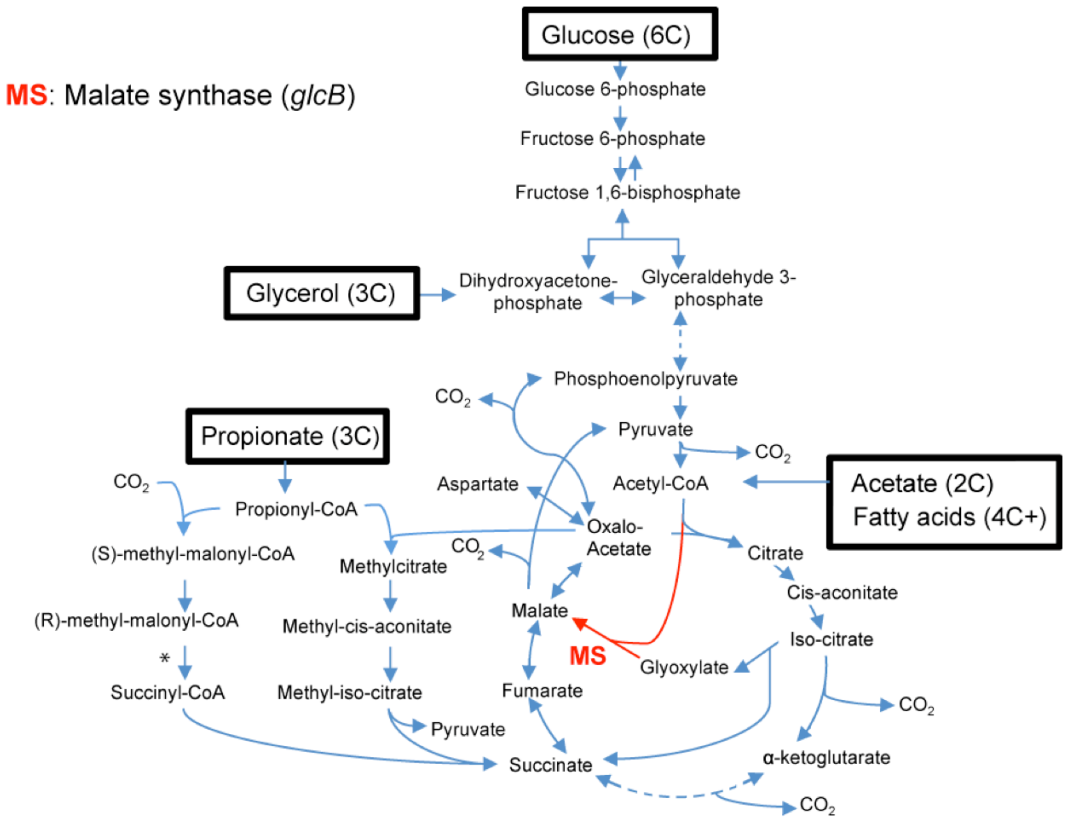

Figure 3.1. Schematic depicting the role of malate synthase in *Mtb* central carbon metabolism. The malate synthase (MS) step is highlighted in red and the entry points of carbon sources glucose (6 carbons), acetate (2 carbons), fatty acids (4+ carbons), glycerol (3 carbons) and propionate (3 carbons) are in black boxes. Pathways involving steps non-depicted steps are in dotted lines. The asterisk indicates the enzymatic step catalyzed by methylmalonyl-CoA mutase, a vitamin B_{12}-dependent enzyme.

enzyme does have malate synthase activity (Smith et al., 2003). Further efforts to understand the mechanism of the reaction have been undertaken (Bauzá et al., 2014; Quartararo and Blanchard, 2011). The enzyme is thought to exist either as a monomer or a dimer, with amino acid residues Asp-633, Glu-434, and Asp-462 and a catalytic Mg^{2+} ion playing probable roles in its enzymatic function (Kumar and Bhakuni, 2010; Smith et al., 2003). MS from *Mtb* has ~60% identity to the MSG of *Corynebacterium glutamicum* and *Escherichia coli*. Unlike isocitrate lyase, malate synthase does not appear to be largely upregulated in *Mtb* within macrophages, mice, in microaerophilic conditions, or in carbon sources acetate or palmitate (Rohde et al., 2012; Schnappinger et al., 2003; Shi et al., 2010; Smith et al., 2003; Wayne and Lin, 1982). The only carbon source reported to increase MS expression was glycolate, and this was only a 2-fold upregulation (Smith et al., 2003). Furthermore, unlike in *C. glutamicum*, the ICL and MS genes are located in separate regions of the genome. Therefore it appears that regulation of the glyoxylate shunt occurs primarily through regulation of ICL expression, and that regulatory mechanisms affecting expression of ICL do not also regulate MS.

Outside of its enzymatic function, MS may also play a role in *Mtb* cell adhesion to host proteins. MS is predominately cytosolic, but is also secreted. MS can localize to the cell wall, and has been shown to bind host laminin and fibronectin (Kinhikar et al., 2006). A 15 amino acid C-terminal tail unique to the *Mtb* MS was shown to play a role in this adhesion. MS is currently being developed as an antigen for testing of latent tuberculosis in rheumatoid arthritis patients, as the body develops a Th1-specific response to the MS antigen (Silva et al., 2014).

While genetic studies are lacking for the *Mtb* malate synthase, the characterization of a MS knockout in *M. smegmatis* was described in a dissertation by L. Merkov (Merkov,

2006). The *M. smegmatis* MS protein is homologous to the *Mtb* protein, with an identity of 80%. Surprisingly, this *M. smegmatis glcB* knockout grew on media containing single carbon sources glucose, acetate, propionate, butyrate, and valerate. Additional knock out of *ald*, a gene encoding an alanine dehydrogenase that could potentially act as a glyoxylate aminase, did not prevent growth on acetate. A transposon mutagenesis screen in the Δ*glcB*Δ*ald* background for mutants that could not grow on acetate uncovered an alternative glyoxylate metabolic pathway (the d-glycerate pathway) involving glyoxylate carboligase (encoded by the gene *gcl*). Deletion of *glcB* and *gcl* in the same strain resulted in inability of *M. smegmatis* to grow on acetate (2C), butyrate (4C), and hexanoate (6C), and this growth was restored upon complementation with the *Mtb glcB*. However, the Δ*glcB*Δ*gcl* mutant grew on propionate (3C), suggesting that glyoxylate metabolism is not required for propionyl-CoA utilization in *M. smegmatis*. Importantly, homologs for *gcl* and other glycerate pathway enzymes are absent in *Mtb* (Chopra et al., 2014).

Research concerning the *Mtb* isocitrate lyase (ICL), the first enzyme of the glyoxylate shunt, has been far more extensive than for malate synthase. Genetic knockout and knockdown studies targeting the genes encoding ICL (*icl1* and *icl2*) have demonstrated that ICL is required for establishment and maintenance of infection in mice (Blumenthal et al., 2010; McKinney et al., 2000; Munoz-Elias and McKinney, 2005). Subsequent studies have revealed that a secondary function outside of the glyoxylate shunt could contribute to this dramatic mouse phenotype. ICL also acts as a methylisocitrate lyase, an enzyme in the methylcitrate pathway that is involved in propionate detoxification (Gould et al., 2006; Upton and McKinney, 2007). Growth of ICL-deficient *Mtb* is inhibited by propionate, even in the presence of other carbon sources. Furthermore, loss of ICL results in accumulation of methylcitrate cycle

intermediates in glucose, acetate, and especially in propionate (Eoh and Rhee, 2014). In 0.05% propionate and 0.2% glucose, growth is rescued by addition of 10μg/ml vitamin B_{12}, a cofactor required for the function of methylmalonyl CoA mutase, an enzyme in the methylmalonyl-CoA pathway (Eoh and Rhee, 2014). This is an alternative propionyl-CoA metabolic pathway and alleviates propionate toxicity in the absence of a functional methylcitrate cycle (Savvi et al., 2008). The lack of mouse phenotype of a *prpDC* mutant, which lacks methylcitrate synthase and dehydratase activity in the methylcitrate cycle, suggests that *Mtb* either has access to vitamin B_{12} within the host which alleviates propionate toxicity via the methylmalonyl pathway, and/or that *Mtb* requires *prpDC* to make toxic metabolites from propionate (Muñoz-Elías et al., 2006; Savvi et al., 2008; Upton and McKinney, 2007). Indeed, a lack of methylisocitrate lyase activity caused by ICL deficiency would lead to an accumulation of methylcitrate and methylisocitrate, two potentially toxic metabolites that should not be generated in the *prpDC* knockout. Therefore, it is possible that a lack of methylisocitrate lyase activity, a lack of isocitrate lyase activity, or both together cause death of ICL-deficient *Mtb* in the mouse model.

In vitro studies have emphasized a role for ICL in *Mtb* survival in several contexts relevant to the host environment. During human infection, *Mtb* encounters a hypoxic environment potentially rich in fatty acids and other lipids. In hypoxia *in vitro*, *Mtb* adopts a bifurcated, reductive TCA cycle, whose end product is succinate (Eoh and Rhee, 2013; Watanabe et al., 2011). In this context, ICL is upregulated and plays a role in succinate generation, which helps *Mtb* adapt to hypoxia and maintain membrane potential, appropriate ATP levels, NAD^+/NADH ratio, and metabolite levels to prevent death (Eoh and Rhee, 2013). During exposure to 0.2% acetate or 0.2% propionate, ICL-deficient *Mtb* also died, and this death was rescued up to 3 days

by addition of vitamin B_{12}, suggesting that a lack of a functional methylcitrate cycle was the cause of death. ICL also plays a role in broad-spectrum antibiotic resistance, as Δ*icl1*Δ*icl2* bacteria were much more susceptible to killing by streptomycin, isoniazid, and rifampicin (Nandakumar et al., 2014). Addition of antioxidants thiourea or tempol to the bacteria enhanced viability of Δ*icl1*Δ*icl2* in these antibiotics, suggesting that ICL could also play a role in alleviating or preventing oxidative stress. Whether *Mtb* lacking malate synthase would also have similar phenotypes to ICL-deficient *Mtb* in these contexts remains to be determined.

There has been interest in development of malate synthase inhibitors as novel anti-TB therapeutics. Phenyl-diketo acid (PDKA) inhibitors, which contain structural similarities to glyoxylate, have shown efficacy at inhibiting growth of *Mtb* H37Rv in acetate and in glucose (Krieger et al., 2012). One specific inhibitor had an MIC_{99} of 2 μM in acetate and 8 μM in glucose against H37Rv *in vitro*, and reduced the ability of *Mtb* to establish infection in mice. Furthermore, overexpressing *glcB* in strains treated with the inhibitor raised the MIC in both acetate and glucose, but did not raise the MIC in strains treated with rifampicin, suggesting that the inhibitor has on-target effects in both conditions. These data support a role for malate synthase for growth in a variety of carbon sources, although the reason for its requirement in glucose is unclear.

We aimed to use genetic methods to further validate malate synthase as a drug target in *Mtb* and to better understand the role of the glyoxylate shunt during infection. In doing so, we uncovered a role for malate synthase in virulence and in *Mtb* fatty acid resistance.

3.3 Results

3.3.1 Generation of the malate synthase knockdown strain

Due to conflicting reports of *glcB* essentiality and a described inability to directly generate a *glcB* knockout strain, we first introduced a second copy of *glcB* into the attL5 phage integration site to generate a merodiploid strain. We transformed this merodiploid strain with a temperature-sensitive knockout plasmid containing a hygromycin resistance cassette flanked with DNA regions homologous to those surrounding *glcB* in the native locus. After selecting for double crossover a few colonies were obtained. These were confirmed to contain the expected deletion by Southern blot (Figure 3.2A-B). Candidate number one was used for the generation of all *glcB* mutants described here and will be referred to as the *glcB* att site mutant.

We then generated a dual control (DUC) strain, in which both transcription of *glcB* and proteolysis of MS were controlled by addition of anhydrotetracycline (atc) (Kim et al., 2011). After confirming that atc addition reduced expression of MS to undetectable levels (Figure 3.2C), we tested growth of *glcB*-DUC in media with single carbon sources plus and minus atc (Figure 3.3). As expected, *glcB*-DUC could not grow plus atc in acetate alone. However, *glcB*-DUC plus atc could grow in glucose alone with a slight growth defect compared to WT. This suggested that *glcB* is not essential for growth in all conditions.

3.3.2 Generation of the *glcB* knockout strain (Δ*glcB*)

To determine whether *glcB* is essential on plate media, we attempted to generate a *glcB* knockout by replacement transformation of the *glcB* att-site mutant with a plasmid lacking *glcB*. Successful transformants lose the *glcB* plasmid but gain kanamycin resistance. We tried plating on conditions identical to those used to

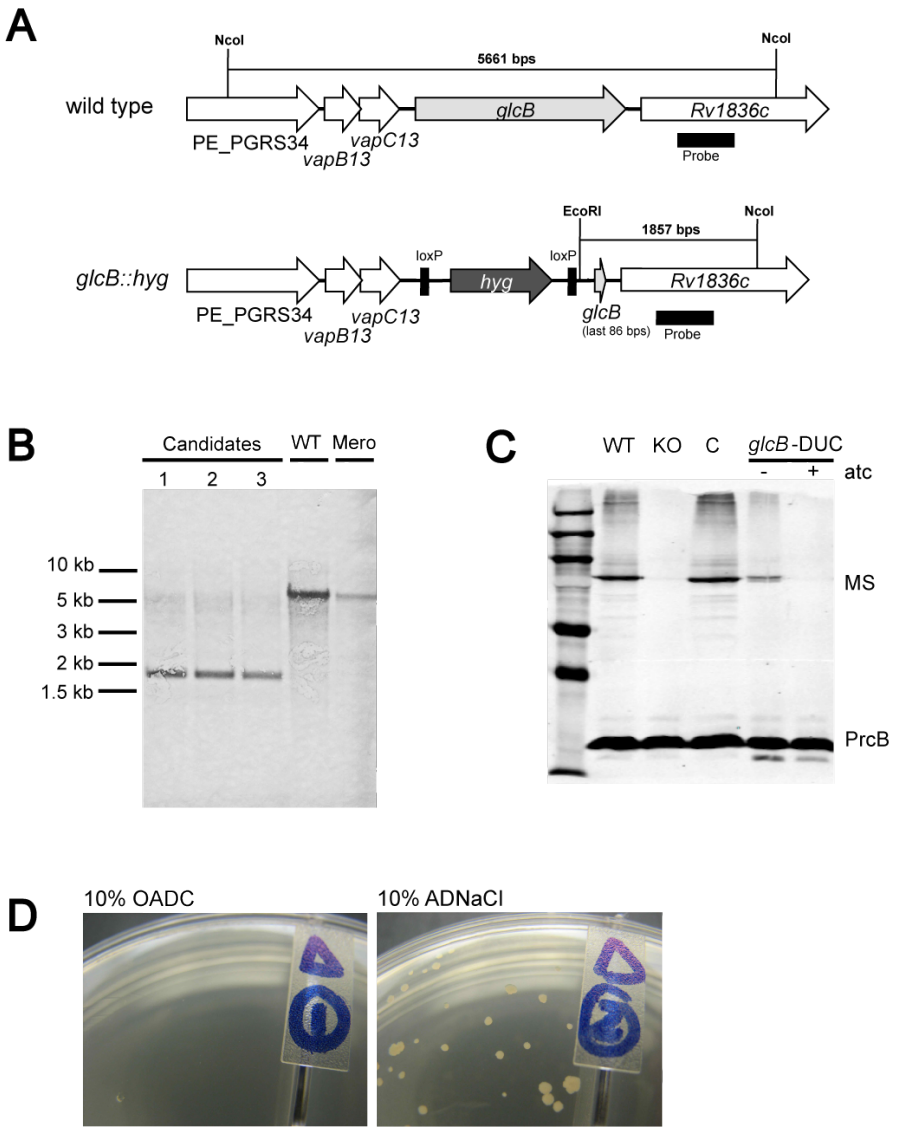

Figure 3.2. Confirmation of the generation of the *glcB* conditional knockdown and knockout strains. (**A**) Southern blot design showing the genomic locus of *glcB* and the same locus after successful replacement of 2140 bps of *glcB* with a hygromycin resistance cassette via homologous recombination with a knockout plasmid. (**B**) Southern blot showing three candidates derived from the merodiploid (Mero) strain which express *glcB* at the attL5 site but lack a functional *glcB* in the native locus, as indicated by the expected shift in band size. Candidate 1 was used for generation of all *glcB* mutant strains. (**C**) Western blot showing malate synthase (MS) protein expression level of wildtype (WT), Δ*glcB* (KO), *glcB* complemented (C), and *glcB*-dual control (DUC) strains minus or plus anhydrotetracycline (atc). (**D**) 7H10 agar plates containing 10% OADC supplement do not support growth of the Δ*glcB* while plates containing 10% ADNaCl supplement support growth of small, slow-growing colonies. OADC contains oleic acid and catalase, while ADNaCl does not.

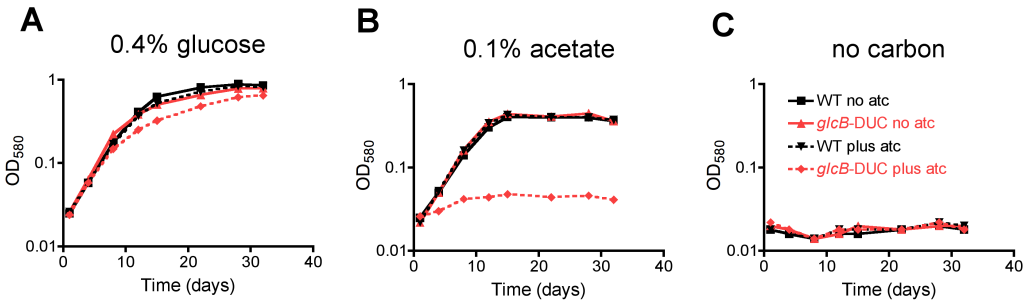

Figure 3.3. Silencing of *glcB* inhibits *Mtb* growth in acetate but does not prevent growth in glucose. Wildtype (WT) and *glcB*-DUC strains were grown plus and minus 500ng/ml atc in (**A**) 0.4% glucose, (**B**) 0.1% acetate, or (**C**) no carbon in minimal carbon-defined media.

generate the *fba* knockout (see Chapter 2). Similar to the *fba* mutant, no colonies grew on standard *Mtb* kanamycin plates containing 10% OADC and 0.5% glycerol, while colonies did appear on kanamycin plates containing 10% ADNaCl and 0.5% glycerol. OADC supplement contains oleic acid and catalase, while ADNaCl does not. However, unlike with the *fba* knockout, addition of 0.2% extra glucose did not allow for growth on plates containing OADC (not shown). This suggested that *glcB* is not essential for *Mtb* growth on plates lacking oleic acid and catalase.

We selected several *glcB* knockout candidates from the ADNaCl plate and successfully grew them in standard *Mtb* liquid media containing 0.2% glucose and 0.2% glycerol. The *glcB* knockout candidate (Δ*glcB*) we chose for this study lacked MS expression and recapitulated the OADC sensitivity when re-cultured on agar plates (Figure 3.2C-D). Growth of Δ*glcB* takes roughly 40 days to appear on plates. In collaboration with Dr. Jim Sacchettini and Dr. Tom Ioerger, the genomic DNA of the *glcB* knockout was sequenced and confirmed to have the expected *glcB* deletion. Δ*glcB* also had a point mutation in *embC* (N693K), a gene involved in synthesis of cell wall component arabinan, and a 5.5 kilobase deletion in *ppsA* and *ppsB*, genes involved in biosynthesis of phthiocerol dimycocerosate (PDIM), a cell wall lipid. Mutations in PDIM are common in *Mtb* strains passaged *in vitro* in laboratory conditions (Domenech and Reed, 2009). To rule out effects these secondary mutations may have on phenotypes we observed, we generated a Δ*glcB* complemented strain derived from the Δ*glcB* strain, in which *glcB* is expressed at the attL5 site from its native promoter (Figure 3.2C). We used this strain as a control in subsequent experiments throughout this chapter.

3.3.3 Malate synthase is essential for *Mtb* growth and persistence in the mouse

To determine the importance of malate synthase for establishment and maintenance of infection in an animal model, we infected mice with WT Erdman, Δ*glcB*, and *glcB*-DUC *Mtb* strains. Mice infected with *glcB*-DUC were fed mice doxy food to silence *glcB* at different timepoints during and after establishment of infection (Figure 3.4). We found that *glcB* was required for both growth and maintenance of infection in mouse lungs and spleens. Furthermore, silencing *glcB* after establishment of infection reduced lung lesion size by day 113 post-infection. These data showed that targeting MS can kill *Mtb in vivo* and validates further work on MS inhibitors.

3.3.4 Malate synthase is dispensable for growth in glucose and glycerol, but not in acetate, fatty acids, and cholesterol

To better understand the conditional essentiality of the *glcB* knockout, we assessed growth of Δ*glcB* in various single carbon sources. Similar to growth of the *glcB*-DUC strain plus atc, growth of Δ*glcB* was achieved in glucose but not acetate (2-carbon). Δ*glcB* also grew in glycerol but failed to grow in fatty acids propionate (3-carbon) and butyrate (4-carbon) (Figure 3.5). We also tested growth in media containing 0.01% cholesterol, a physiologically-relevant carbon source that is broken down into pyruvate, acetyl-CoA, and propionyl-CoA, as described (Griffin et al., 2012) (Figure 3.6A). While the WT enhanced its growth in cholesterol, Δ*glcB* did not. This demonstrated that malate synthase is essential for growth on acetate, cholesterol, and fatty acids, including carbon sources that feed into the methylcitrate cycle.

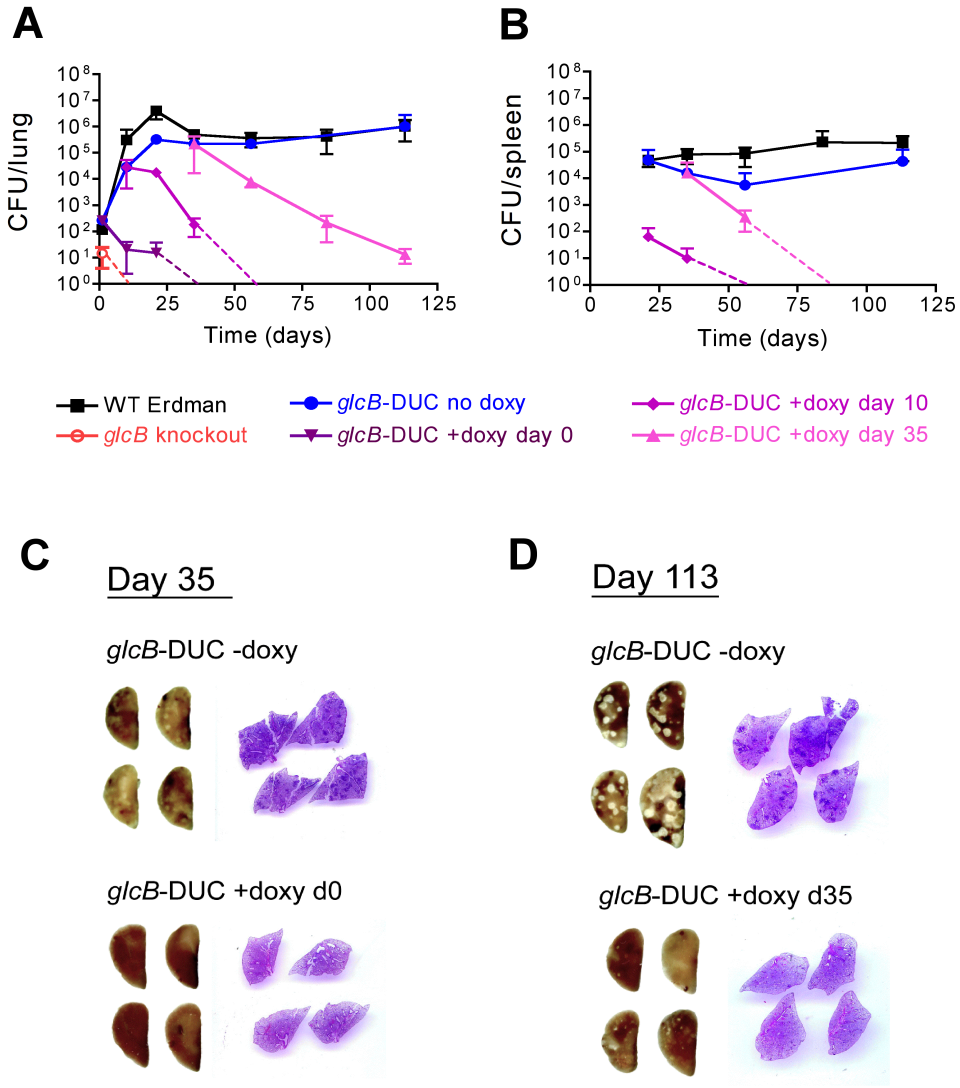

Figure 3.4. Malate synthase is required for growth and survival of *Mtb* in the mouse model. (**A**) Lung and (**B**) spleen bacterial burden over time in mice infected on day 0 with WT or the *glcB*-DUC *Mtb* strains. Organ homogenates were plated on 7H10 ADNaCl plates. Mice infected with *glcB*-DUC were given doxy mouse chow on the indicated days. There were no detected atc-resistant revertants. Similar results for the early timepoints were observed in a short-term (28-day) infection. Data are means +/-SD. (**C-D**) Gross pathology and H&E staining of lung sections from mice infected with *glcB*-DUC on day 35 day 113 post-infection.

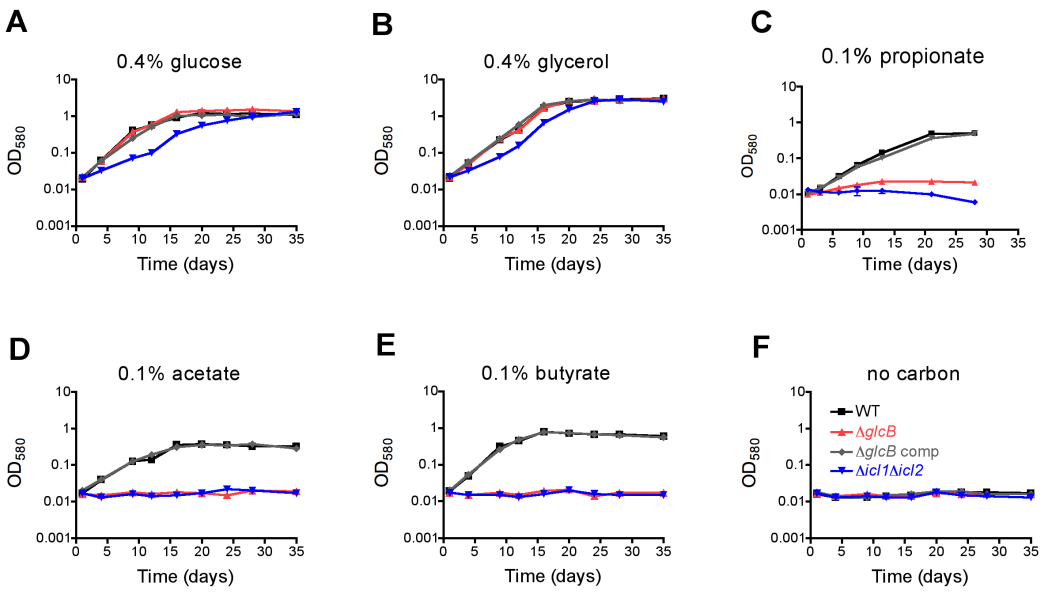

Figure 3.5. Malate synthase is required for growth in acetate, propionate, and butyrate but not in glucose or glycerol. The WT, Δ*glcB*, Δ*glcB* complemented (comp), and Δ*icl1*Δ*icl2* strains were grown in single carbon sources (**A**) 0.4% glucose, (**B**) 0.4% glycerol, (**C**) 0.1% propionate, (**D**) 0.1% acetate, (**E**) 0.1% butyrate, or (**F**) no carbon, in carbon-defined minimal media. Data are representative of at least two experiments.

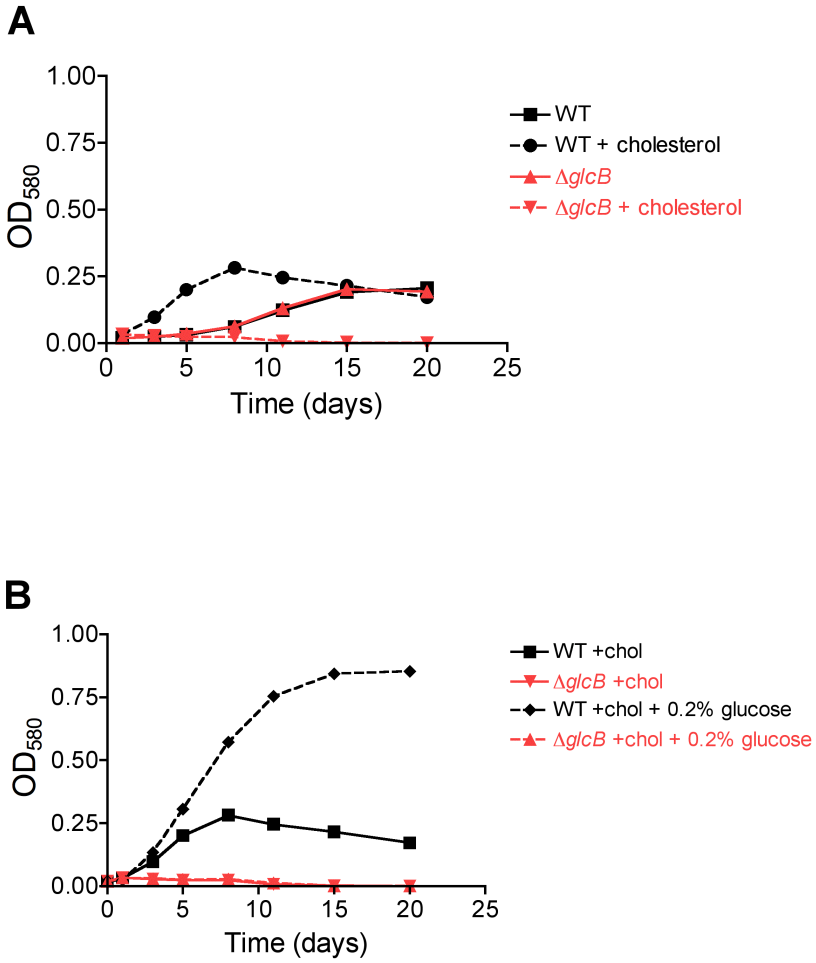

Figure 3.6. Growth of Δ*glcB* is inhibited by cholesterol. (**A**) Growth of WT Erdman and Δ*glcB* in Sassetti base medium, plus or minus 0.01% cholesterol. (**B**) Growth of WT Erdman and Δ*glcB* in Sassetti base medium plus 0.01% cholesterol with or without 0.2% glucose. Data are representative of two experiments.

3.3.5 Acetate alters growth of Δ*glcB* in glucose in a dose-dependent manner

Mtb is thought to encounter fatty acids and other lipids within the host environment, but may also encounter carbon sources such as carbohydrates. In order to mimic the effect of exposure to fatty acids we chose to use acetate as a carbon source, as it does not have solubility issues. Similar to fatty acids, acetate enters the TCA cycle after conversion to acetyl-CoA. In order to determine whether presence of a carbohydrate (glucose) could rescue growth in acetate, we performed 96-well plate growth assays and growth curves in flasks in which glucose concentration was kept constant (0.2%) while acetate concentration varied (Figure 3.7, 3.8A). WT *Mtb* is known to co-catabolize carbon sources glucose and acetate to enhance its growth, which is what we observed (de Carvalho et al., 2010a). We also observed that growth of Δ*glcB* was enhanced by low concentrations of acetate. However, acetate was growth inhibitory for the Δ*glcB* at a concentration of 0.1% and higher, whereas acetate did not become growth inhibitory for the WT until 0.4%. Growth of Δ*glcB* in media containing 0.01% cholesterol was also not rescued by 0.2% glucose (Figure 3.6B). These data showed that Δ*glcB* is able to co-catabolize glucose and acetate at lower acetate concentrations to enhance its growth. However, high acetate concentrations and 0.01% cholesterol have a dominant negative effect, as glucose could not rescue growth of Δ*glcB* in these conditions.

3.3.6 Δ*glcB* slowly in acetate, and glucose exacerbates this phenotype

To understand whether acetate kills *Mtb* lacking malate synthase and whether glucose can rescue this effect, we determined viability with colony forming unit (CFU) assays in 0.025% acetate, 0.2% acetate, 0.2% acetate plus 0.2% glucose, and 0.2% plus 0.4%

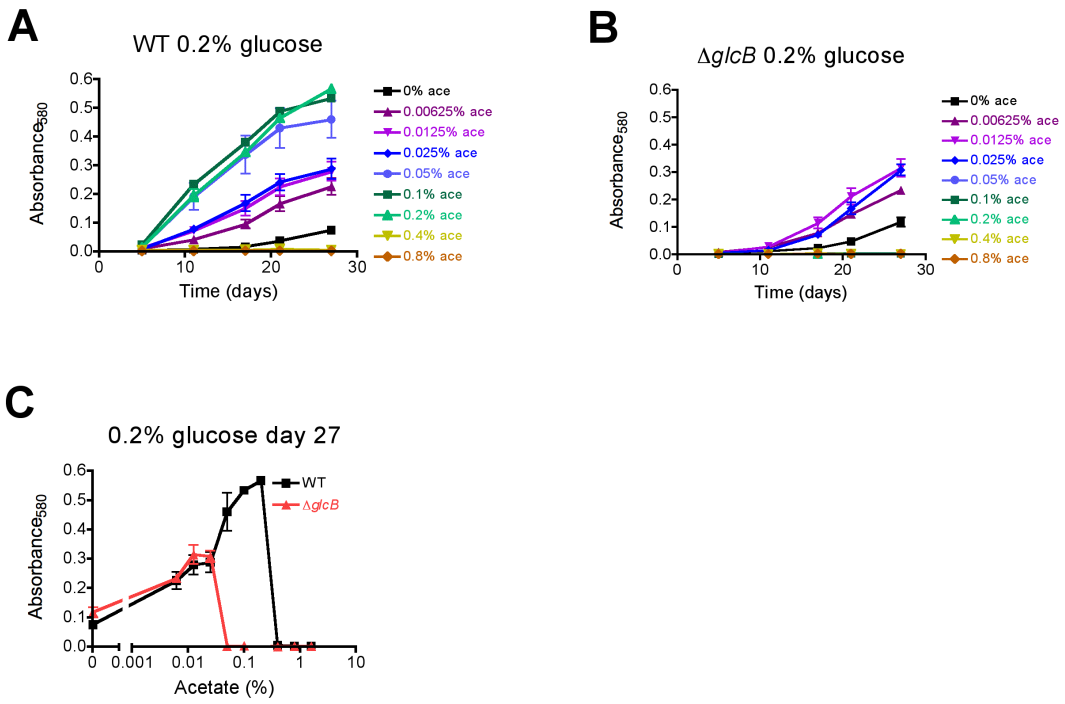

Figure 3.7. Growth of *Mtb* lacking *glcB* is enhanced or inhibited by acetate, depending on the concentration. Growth of (**A**) WT or (**B**) Δ*glcB* strains in 0.2% glucose supplemented with the indicated concentrations of acetate. (**C**) Comparison of WT and Δ*glcB* growth on day 27 at varying acetate concentrations. Assays were performed in 96-well plate format and data are means +/- SEM of triplicate cultures with carbon-defined minimal media.

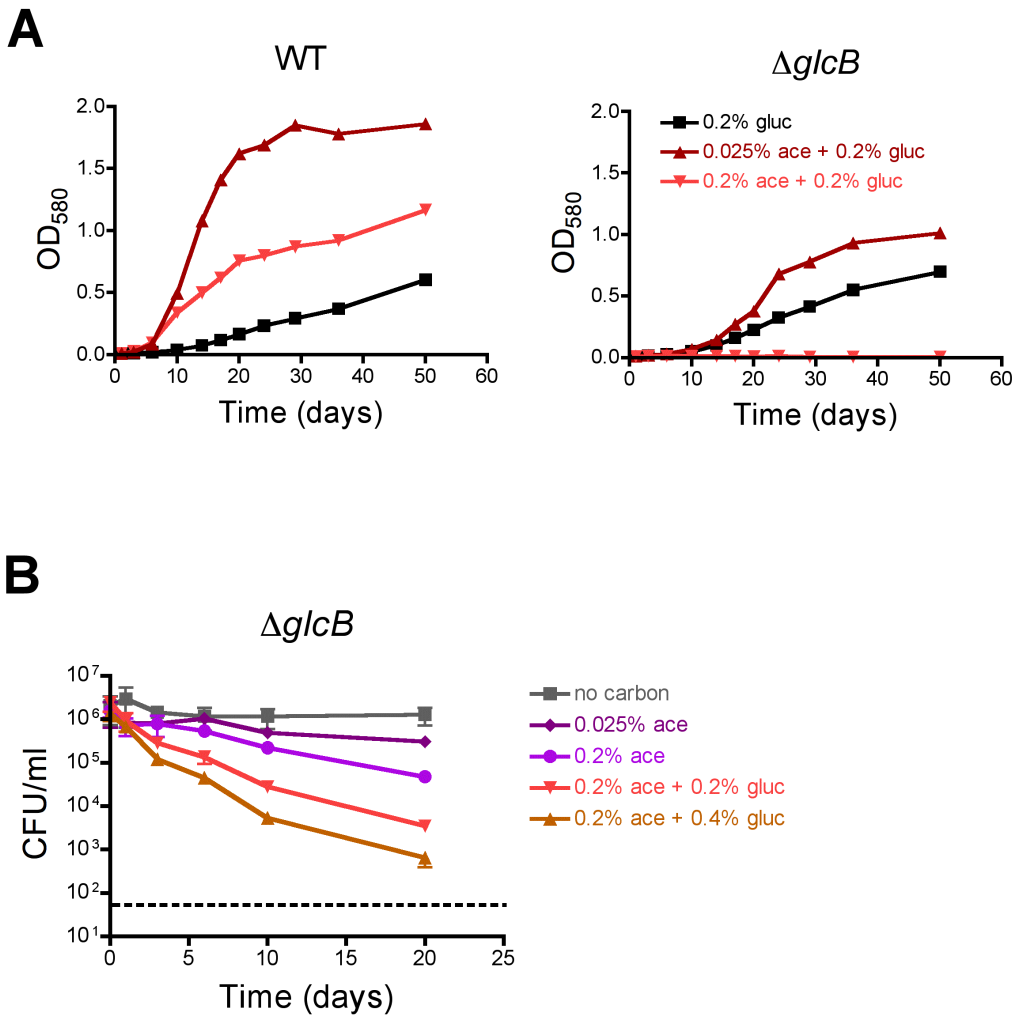

Figure 3.8. Δ*glcB* growth and survival is impaired by high but not low acetate concentrations. (**A**) WT Erdman and Δ*glcB* were grown in T25 flasks in carbon-defined minimal medium plus the indicated carbon sources. (**B**) Δ*glcB* was exposed to the indicated carbon source(s) in T25 flasks and aliquots were plated for CFU at the indicated time points. Survival data are the means +/- SD of triplicate cultures.

glucose (Figure 3.8B). We found that survival of Δ*glcB* bacteria was dependent on the concentration of acetate in the media and that death in 0.2% acetate was exacerbated by glucose. In media with no added carbon, Δ*glcB* persisted. A concentration of 0.025% acetate led to ~½ $\log_{10}$ killing by day 20, while 0.2% acetate resulted in ~1 $\log_{10}$ killing. Addition of 0.2% glucose to 0.2% acetate resulted in over 2 $\log_{10}$ drop in CFU and addition of 0.4% glucose to 0.2% acetate resulted in a ~3 $\log_{10}$ reduction by day 20. These data showed that acetate exposure impairs survival of Δ*glcB* in the absence of glucose, and that glucose enhances killing in 0.2% acetate in a concentration-dependent manner.

3.3.7 Δ*glcB* experiences metabolic perturbations in acetate

In order to confirm that *glcB* deletion inhibited malate synthase activity, and to determine the metabolic changes associated with growth-permissive and non-permissive conditions, we used a metabolomics approach. WT, Δ*glcB*, and Δ*glcB* complemented strains were grown on filters and exposed to 0.2% glucose, 0.2% acetate, 0.025% acetate plus 0.2% glucose or 0.2% acetate plus 0.2% glucose for one day. Analysis of the metabolite pool sizes in bacterial lysates by liquid chromatography-mass spectrometry (LC-MS) indicated drastic changes in Δ*glcB* exposed to high levels of acetate (Figure 3.9 and Table 3.1).

Glyoxylate, a substrate for the malate synthase reaction, accumulated in the knockout compared to WT and the complemented strain in all conditions tested. Compared to WT, Δ*glcB* accumulated glyoxylate 9.9-fold more in 0.2% glucose, 37.0-fold more in 0.2% acetate, 21.2-fold more in 0.025% acetate plus 0.2% glucose, and 73.2-fold more in 0.2% acetate plus 0.2% glucose. Accumulations were also observed for other metabolites in 0.2% acetate plus 0.2% glucose, including alpha-ketoglutarate, cis-

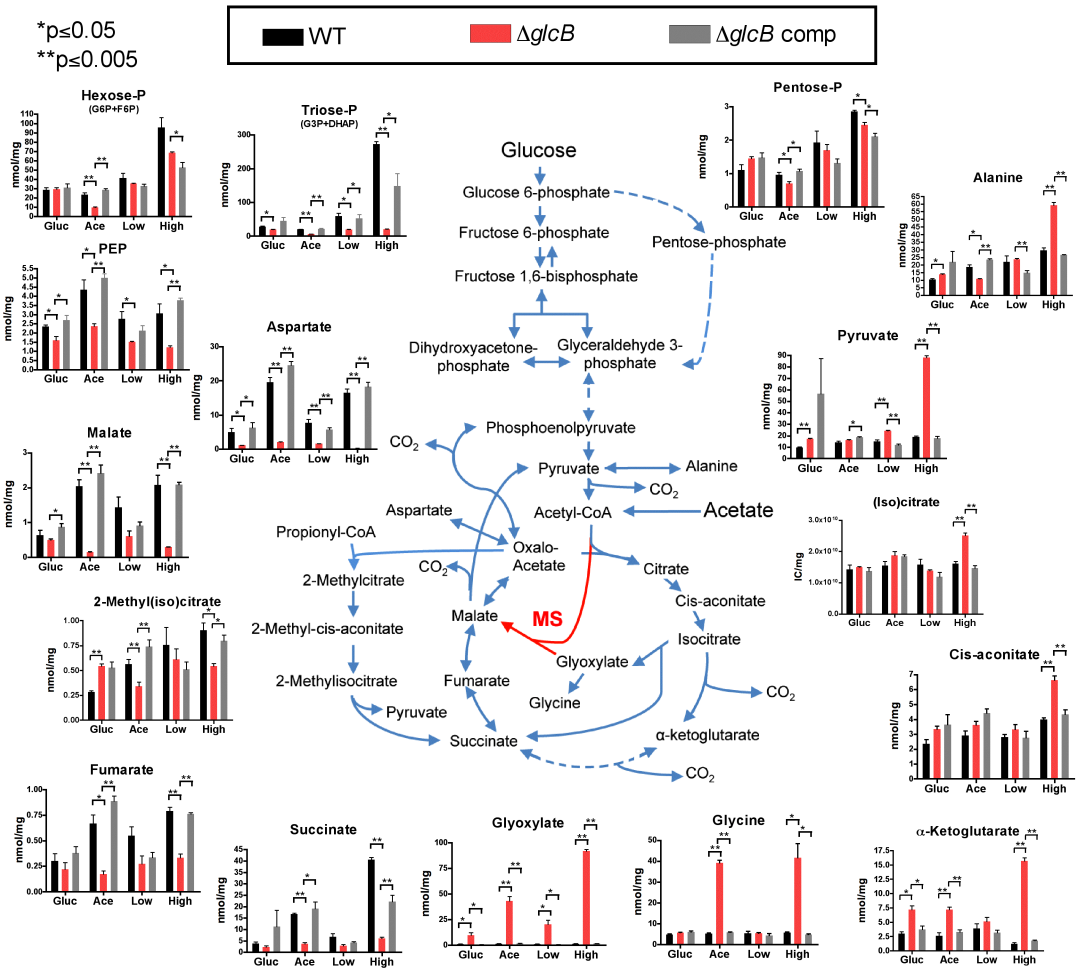

Figure 3.9. Metabolic profiling reveals accumulation of metabolites upstream of MS reaction and depletion of downstream metabolites in acetate. Liquid chromatography mass spectrometry (LCMS) analysis of bacterial lysates after bacterial exposure to 0.2% glucose (Gluc), 0.2% acetate (Ace), 0.2% glucose plus 0.025% acetate (Low), or 0.2% glucose plus 0.2% acetate (High) for one day. Metabolite levels are reported as nmol per mg protein, except in the case of (iso)citrate reported in ion counts (IC) per mg protein (these ion counts were outside the range of the standards). G6P is glucose 6-phosphate, F6P is fructose 6-phosphate, DHAP is dihydroxyacetone phosphate, G3P is glyceraldehyde 3-phosphate, PEP is phosphoenolpyruvate. Statistical analysis was performed using students two-tailed T-test *p≤0.05 **p≤0.005.

Table 3.1. Δ*glcB* fold change compared to WT. Bold values are statistically significant.

Metabolite	0.2% glucose (Gluc)	0.2% acetate (Ace)	0.025% acetate + 0.2% glucose (Low)	0.2% acetate + 0.2% glucose (High)
alanine	**1.33**	**-1.70**	1.07	**1.99**
α-ketoglutarate	**2.36**	**2.76**	1.30	**12.87**
aspartate	**-4.41**	**-9.49**	**-4.80**	**-73.34**
cis-aconitate	1.43	1.24	1.19	**1.66**
citrate/isocitrate	1.05	1.21	-1.14	**1.56**
fumarate	-1.38	**-3.86**	-2.00	**-2.37**
glycine	1.20	**7.20**	1.00	**7.20**
glyoxylate	**9.87**	**36.96**	**21.23**	**73.21**
hexose-P	-1.48	**-3.42**	-3.13	-1.40
malate	-1.28	**-13.93**	-2.39	**-7.15**
methylcitrate	**1.92**	**-1.64**	-1.23	**-1.66**
pentose-P	1.30	**-1.36**	-1.13	**-1.16**
PEP	**-1.46**	**-1.84**	**-1.82**	**-2.50**
pyruvate	**1.80**	1.13	**1.60**	**4.69**
succinate	-1.63	**-4.55**	-2.37	**-6.67**
triose-P	**-0.98**	**-2.43**	**-1.17**	**-13.93**

aconitate, (iso)citrate, pyruvate, glycine, and alanine. The metabolite extraction method used for this experiment could not be used to measure acetyl-CoA levels, the other substrate of the malate synthase reaction. Glycine, a potential downstream product of glyoxylate via a glyoxylate aminase reaction increased in Δ*glcB* in 0.2% acetate-containing conditions.

In contrast to accumulations upstream of malate synthase, depletions were observed in downstream metabolites malate and aspartate. Malate levels were decreased in the knockout compared to WT 13.93-fold in 0.2% acetate and 7.15-fold in 0.2% acetate plus 0.2% glucose. Aspartate, which is indicative of oxaloacetate levels, was also decreased 4.41-fold in glucose, 9.49-fold in acetate, and 4.8-fold in 0.2% glucose plus 0.025% acetate and 73.34-fold in 0.2% glucose plus 0.2% acetate. Other metabolite decreases in Δ*glcB* included hexose-phosphates, triose-phosphates, pentose-phosphates, 2-methyl(iso)citrate, alanine, and succinate in 0.2% acetate-containing conditions. Many of these changes are absent or reduced in the 0.025% acetate plus 0.2% glucose condition, a growth-permissive condition.

These results indicate that upon exposure to high levels of acetate, Δ*glcB* experiences many metabolic perturbations within glycolysis/gluconeogenesis, the TCA cycle, and the glyoxylate shunt. Accumulations of metabolites upstream of the malate synthase reaction and depletion of metabolites downstream of the reaction confirm the expected role of *glcB* as the primary malate synthase gene in *Mtb*. These perturbations may contribute to the growth and survival phenotypes of Δ*glcB* in acetate. Interestingly, addition of glucose to acetate largely exacerbates the metabolic changes that we observe and does not improve aspartate or malate levels. Adding exogenous malate or aspartate did not rescue growth of Δ*glcB* in acetate (Figure 3.10). These data suggest that in *Mtb* lacking malate synthase, the presence of high amounts of acetate leads to

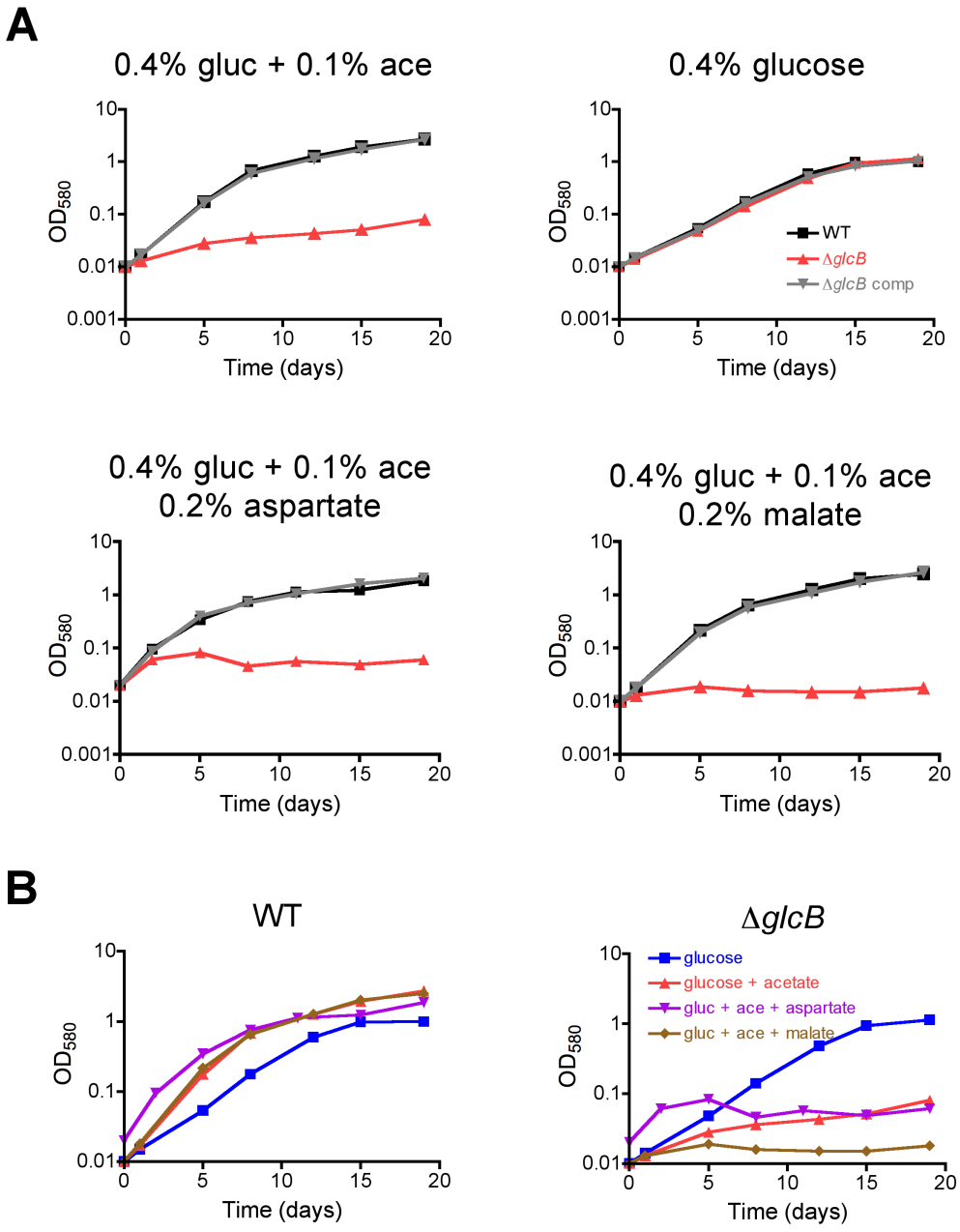

Figure 3.10. Exogenous malate and aspartate do not rescue acetate-mediated growth inhibition. (**A**) WT, Δ*glcB*, and Δ*glcB* complemented strains were grown in 0.4% glucose and 0.1% acetate; 0.4% glucose; 0.4% glucose, 0.1% acetate, and 0.2% malate; or 0.4% glucose, 0.1% acetate, and 0.2% aspartate in carbon-defined minimal medium. (**B**) Same data as in (**A**) but comparing growth of WT or Δ*glcB* in the four media types used in (**A**).

accumulation of toxic metabolites (such as glyoxylate) or flux of carbon away from the glyoxylate shunt that leads to detrimental effects to the cell.

3.3.8 Δ*glcB* accumulates metabolites in branched-chain amino acid synthesis in acetate

In order to get a global picture of metabolic changes within the *glcB* KO exposed to acetate, we also identified metabolites based on their expected mass over charge ratio, in the absence of standards. This approach is hypothesis generating, and there is the possibility that metabolites are incorrectly annotated. We found that many amino acid pools were depleted in the *glcB* knockout compared to WT in 0.2% acetate and in 0.2% acetate plus 0.2% glucose (Figure 3.11). However, metabolites involved in branched-chain amino acid synthesis, including α-methylmalate, α-acetolactate, and keto(iso)leucine were increased. This suggests that deletion of *glcB* affects branched chain amino acid synthesis and/or degradation pathways.

A reaction that is similar to the malate synthase reaction is the first committed step of leucine biosynthesis catalyzed by α-isopropylmalate synthase. This reaction uses acetyl-CoA and α-ketoisovalerate as substrates (Koon et al., 2004). α-ketoisovaleric acid ($C_5H_8O_3$) and glyoxylic acid ($C_2H_2O_3$) are both α-keto acids, containing a carboxylic acid and ketone group. Due to the observed accumulation of metabolites upstream of this enzymatic step, we hypothesized that high glyoxylate may compete with α-ketoisovalerate to inhibit this reaction, or that high levels of acetyl-CoA could contribute to substrate inhibition. Therefore, we tried adding exogenous leucine or isoleucine (as a control) to rescue growth of Δ*glcB*. However, we did not observe a substantial enhancement of growth with leucine (Figure 3.12). It is possible that leucine does not enter *Mtb* efficiently enough to rescue growth, that leucine deficiency

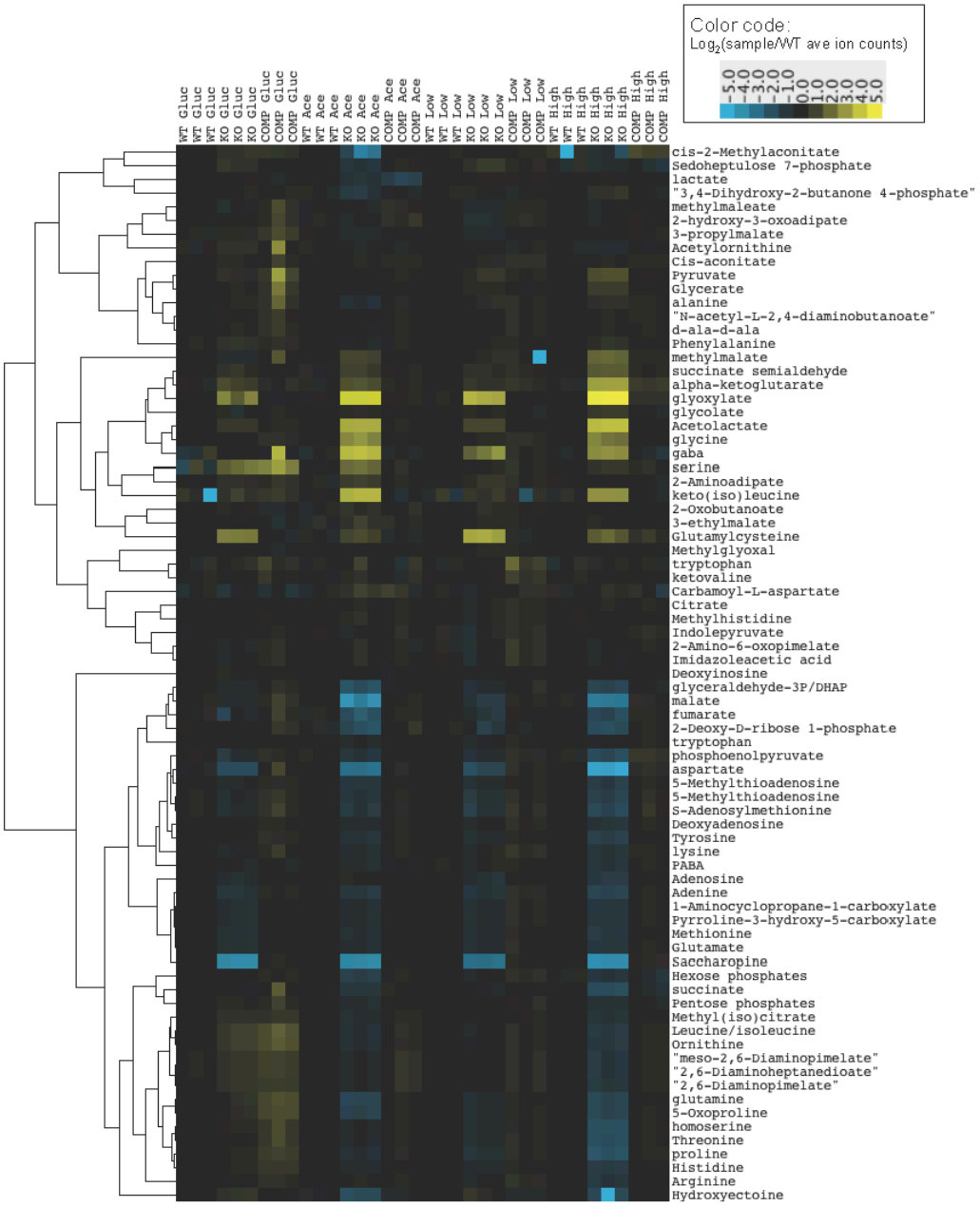

Figure 3.11. Clustered heatmap of metabolite levels in the WT, Δ*glcB*, and Δ*glcB* complemented strains. Wild-type (WT), Δ*glcB* (KO), and *glcB* complemented (COMP) strains were exposed for 1 day to 0.2% glucose (Gluc), 0.2% acetate (Ace), 0.025% acetate and 0.2% glucose (Low), or 0.2% acetate and 0.2% glucose (High) prior to metabolite extraction. Metabolite levels are represented as yellow (accumulation) or blue (depletion), as determined by the $\log_2$ value of the ion counts of the sample divided by the average of the ion counts of three WT samples in that condition. Profinder was used to analyze the data and generate ion counts while hierarchical complete linkage clustering by the Cluster software was used along with Java TreeView to organize and present the data.

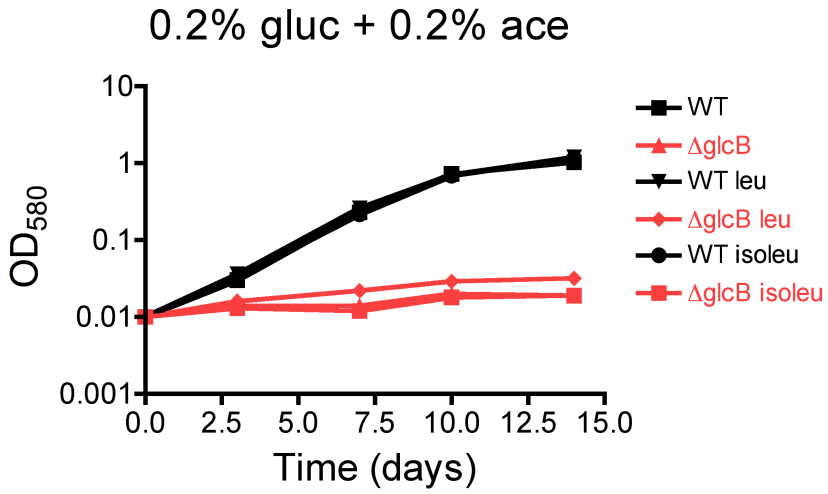

Figure 3.12. Leucine does not rescue growth of Δ*glcB* in acetate. Erdman (WT) and Δ*glcB* (*glcB* KO) were grown in 0.2% glucose plus 0.2% acetate and incubated +/- 0.2% leucine (leu) or 0.2% isoleucine (isoleu) (as a control).

does not contribute to acetate-mediated growth inhibition, or that other factors also contribute to the growth phenotype.

Using this global analysis approach we also examined metabolic changes in 0.025% acetate plus 0.2% glucose, a condition in which the growth rate of Δ*glcB* is enhanced compared to 0.2% glucose alone. In general, depletions and accumulations were less severe in this condition compared to 0.2% acetate or 0.2% acetate plus 0.2% glucose, and metabolite levels were comparable to those in 0.2% glucose.

3.3.9 Potential increase in protein acetylation in glyoxylate shunt mutants

Although we could not measure acetyl-CoA levels in the metabolomics samples used for the previous analysis, we hypothesized that deleting malate synthase could result in enhanced levels of acetyl-CoA, or activation of pathways that use acetyl-CoA as a substrate. Lysine acetylation has received attention as a post-translational modification involved in the regulation of carbon metabolic pathways, and also uses acetyl-CoA as a substrate (Liu et al., 2014). Therefore, we aimed to determine whether acetylation profiles change in Δ*glcB* in 0.2% acetate, which could contribute to growth inhibition. We also included Δ*icl1*Δ*icl2* as a control. Interestingly, we observed enhancement of band intensities of lysates probed with acetylated lysine antibody from both *glcB* and *icl1icl2* knockouts (Figure 3.13). Future work will need to involve confirmation of the specificity of the antibody in detection of acetylated proteins, as adjuvants used for antibody generation can include *Mtb* components. However, this suggests that acetylation may occur similarly between the two knockouts in 0.2% acetate.

3.3.10 Evidence for glyoxylate toxicity

Glyoxylate has been implicated as a potentially toxic metabolite (Vereecke et al., 2002). To determine whether glyoxylate toxicity plays a role in acetate-mediated

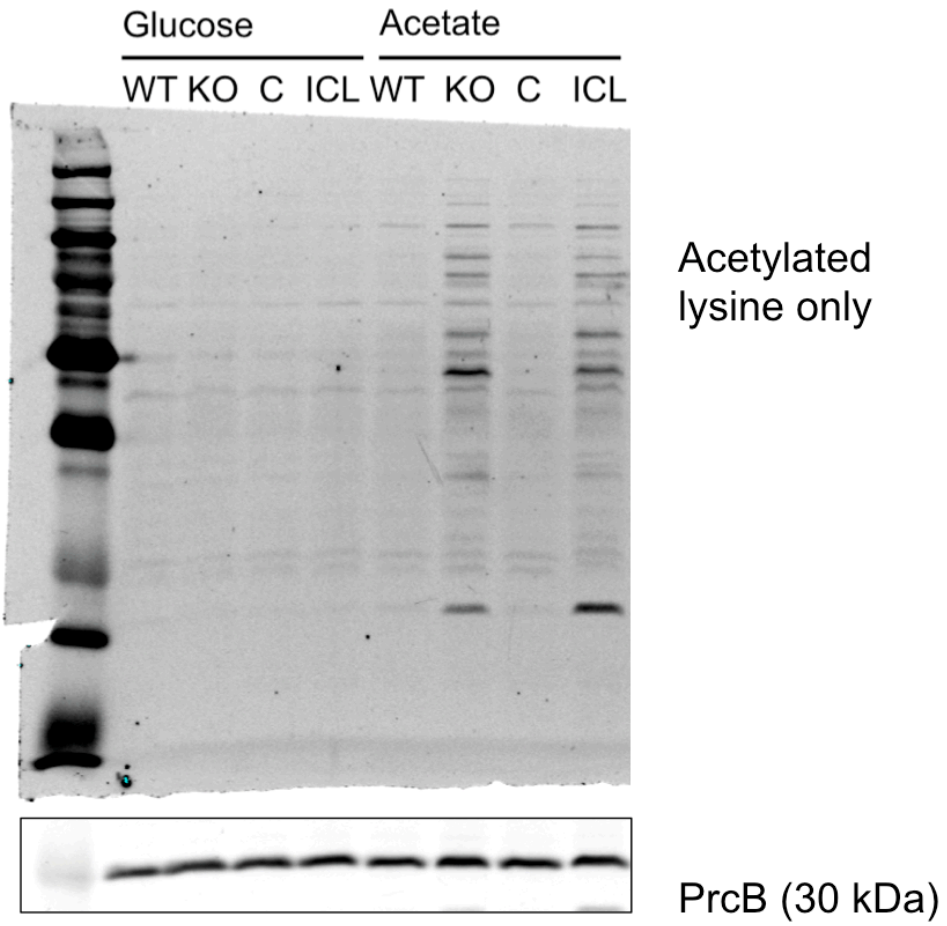

Figure 3.13. Global acetylation profiles of Δ*glcB* and Δ*icl1*Δ*icl2* change in acetate. Erdman (WT), Δ*glcB* (KO), Δ*glcB* complemented (C) and Δ*icl1*Δ*icl2* (ICL) strains were grown in 0.4% glucose and resuspended in 0.2% glucose or 0.2% acetate for one day. Protein lysates were probed using the commercially available anti-acetylated lysine antibody (Cell Signaling). Blot was subsequently probed with PrcB antibody as a loading control.

growth inhibition, we assessed whether adding exogenous glyoxylate could render Δ*glcB* more sensitive to acetate. A dose response assay in which growth of Δ*glcB* was measured at different acetate concentrations revealed that without glyoxylate, 0.05% acetate is growth inhibitory (Figure 3.14A). The presence of 0.2% or 0.3% glyoxylate rendered Δ*glcB* sensitive to 0.025% acetate. To obtain a more precise quantification of the inhibitory acetate concentration, we repeated this experiment with six acetate concentrations between 0 and 0.04% acetate (Figure 3.14B). While growth of the knockout was completely inhibited in 0.04% acetate, growth of the knockout plus 0.2% glyoxylate was completely inhibited by 0.02% acetate. Although the WT biomass (as measured by absorbance at 580 nm) was slightly reduced with glyoxylate treatment, the minimum amount of acetate that inhibited growth completely (0.4%) did not change. This suggests that glyoxylate toxicity may contribute to acetate-mediated toxicity. Inefficient glyoxylate entry or potential glyoxylate efflux may explain the absence of a more dramatic phenotype.

More evidence supporting the idea of glyoxylate toxicity comes from the existence of growth conditions in which Δ*icl1*Δ*icl2* grows better than Δ*glcB*. In media containing glucose or glycerol alone, Δ*glcB* grew better than Δ*icl1*Δ*icl2* (Figure 3.5A-B), which is likely attributed to the dual function of *icl* in the methylcitrate cycle and the glyoxylate shunt. However, Δ*icl1*Δ*icl2* grew normally on agar plates containing 10% OADC supplement (which contains the carbon source oleic acid) but lacking malachite green (not shown), whereas Δ*glcB* did not grow on plates containing OADC (Figure 3.2D) and also grew more slowly on plates lacking OADC than the *icl* KO. We investigated whether this was true for liquid culture conditions as well and found that Δ*glcB* displayed a growth lag in rich media containing 10% OADC and 0.5% glycerol compared to both the WT and Δ*icl1*Δ*icl2* strains (Figure 3.15). This growth

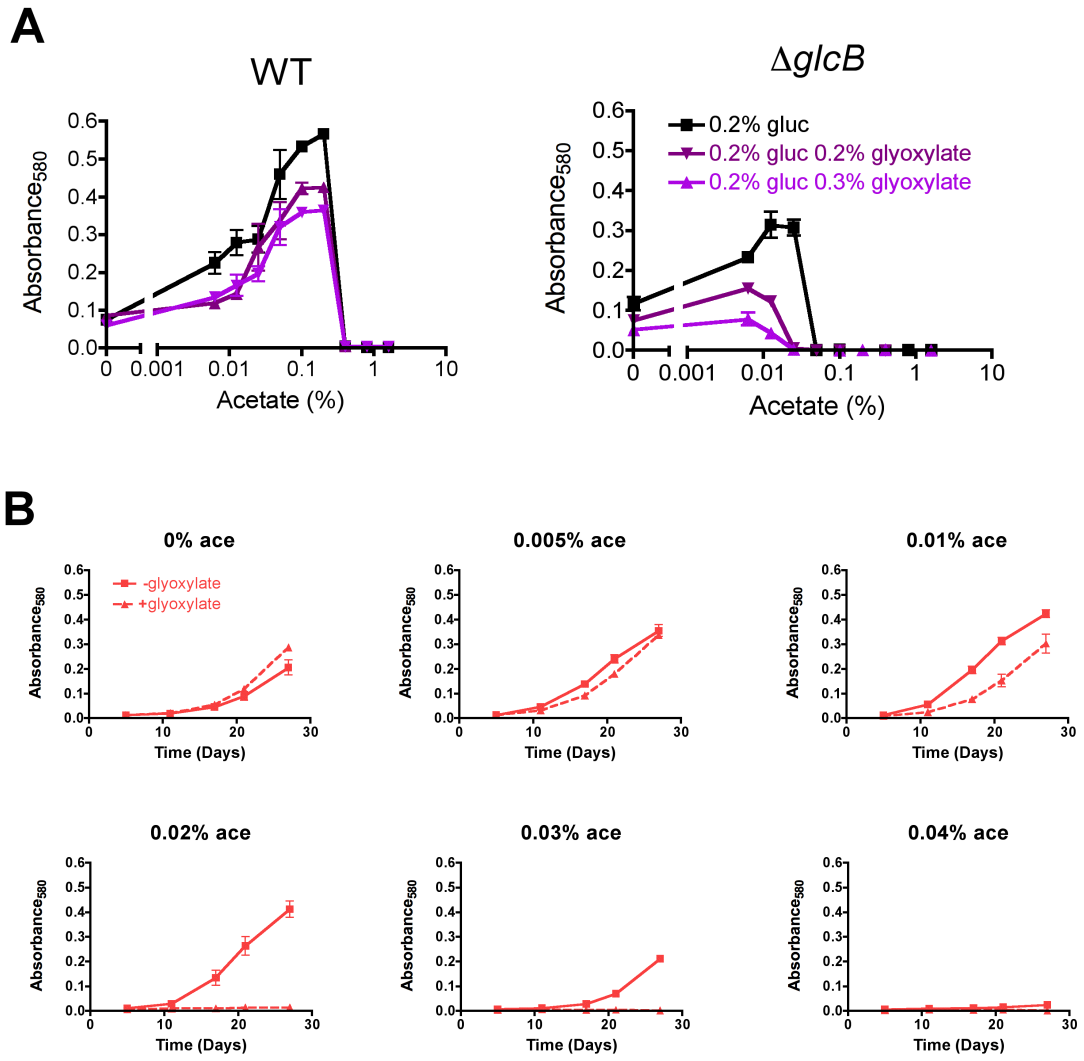

Figure 3.14. Exogenous glyoxylate exacerbates acetate-induced growth inhibition of Δ*glcB*. (**A**) Sensitivity of the WT and Δ*glcB* to acetate in constant 0.2% glucose (gluc), 0.2% glucose plus 0.2% glyoxylate, or 0.2% glucose plus 0.3% glyoxylate on day 27. This data +/- 0.2% glyoxylate is representative of two (WT) or three (Δ*glcB*) experiments. (**B**) Kinetics of growth of Δ*glcB* in 0.2% glucose plus varied acetate concentrations, plus (dotted line) or minus (solid line) 0.2% glyoxylate. Data in (**A**) and (**B**) are means of triplicate culture +/- SEM in 96-well plates.

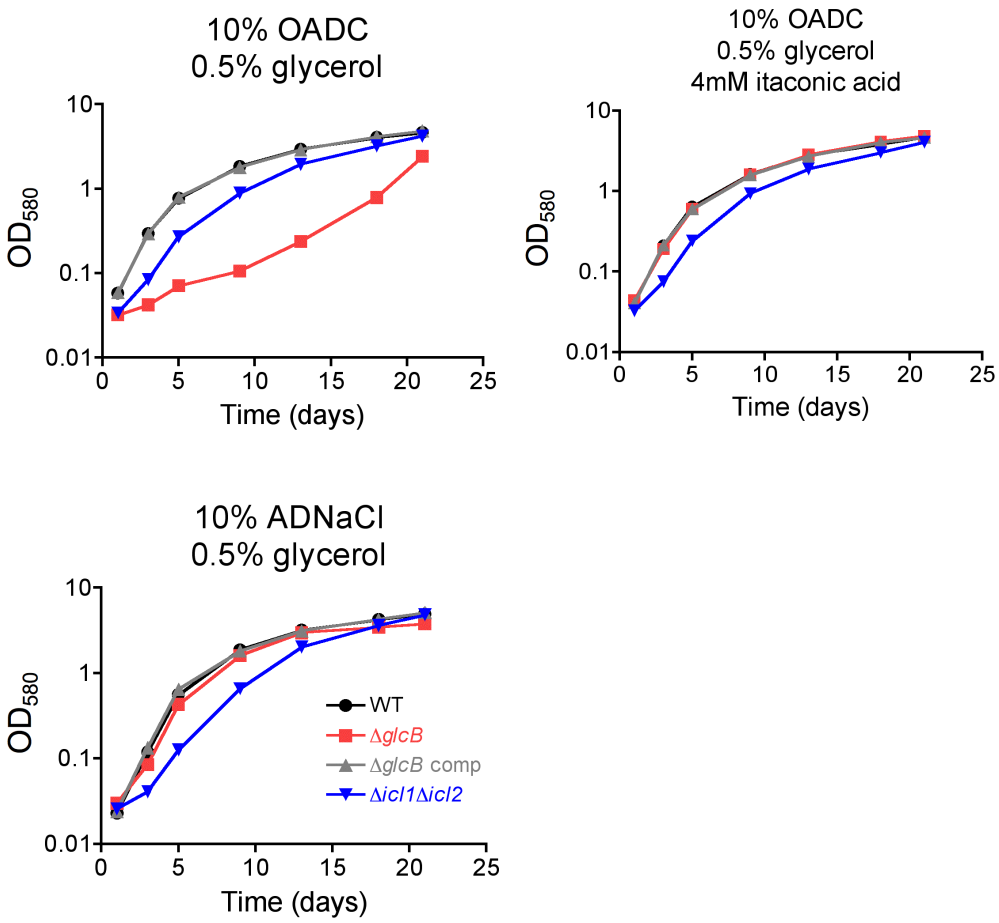

Figure 3.15. Itaconic acid rescues growth of the *glcB* KO in OADC. WT Erdman (WT), Δ*glcB*, the *glcB* complemented strain, and the Δ*icl1*Δ*icl2* were grown in 7H9 base media supplemented with 0.5% glycerol and either 10% OADC (with or without 4 mM itaconic acid) or 10% ADNaCl.

lag disappeared when the supplement ADNaCl (which lacks oleic acid) was used in place of OADC. Importantly, addition of the isocitrate lyase inhibitor itaconic acid to cultures with OADC also abolished the growth lag of the *glcB* KO. This suggests that the oleic acid in OADC may enhance glyoxylate levels, which were likely reduced upon ICL inhibition, allowing for growth of Δ*glcB*.

Although growth of Δ*glcB* was comparable to WT in liquid media lacking OADC, the time it took for colony formation on plates lacking OADC (~40 days) was approximately double that of the WT. To determine whether growth of Δ*glcB* was enhanced by ICL inhibition on plates, itaconic acid was added directly atop 7H10 agar containing 10% ADNaCl and 0.5% glycerol. This enhanced colony size of Δ*glcB*, suggesting that the beneficial effect of ICL inhibition on growth is not limited to OADC-containing media (Figure 3.16).

3.3.11 Malate synthase plays a role in detoxification of odd-chain fatty acids

Break down of long odd-chain fatty acids results in the generation of acetyl-CoA via β-oxidation, but also produces propionyl-CoA. Propionyl CoA-feeds into the methylcitrate pathway, and block of this pathway by deletion of ICL rendered *Mtb* unable to grow in propionate, even in the presence of glucose (Eoh and Rhee, 2014; Munoz-Elias and McKinney, 2005). Survival on 0.2% propionate was also impaired. Activation of an alternative propionyl-CoA metabolic pathway, the methylmalonyl pathway, rescued survival of the ICL-deficient strain on propionate, showing that buildup of propionate-derived metabolites due to methylcitrate cycle block can be toxic (Eoh and Rhee, 2014). Unlike ICL, MS does not play a role in the methylcitrate cycle pathway, so we hypothesized that Δ*glcB* bacteria may grow in media with propionate.

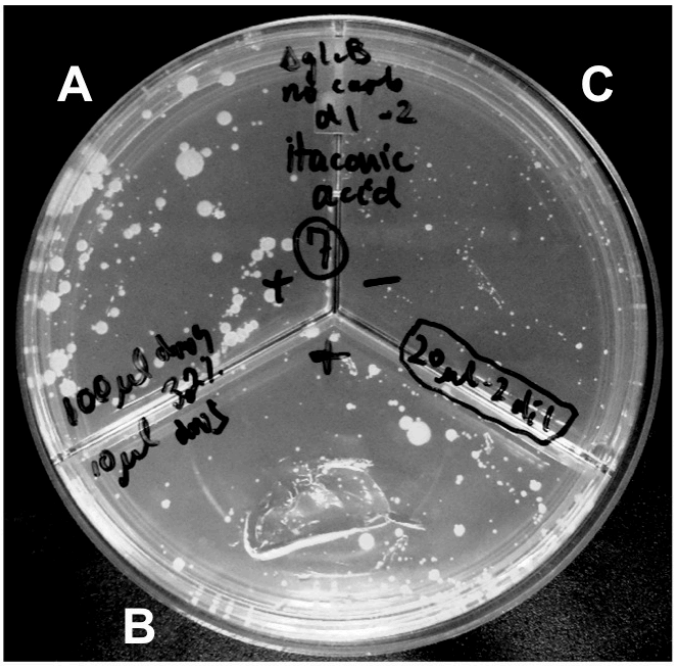

Figure 3.16. Addition of itaconic acid enhances growth of Δ*glcB* on solid media lacking OADC. Δ*glcB* was plated onto a 7H10 Y plate supplemented with 10% ADNaCl and 0.5% glycerol. Itaconic acid was added on top of the agar during plating in the following amounts: (**A**) 100ul of 246 mM (3.2%) itaconic acid, (**B**) 10ul of 246 mM (3.2%) itaconic acid, or (**C**) no itaconic acid. The same volume of *glcB* culture was added to each section.

We were surprised to find that *Mtb* lacking *glcB* was unable to grow in 0.1% propionate (Figure 3.5C). Also, exposure to 0.1% propionate led to eventual killing of Δ*glcB* after 30 days of incubation (Figure 3.17). Furthermore, we found 0.4% glucose did not rescue growth of Δ*glcB* in 0.1% propionate or in 0.05% valerate (Figure 3.18A,C). However, growth of Δ*glcB* in these conditions was improved by addition of 10 μg/ml vitamin B_{12}, which activates the methylmalonyl pathway by enabling activity of methylmaylonyl-CoA mutase (Figure 3.18B,D). In comparison with Δ*icl1*Δ*icl2*, Δ*glcB* had a reduced growth lag in propionate, whereas in valerate Δ*glcB* did not grow as well as Δ*icl1*Δ*icl2*. The Δ*icl1*Δ*icl2* growth lag in 0.1% propionate can be explained by an accumulation of propionyl-CoA-derived metabolites to a certain extent despite the activation of the methylmalonyl pathway. This lag has been previously observed and is less pronounced or absent in 0.05% and 0.01% propionate, respectively (Eoh and Rhee, 2014). Perhaps in 0.05% valerate, which is converted into propionyl-CoA and acetyl-CoA by β-oxidation, propionyl-CoA and downstream metabolites accumulate to a lesser extent than in 0.1% propionate, and therefore do not inhibit growth of Δ*icl1*Δ*icl2*. Also, the growth lag of Δ*glcB* in valerate could be explained by glyoxylate toxicity coming from acetyl-CoA. These data support a role for malate synthase in metabolism and resistance to odd-chain fatty acids.

We also determined whether growth of Δ*glcB* in acetate would be enhanced by activation of the methylmalonyl pathway. Addition of 10 μg/ml vitamin B_{12} did not stimulate growth of either Δ*glcB* or Δ*icl1*Δ*icl2* in 0.2% acetate, with or without 0.2% glucose (Figure 3.19A-D). Previously, vitamin B_{12} improved growth of the Δ*icl1*Δ*icl2* in 0.2% acetate, in the presence of aspartate and glucose (Eoh and Rhee, 2014). Also, addition of vitamin B_{12} rescued survival of Δ*icl1*Δ*icl2* in 0.2% acetate alone (Eoh and Rhee, 2014). We found that addition of vitamin B_{12} did not help survival of Δ*glcB* in

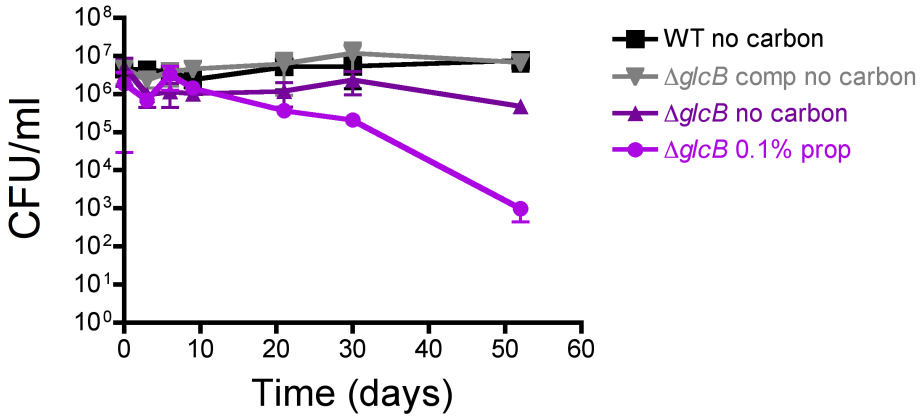

Figure 3.17. Propionate kills Δ*glcB* over time. Survival of the WT Erdman, Δ*glcB*, and Δ*glcB* complemented strain in no carbon compared to survival of Δ*glcB* in 0.1% propionate. The base media is carbon-defined minimal media and each data point is the mean +/- SD of three biological replicates.

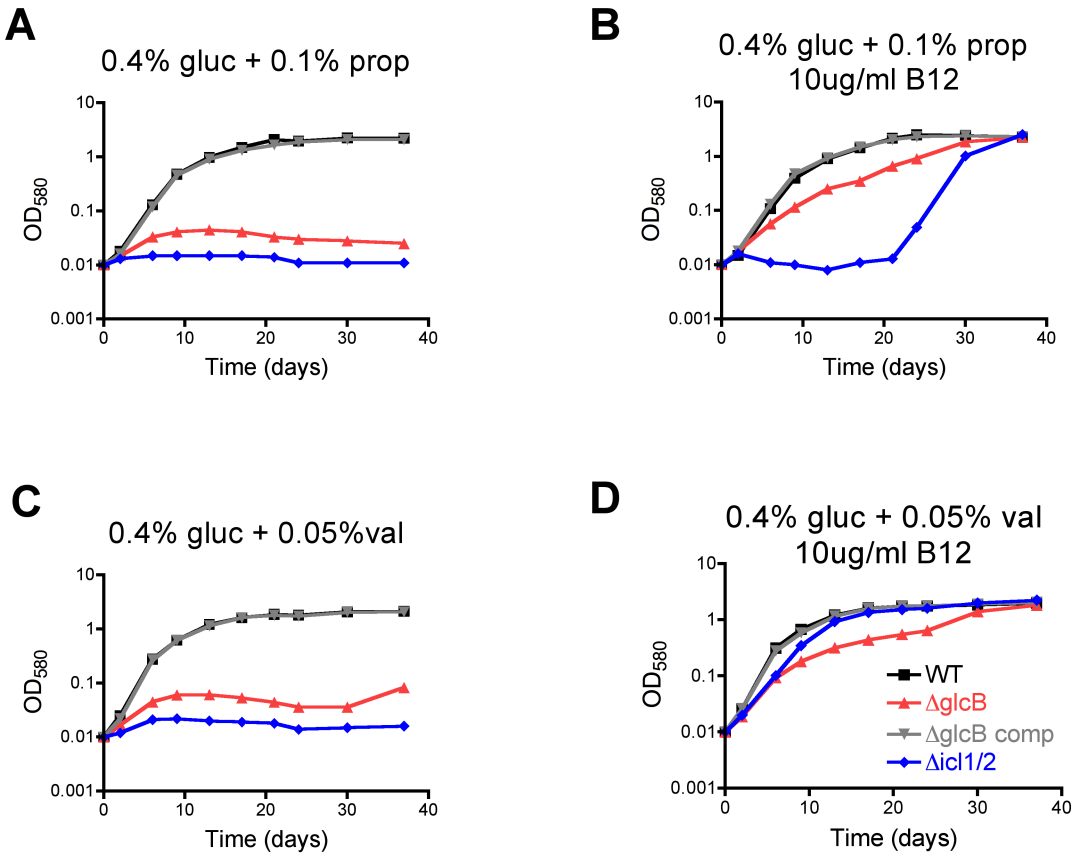

Figure 3.18. Propionate and valerate inhibit growth of Δ*glcB*, which is rescued by vitamin B_{12}. Growth of WT Erdman, Δ*glcB,* Δ*glcB* complemented, and Δ*icl1*Δ*icl2* strains in (**A**) 0.4% glucose and 0.1% propionate, (**B**) 0.4% glucose, 0.1% propionate, and 10 µg/ml vitamin B_{12}, (**C**) 0.4% glucose and 0.05% valerate, and (**D**) 0.4% glucose, 0.05% valerate, and 10 µg/ml vitamin B_{12}.

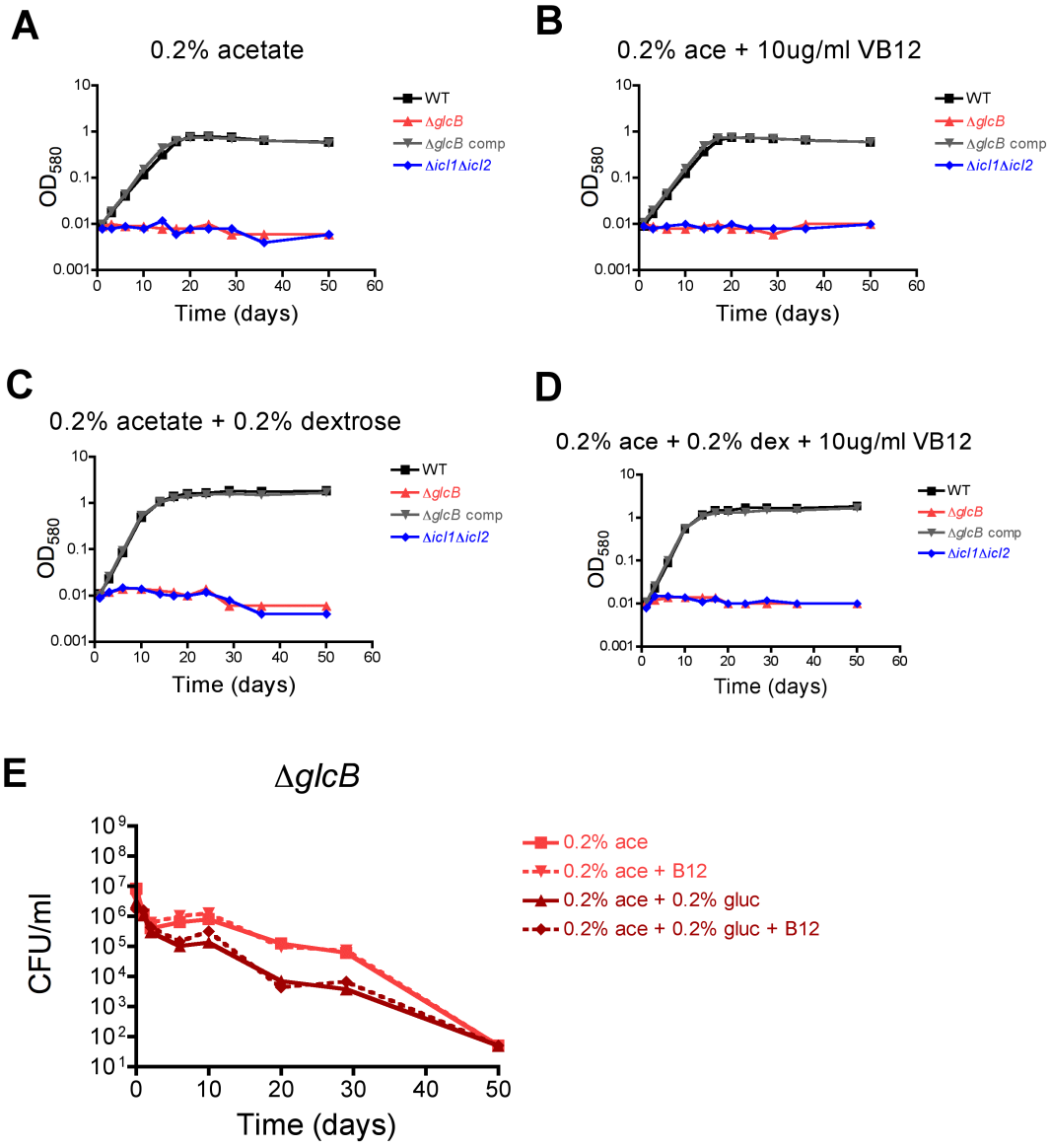

Figure 3.19. Vitamin B_{12} does not rescue acetate-induced toxicity. WT, Δ*glcB*, Δ*glcB* complemented, and Δ*icl1*Δ*icl2* strains were grown in (**A**) 0.2% acetate, (**B**) in 0.2% acetate plus 10 µg/ml vitamin B_{12}, (**C**) 0.2% acetate plus 0.2% glucose, and (**D**) 0.2% acetate, 0.2% glucose, and 10 µg/ml vitamin B_{12}. (**E**) Survival of Δ*glcB* in 0.2% acetate with or without 0.2% glucose and 10 µg/ml vitamin B_{12}.

acetate (Figure 3.19E). This suggests that activation of the methylmalonyl pathway is not sufficient to overcome acetate-mediated toxicity in *Mtb* lacking malate synthase.

3.3.12 Mutation in *gltA2* confers partial acetate resistance in *Mtb* lacking *glcB*

As another approach to understanding acetate-mediated toxicity, we aimed to identify suppressor mutations that could confer resistance to acetate in the Δ*glcB* background. We plated a dense culture (~6.8 x 10^8 bacteria) and dilutions of Δ*glcB* onto plates containing 0.2% acetate and 0.4% glucose. Unfortunately, no colonies were obtained after 2.5 months of incubation.

However, while performing growth curves with Δ*glcB*, we observed that in an intermediate amount of acetate (0.1%) plus 0.4% glucose, growth was inhibited for approximately twenty days, after which Δ*glcB* ultimately reached WT density at around day 35 (Figure 3.20A). To determine whether growth was due to a suppressor mutation, we passaged Δ*glcB* into identical media. While Δ*glcB* still had a growth lag, it was much reduced compared to Δ*glcB* strain that had never been exposed to acetate (Figure 3.20B). To confirm that Δ*glcB* had not been contaminated with a *glcB* expressing strain, we confirmed absence of MS in protein lysates harvested from the end of the growth curve (Figure 3.19C). We then single-colony purified this culture by plating, and colonies exhibited the same slow growth and small, ridged colony phenotype of the parent Δ*glcB* strain. Importantly, culture of these colonies retained the acetate-resistant phenotype when grown in 0.4% glucose and 0.1% acetate (Figure 3.20D). Sequencing of the chromosomal DNA of two of these isolates in collaboration with Dr. Jim Sacchettini and Dr. Tom Ioerger identified a stop mutation (Y147*) in the gene *gltA2* (*Rv0896*). This gene encodes a probable citrate synthase with 431 amino acids and is similar to *citA* (*Rv0889c*), a citrate synthase (31.8% identity in 371 aa overlap), and *prpC* (Rv1131 or *gltA1)*, a methylcitrate synthase (33.1% identity in

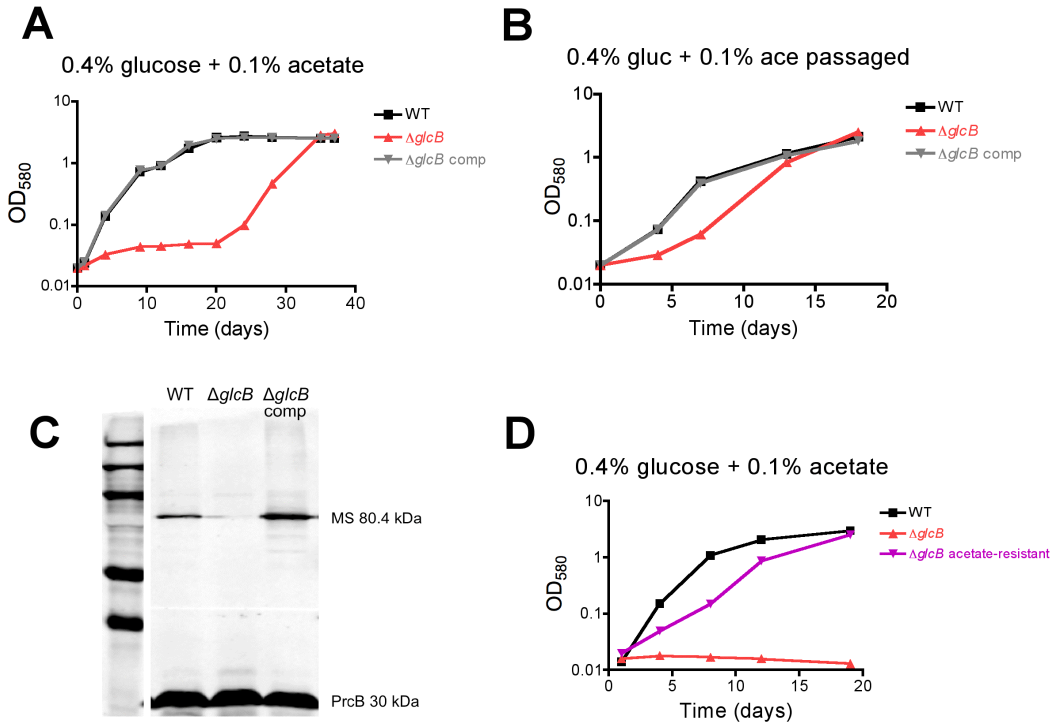

Figure 3.20. Selection for an acetate-resistant Δ*glcB* strain. (**A**) Growth of the WT, Δ*glcB*, and Δ*glcB* complemented strains in 0.4% glucose plus 0.1% acetate in carbon-defined minimal media. (**B**) Growth of cultured passaged from (**A**) on day 37 into the same media condition. (**C**) Western blot examining MS and PrcB expression in lysates harvested from (**B**) on day 18. (**D**) Growth of WT, Δ*glcB* (never exposed to acetate), and the acetate-resistant Δ*glcB* strain isolated from a single colony after plating of Δ*glcB* from (**B**) onto 7H10 ADNaCl plates.

381 aa overlap) according to TubercuList. Considering this potential functional redundancy with *citA* and *prpC*, inactivation of this gene could potentially result in reduced, but not abolished, citrate synthase and/or methylcitrate synthase activity (Figure 3.21). This suggests that the growth-inhibitory phenotype in acetate is caused by metabolism of carbon substrates downstream of the citrate synthase reaction.

We tested the sensitivity of this acetate-resistant Δ*glcB* strain as well as the parent Δ*glcB* strain to acetate (2 carbons), propionate (3 carbons), octanoic acid (8 carbons), and oleic acid (18 carbons). We found that the acetate-resistant mutant was more resistant to acetate, propionate, octanoic acid, and oleic acid than Δ*glcB*, but was not as resistant as WT (Figure 3.22). We also determined whether addition of itaconic acid would help protect against acetate-mediated toxicity, considering that it should reduce glyoxylate buildup by blocking isocitrate lyase. However, addition of 4 mM itaconic acid did not shift the minimum inhibitory concentration of acetate for Δ*glcB*, suggesting that factors other than glyoxylate buildup may contribute to growth inhibition in this condition. These data show that in addition to acetate and propionate, Δ*glcB* growth is also sensitive to long-chain fatty acids. Also, a mutation in *gltA2* resulting in a truncated protein provided intermediate resistance to all of these fatty acids tested. More work is needed to confirm the function of *gltA2* and to confirm that loss of *gltA2* alters metabolic flux downstream of citrate synthase.

3.4 Discussion

Data reported here promotes malate synthase (MS) as a drug target and reveals fatty acid sensitivity in MS-deficient *Mtb*. We found that *glcB*, the gene encoding MS in *Mtb*, was essential for establishment and maintenance of infection in the mouse and that it was required for growth and survival of *Mtb* in high levels of acetate. Acetate, similar to long-chain fatty acids, is converted to acetyl-CoA for entrance into the TCA

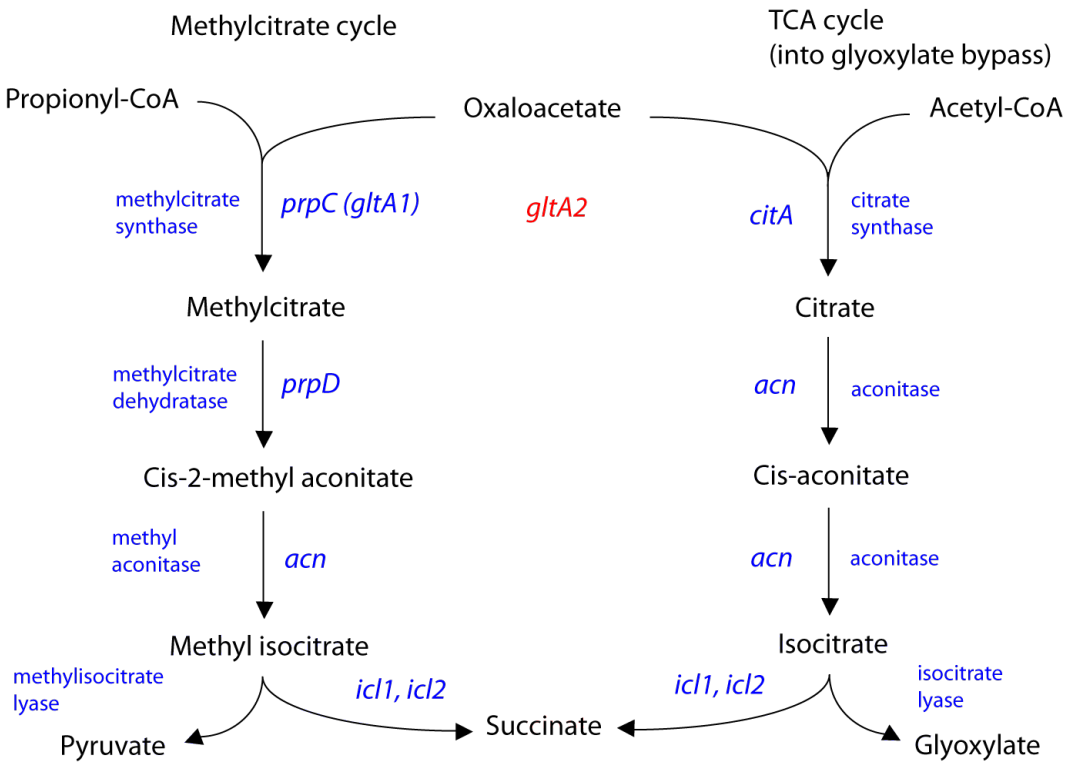

Figure 3.21. Potential roles of *gltA2* in the methylcitrate and TCA cycles. The gene *gltA2* is annotated as a probable citrate synthase in the H37Rv *Mtb* genome and has 33.1% identity with the citrate synthase *citA* and 31.8% identity with the methylcitrate synthase *prpC*.

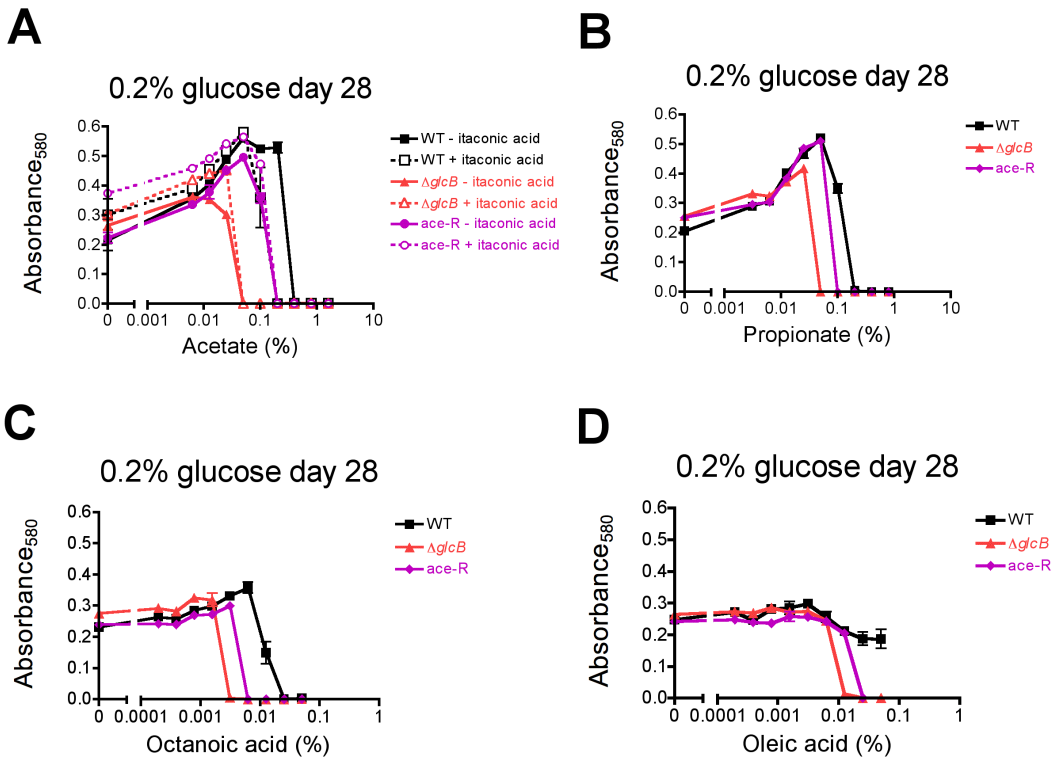

Figure 3.22. The acetate-resistant Δ*glcB* strain is also more resistant to other fatty acids compared to the Δ*glcB* strain. Sensitivity of the WT, Δ*glcB*, and acetate-resistant (ace-R) Δ*glcB* strains (with a truncated *gltA2*) to (**A**) acetate plus or minus 4mM itaconic acid, (**B**) propionate, (**C**) octanoic acid, and (**D**) oleic acid on day 28. Variable carbon source was added to carbon-defined minimal media with 10% ADNaCl (for a final concentration of 0.5% fatty acid-free bovine serum albumin, 0.2% glucose, and 0.085% sodium chloride) in 96-well plate format. Data are means +/- SEM of triplicate wells.

cycle and the glyoxylate shunt. Also, *glcB* was required for growth in cholesterol, a physiologically relevant carbon source that is degraded into a mixture of acetyl-CoA, propionyl-CoA, and pyruvate. Unexpectedly, we found that glucose did not rescue growth or survival of the *glcB* knockout strain (Δ*glcB*) in high acetate concentrations. This suggests that the presence of glycolytic carbon sources in the host environment may not overcome fatty acid toxicity in the absence of MS. As evidence suggests that the host provides *Mtb* with fatty acids and other lipids, it is possible that these contribute to the killing we observe upon MS depletion *in vivo*. This promotes further work on MS inhibitors as an antibacterial strategy.

Why is *Mtb* lacking MS impaired for growth and survival by the presence of carbon sources that enter carbon metabolism as acetyl-CoA? And why would glucose exacerbate this phenotype rather than lead to rescue? We first wanted to investigate whether accumulation of a toxic metabolite could contribute to this phenotype. Two metabolites likely to accumulate in Δ*glcB* are acetyl-CoA and glyoxylate, the substrates of the MS reaction. While it was not possible to measure acetyl-CoA levels using the metabolite preparation protocol we used, we were able to detect elevated glyoxylate levels in Δ*glcB* compared to the wildtype and complemented strains in glucose, acetate, and combinations of glucose and acetate. Glyoxylate accumulations were highest in 0.2% acetate and 0.2% acetate plus 0.2% glucose, and higher glyoxylate levels correlated with a greater extent of killing. Furthermore, glyoxylate accumulated the most out of any metabolite we examined in relation to WT pool sizes in these conditions. Therefore, glyoxylate buildup was linked with growth inhibition and death of Δ*glcB*.

Is glyoxylate buildup toxic for *Mtb*? Glyoxylate toxicity has been proposed as a reason for the pathogenicity defect of a *Rhodococcus fascians* strain with a mutation in MS

(Vereecke et al., 2002). Glyoxylate may be toxic for several reasons. Glyoxylate exists primarily as a gem-diol hydrate in which one carbon is bonded with two hydroxyl groups, but can also exist in a reactive form containing an aldehyde group (Jiang et al., 2012). This can potentially react with proteins or DNA within the cell, causing damage. Also, glyoxylate can act as a metabolic regulator in several ways. Glyoxylate can compete with structurally similar metabolites for the active sites of metabolic enzymes, as has been demonstrated in its ability to compete with pyruvate and inhibit pyruvate dehydrogenase (Beatty and Hamilton, 1985; Dangelmaier and Holmsen, 2014). Glyoxylate can also condense with metabolites such as oxaloacetate and pyruvate, and those products can act as regulators to inhibit enzymes like isocitrate dehydrogenase, α-ketoglutarate dehydrogenase, or aconitase (El-Mansi et al., 1986; Ruffo et al., 1967; Yushok, 1971). Finally, abundance of glyoxylate may activate or inhibit enzymes whose reaction involves glyoxylate as a substrate or product, such as isocitrate lyase (ICL), alanine dehydrogenase (ALD, which has glyoxylate reductive aminase activity), or 2-hydroxy-3-oxoadipate synthase (HOAS). Glyoxylate accumulation can therefore be problematic for the cell by many potential mechanisms.

To investigate this glyoxylate toxicity hypothesis, we determined whether adding exogenous glyoxylate increased sensitivity of Δ*glcB* to acetate. We found that glyoxylate prevented growth of Δ*glcB* in 0.02% acetate, whereas 0.04% acetate was required to prevent growth without glyoxylate. This slight shift in acetate sensitivity suggests that glyoxylate may contribute to toxicity, but inefficient uptake or efficient efflux of glyoxylate may have prevented the phenotype from being more extreme.

We also observed phenotypic differences between the isocitrate lyase and MS-deficient bacteria that supported the glyoxylate toxicity hypothesis. While both strains are similarly inhibited for growth in 0.2% acetate in liquid media, Δ*icl1icl2* grows

much better than Δ*glcB* in liquid media with OADC. OADC contains oleic acid, which can be catabolized into acetyl-CoA to enter into the TCA cycle. It is possible that bacteria growing on 0.006% oleic acid do not generate acetyl-CoA as efficiently as during growth on 0.2% acetate, but that this lower amount of acetyl-CoA is sufficient to contribute to glyoxylate toxicity. Adding OADC to solid media also prevented growth of the Δ*glcB* but not Δ*icl1icl2*. This suggested that growth inhibition of the Δ*glcB* in the presence of oleic acid could be caused by a metabolite buildup that did not occur in Δ*icl1*Δ*icl2* bacteria, such as glyoxylate buildup.

We aimed to determine whether reducing glyoxylate accumulation in Δ*glcB* would enhance growth in media containing OADC. We found that addition of the ICL inhibitor itaconic acid restored growth of Δ*glcB* in OADC to WT levels. Future work using metabolomics to assess the intracellular levels of glyoxylate and other metabolites in conditions with OADC in the presence and absence of itaconic acid could provide further evidence for this glyoxylate toxicity hypothesis. Also, overexpressing enzymes such as ALD (glyoxylate + NADH → glycine + NAD^+) or HOAS (glyoxylate + α-ketoglutarate → 2-hydroxy-3-oxoadipate) could drain glyoxylate levels and rescue growth of Δ*glcB* in OADC if glyoxylate toxicity is the culprit (de Carvalho et al., 2010b; Giffin et al., 2012). However, in lieu of these experiments, glyoxylate toxicity remains the most straightforward explanation for the growth inhibition of Δ*glcB* in OADC.

Surprisingly, addition of itaconic acid to plate media lacking OADC also enhanced growth of the Δ*glcB* strain, suggesting that glyoxylate toxicity also occurs on plates in the absence of oleic acid. Is it possible that itaconic acid enhances growth via a mechanism other than glyoxylate buildup prevention? Macrophages are known to secrete itaconic acid as a defense mechanism and as a response, intracellular

pathogens have evolved itaconic acid degradation pathways (Michelucci et al., 2013; Sasikaran et al., 2014). In *Yersinia pestis* and *Pseudomonas aeroginosa*, itaconic acid break-down results in the production of succinate, pyruvate, and acetyl-CoA (Sasikaran et al., 2014). It is possible that *Mtb* also encodes such pathways and uses them to generate these metabolites, which could potentially act as carbon sources and contribute to growth. However, considering that addition of itaconic acid does not enhance growth of Δ*icl1*Δ*icl2*, it seems unlikely that itaconic acid promotes growth due to this reason. It seems more likely that low levels of glyoxylate produced in plates lacking OADC is sufficient to slow down, but not abolish growth of Δ*glcB*.

Is acetyl-CoA buildup toxic? Acetyl-CoA is a substrate for acetylation, participates in fatty acid and amino acid biosynthesis, and acts as an allosteric regulator of several metabolic enzymes. By western blot, we detected higher reactivity with the acetylated lysine antibody when we probed Δ*glcB* lysate but not WT lysate after cells were exposed for one day to acetate. However, we observed similar levels of reactivity with proteins of the same sizes in Δ*icl1*Δ*icl2*, suggesting that enhanced acetylation is not specific to Δ*glcB* and may not explain the differences we observe between the two knockouts. Future work will need to confirm the specificity of the acetylated lysine antibody to acetylated proteins. Incubation of acetylated lysine antibodies with known acetylated proteins prior to use should result in reduced band intensities in a blot with *Mtb* lysates. Following this confirmation, it would be of interest to determine whether acetylation in Δ*glcB* occurs in other fatty acids, and does not occur in 0.025% acetate plus 0.2% glucose, to better link the occurrence of acetylation with growth inhibition. This could be followed with purification and identification of acetylated proteins that are present in all growth inhibitory conditions. An alternative experiment would be to

overexpress a deacetylase in Δ*glcB* to see whether reducing acetylation rescues growth in 0.2% acetate.

However, identification of a mutation in the Δ*glcB* background that enhances acetate resistance provided evidence against the acetyl-CoA toxicity hypothesis. This is because the loss-of-function mutation is in *gltA2*, a gene that encodes a probable citrate synthase. Loss of this function would likely exacerbate acetyl-CoA accumulation while slowing down accumulation of downstream metabolites. This suggests that whatever metabolic activity that causes growth inhibition is downstream of the citrate synthase reaction, and that acetyl-CoA buildup may not be the cause of toxicity. It may be interesting to further investigate whether acetylation profiles in acetate-resistant Δ*glcB* strain are enhanced due to citrate synthase inhibition, arguing against a role for acetylation-induced toxicity.

In addition to altered levels of substrate and products of the MS reaction, we observed other metabolic changes in Δ*glcB*. We observed accumulation of glycine and α-ketoglutarate in conditions with acetate (and in glucose for α-ketoglutarate). Levels of glyoxylate and α-ketoglutarate were especially high in 0.2% glucose + 0.2% acetate. Conversely, we observed a reduction in aspartate in all conditions tested, showing that 0.2% glucose is not sufficient to maintain aspartate levels. We also observed a reduction in succinate and fumarate in conditions with 0.2% acetate. It was previously noted that there was a partial bifurcation of the TCA cycle between α-ketoglutarate and succinate as determined by disparate pool sizes and carbon flux, despite existing enzymatic reactions that link the two metabolites (de Carvalho et al., 2010a). However, ICL should be able to generate succinate, and the succinate depletion we observe remains unexplained. We also observed increases in branched chain amino acid pathway metabolites, which could be linked to acetyl-CoA or glyoxylate accumulation.

For example, the α-isopropylmalate synthase reaction is the first step of leucine synthesis and uses acetyl-CoA as a substrate (Koon et al., 2004). However, the reasons for these accumulations remain to be clearly defined. It is possible that these metabolic changes contribute to the death phenotype that we observe in 0.2% acetate.

While there are differences in the growth phenotypes of Δ*glcB* and Δ*icl1*Δ*icl2* in OADC, growth of both knockouts is inhibited by 0.2% acetate (Eoh and Rhee, 2014). It is probable that a combination of similar and contrasting mechanisms contribute to the phenotypes of these knockouts in this condition. For example, starvation induced by blockage of the glyoxylate shunt, channeling of carbon away from the glyoxylate shunt and into the TCA cycle, and mutant-specific factors (glyoxylate accumulation or methylcitrate cycle block) could all contribute. It may be interesting to test whether blockage of the glyoxylate shunt lead to alterations in NAD^+/NADH ratio, ATP generation, and/or redox balance. Enhanced antibiotic sensitivity of Δ*icl1*Δ*icl2* was alleviated by addition of antioxidants, suggesting that Δ*icl1*Δ*icl2* is either more susceptible to oxidative stress or generates more reactive oxygen species than WT during antibiotic treatment (Nandakumar et al., 2014). *Mtb* under anaerobic conditions was shown to upregulate both isocitrate lyase and glycine dehydrogenase (which can perform the reductive amination of glyoxylate and convert NADH to NAD^+). Therefore, deletion of ICL may have a more dramatic effect on redox balance than an MS deletion. It will be of interest to determine whether addition of an antioxidant such as thiourea could rescue growth or survival in acetate for both knockouts. If so, this would support a role for the glyoxylate shunt in minimizing oxidative stress.

We found that acetate-mediated growth inhibition is a concentration-dependent phenotype. Despite inhibiting growth at high concentrations, low concentrations of acetate (0.025%) helped growth of Δ*glcB* in the presence of glucose, similarly to WT.

Metabolomics analysis showed that at 0.025% acetate plus 0.2% glucose, many of the metabolic changes observed in 0.2% acetate were absent or less severe. Therefore, the glyoxylate shunt is not required for co-catabolism of acetate and glucose at low acetate concentrations.

Growth inhibition of Δ*glcB* mediated by fatty acids is not limited to even-chain fatty acids. We observe that Δ*glcB* is inhibited by 0.1% propionate (3 carbons) and 0.05% valerate (5 carbons), whereas the WT is not. This differs from a *M. smegmatis* mutant lacking *glcb* and *gcl* (involved in the D-glycerate pathway, an alternative glyoxylate metabolic pathway), which did not have problems growing on propionate. Interestingly, activation of an alternative propionyl-CoA metabolic pathway (the methylmalonyl pathway) alleviated growth inhibition for the *Mtb glcB* knockout. This was unexpected, because unlike Δ*icl1*Δ*icl2*, Δ*glcB* should have a functional methylcitrate pathway to detoxify propionyl-CoA-derived metabolites. Indeed, we observe depletions, rather than accumulations, of methyl(iso)citrate in Δ*glcB* in acetate, suggesting that there is no block of the methylcitrate pathway as is observed in Δ*icl1*Δ*icl2*. However, these growth phenotypes in odd-chain fatty acids could be attributed to depletion of oxaloacetate, which feeds into the methylcitrate pathway. While we cannot measure oxaloacetate levels, we observe a depletion of aspartate, whose levels are an indication of oxaloacetate. We also observe a depletion of malate, which directly contributes to oxaloacetate generation by the enzymatic activity of malate dehydrogenase. Perhaps propionyl-CoA itself is toxic and cannot be drained via the methylcitrate cycle during a paucity of oxaloacetate caused by MS deletion.

It is puzzling why a truncation in the probable citrate synthase *gltA2* can augment growth of Δ*glcB* in propionate. It is possible that *gltA2* can also function as a methylcitrate synthase. *Salmonella enterica* expresses a citrate synthase encoded by

gltA, that has 53% amino acid identity and 70% amino acid positives compared to the *Mtb* H37Rv *gltA2* by NCBI BLAST analysis. The *S. enterica gltA* has been shown to function as a methylcitrate synthase, generating isomers of methylcitrate that vary from those produced by the methylcitrate synthase PrpC and are potentially more difficult to be metabolized by the downstream enzyme, methylcitrate dehydratase (Rocco and Escalante-Semerena, 2010). These isoforms could contribute to toxicity. It is possible that something similar occurs in *Mtb*. It would be of interest to see what effect depletion of this enzyme in combination with MS depletion has on TCA cycle and methylcitrate cycle metabolite levels in *Mtb* in propionate.

Does *Mtb* alter its metabolism in response to acetate? It is possible that high levels of acetate trigger metabolic regulation that exacerbates the effect of glyoxylate shunt deletion. In *E. coli*, acetate activates the glyoxylate shunt by triggering phosphorylation of isocitrate dehydrogenase (ICDH) by the kinase AceK, which inhibits ICDH and redirects carbon flow through the glyoxylate shunt (El-Mansi et al., 1986; Quartararo et al., 2013). *Mtb* lacks a homolog for AceK and the ICDH of *Mtb* has no identified phosphorylation sites, suggesting an alternative regulatory mechanism (Quartararo et al., 2013). However, transcriptional regulation in response to carbon source is known to occur in *Mtb*. RamB (encoded by *rv0465c*) is a transcriptional regulator that reduces the expression of *icl1* in glucose, and can also bind its own promoter region (Micklinghoff et al., 2009). RamB is expressed in both acetate and glucose; therefore in acetate other mechanisms must exist to prevent inactivation of *icl1* by RamB.

The post-translational protein modification of lysine acetylation has gained much attention as a mechanism by which metabolic pathways are regulated in bacteria, and is known to occur in *Mtb* (Liu et al., 2014). *Mtb* Acetyl-CoA synthetatse (ACS), the

enzyme that converts acetate to acetyl-CoA and propionate to propionyl-CoA, is inhibited by lysine acetylation (Xu et al., 2011). It is possible that the potential changes in acetylation that we observed in *Mtb* lacking a functional glyoxylate shunt in response to acetate, alter carbon flux in *Mtb*. This could also have an effect on propionate metabolism, or other metabolic pathways (Liu et al., 2014; Nambi et al., 2013).

In conclusion, these data outline a role for *glcB* as the sole malate synthase in *Mtb*, whose function is required for growth and survival in high levels of acetate and in the mouse model of tuberculosis. However, *glcB* is not essential for growth in glucose or glycerol as a sole carbon source, showing that *glcB* essentiality is carbon-source dependent. The question remains, why is *glcB* required in the mouse model? It is plausible that the sensitivity of Δ*glcB* to fatty acids (caused by glyoxylate toxicity, blockage of the glyoxylate shunt, or alternative mechanisms) found in the host environment contributes to the *in vivo* phenotype. This does not rule out a role for *glcB* in response to other host stresses. Considering the many roles of ICL in *Mtb* pathogenesis in different stress conditions, it would be of interest to determine whether the same sensitivities occur in *Mtb* lacking MS. However, considering that fatty acids and other lipids are likely accessible to *Mtb* in the human, they may be sufficient to induce *Mtb* death in humans treated with potent MS inhibitors, supporting further work on MS inhibitor development.

3.5 Materials and Methods

3.5.1 Ethics statement

Animal experiments were performed as according to National Institutes of Health guidelines for housing and care of laboratory animals. The Institutional Animal Care and Use Committee of Weill Cornell Medical College evaluated and approved the

protocol #0601-441A, Conditional Expression of Mycobacterial Genes, which we followed during these experiments.

3.5.2 Bacterial culture conditions

For standard liquid *Mtb* media, Middlebrook 7H9 with 10% homemade ADNaCl (final concentration of 0.5% bovine serum albumin (BSA) fraction V, 0.2% glucose, 0.085% NaCl), 0.2% glycerol, and 0.05% tyloxapol was used. For standard *Mtb* plate media, Middlebrook 7H10 with 10% commercial OADC supplement (final concentration 0.5% bovine serum albumin, 0.2% glucose, 0.085% NaCl, 0.006% oleic acid, and 0.0003% catalase) and 0.5% glycerol was used, prepared according to manufacturers instructions. However, in any experiment involving the confirmed Δ*glcB* strain, 10% ADNaCl (made with Roche BSA fraction V, heat shock, fatty acid-free with total FA≤1.2 mg/g) was used instead of OADC in plate media and instead of regular ADNaCl in liquid media. Carbon-defined media was composed of 0.05% potassium phosphate monobasic, 0.05% magnesium sulfate heptahydrate, 0.2% citric acid, 0.005% ferric ammonium sulfate, 0.05% ammonium sulfate, 0.0001% zinc sulfate, and 0.05% tyloxapol. Carbon sources propionic acid, butyric acid, sodium acetate, valeric acid, octanoic acid, oleic acid, aspartic acid, malic acid, glucose, and glycerol were added at the indicated concentration (%wt/vol or %vol/vol, depending on stock), and pH adjusted to 7.4. Growth curves with cholesterol were performed in "Sassetti base media" according to the protocol from Griffin et. al. 2012. Briefly, a 500x stock of cholesterol was made by addition of 100mg cholesterol to 1 ml of tyloxapol and 1 ml of ethanol. This was heated to 95°C-100°C before addition to minimal media containing 0.5 g/L asparagine, 1 g/L KH_2PO_4, 2.5 g/L Na_2HPO_4, 0.05 g/L ferric ammonium citrate, 0.5 g/L $MgSO_4 \bullet 7H_2O$, 0.5 mg/L $CaCl_2$, and 0.1 mg/L $ZnSO_4$. Media was sterile filtered before addition of bacteria. Optical density (OD)

measurements taken with vitamin B_{12} or cholesterol-containing media required an appropriate blank to account for color or cloudiness. When required, antibiotics hygromycin B (50 μg/ml), streptomycin (10 μg/ml), kanamycin (25 μg/ml) and/or zeocin (25 μg/ml) were added. Where indicated, anhydrotetracycline (atc) was added at 500ng/ml and replenished at 250 ng/ml every 4-5 days. For metabolomics profiling, *Mtb* culture at OD_{580}~1 was seeded onto 0.22 μM nitrocellulose filters atop 7H10 agar plates containing 0.2% glucose and 0.5% glycerol for 4 days, then 0.2% glucose for 2 days, before transfer to the indicated carbon source for 1 day. Bacteria were subsequently quenched in cold acetonitrile:methanol:water (40:40:20) buffer, scraped off of filters, and mechanically lysed using a beadbeater prior to metabolite analysis.

3.5.3 Generation of mutant strains

All mutant strains generated and evaluated in this chapter were generated in the *Mycobacterium tuberculosis* Erdman background. To generate the *glcB* mutant strains, *Mtb* was first transformed with an attL5-integrating plasmid expressing under the control of its native promoter. This merodiploid strain was then transformed with a temperature-sensitive knockout plasmid containing a hygromycin resistance cassette flanked with regions homologous to those surrounding *glcB* in the *Mtb* genome. This plasmid was designed to remove all of *glcB* except for the last 86 base pairs. This plasmid also expressed *xylE* and *sacB* in the backbone, which aided in selection of knockout candidates. *xylE* expression results in colonies turning yellow upon exposure to catechol, and *sacB* confers sucrose sensitivity. After confirming successful transformation with the knockout plasmid by addition of catechol, we grew up and plated this strain on plates containing sucrose at 40°C to select for double crossover events. A double crossover results in the removal of the backbone of the plasmid but retention of the hygromycin resistance cassette in place of the *glcB* gene. After 39

days, a few colonies were obtained, which we propagated and obtained DNA to confirm the lack of native *glcB* by PCR and Southern blot. This att-site mutant strain was then used to generate both the *glcB*-DUC and *glcB* knockout strains. To generate *glcB*-DUC, the att site mutant was transformed with an att-site-integrating plasmid expressing *glcB* C-terminally tagged with DAS+4 under the control of a Tet-OFF promoter (p750) controlled by the tet repressor T38S38, and also a tweety-site integrating plasmid expressing *sspB* under the control of a Tet-ON promoter (P1) controlled by TSC10M repressor as described (Ehrt et al., 2005; Kim et al., 2013). The *glcB* knockout strain (Δ*glcB*) was generated from the att site mutant by replacement transformation of the *glcB*-expressing plasmid in the attL5 site with a plasmid lacking *glcB*. The *glcB* complemented strain was generated by transforming Δ*glcB* with an attL5-site integrating plasmid expressing *glcB* under the control of the native *glcB* promoter. Gateway Cloning technology (Invitrogen) was used to generate all plasmids in this study, via BP and LR recombinase, as instructed by the manufacturer.

3.5.4 Metabolomics

Liquid chromatography mass spectrometry differentiation and detection of *Mtb* metabolites was performed with an Agilent Accurate Mass 6220 TOF coupled with an Agilent 1200 Liquid Chromatography system using a Cogent Diamond Hydride Type C column (Microsolve Technologies) as described (Eoh and Rhee, 2013). Standards of authentic chemicals of known amounts were mixed with bacterial lysates and analyzed to generate the standard curves used to quantify metabolite levels. These were normalized to lysate protein levels, which were quantified using a BCA Protein Assay Kit (Pierce). Data was analyzed using Profinder B.06.00 software. The clustered metabolite heatmap was generated with Gene Cluster 3.0 and Java TreeView 1.1.6r3 software.

3.5.5 Mouse infection

Female C57BL/6 mice (Jackson Laboratory) were exposed to aerosolized *Mtb* using a Glas-Col inhalation exposure system. 5 ml of OD 0.2 *Mtb* single-cell suspension in PBS was injected into the nebulizer to deliver 100 to 200 bacilli per mouse. At the indicated time-points, doxycycline food (2000ppm, Research Diets) was administered in lieu of regular mouse chow for the rest of the experiment. To quantify bacteria, dilutions of lung and spleen homogenates were plated onto 7H10 plates containing 10% ADNaCl (fatty acid-free BSA) and 0.5% glycerol for CFU.

3.5.6 Antibody generation and western blotting

Recombinant malate synthase protein (made from overexpression of *Mtb glcB*) was obtained from the Sacchettini Lab at Texas A&M. Rabbit polyclonal antibodies specific for this protein were generated by GenScript. For western blotting, protein lysates were prepared from *Mtb* cells by mechanical lysis 2x at 4,500RPM for 30 seconds with 0.1mm zirconia/silica beads. Bacterial cell wall components and beads were removed via centrifugation and filtration using 0.2 μm spin-X columns (Corning). Protein quantification was assessed using a DC-Protein Assay Kit (Bio-Rad). Protein lysates were separated using SDS-PAGE and transferred to a nitrocellulose membrane, which was incubated with Odyssey blocking buffer and PBS (1:1). Membrane was cut between 30 and 80 kDa and incubated with either malate synthase antibody (1:3,500) or PrcB (1:20,000) antibody in Odyssey blocking buffer and PBS (1:1) in 0.1% Tween-20. The membranes were washed and then incubated with secondary IRDye 680 Donkey anti-Rabbit IgG (H+L) (LI-COR Biosciences). After washing, proteins were visualized using Odyssey Infrared Imaging System (LI-COR Biosciences). For analysis of acetylated proteins, 80ml *Mtb* strains were grown in roller bottles at 37C in minimal media containing 0.4% glucose until they reached OD~1. Strains were then

centrifuged to remove media and resuspended in minimal media containing 0.2% acetate or 0.2% glucose. After 24 hour incubation, lysates were prepared and used for western blotting as just described. For primary antibody, acetylated lysine antibody (Cell Signaling) was used at a dilution of 1:2,500, followed by secondary at 1:15,000.

3.5.7 Survival assays

Mtb cultures were grown to OD 0.2-1 in 7H9 with 10% ADNaCl (made with fatty acid-free BSA) and spun down to remove the media. Pellets were resuspended in carbon-defined minimal media and used to inoculate 10 mls of the media of interest at an OD of 0.01. Cultures were incubated at 37°C at 5% CO_2 in T25 vented flasks. Flasks were shaken to resuspend bacteria before aliquots were taken for serial dilutions and plating onto 7H10 plates containing 10% ADNaCl (fatty acid-free BSA) and 0.5% glycerol.

3.5.8 Genome sequencing

Genomic DNA was prepared from *Mtb* cultures ~OD 1 by phenol:chloroform extraction. Genomic DNA was sequenced by the Sacchettini Lab at Texas A&M and data analyzed by Dr. Tom Ioerger.

3.6 Acknowledgements

The following Ehrt lab members contributed to this work: Dr. Carolina Trujillo (mouse infections/harvests), Natalia Betancourt (plasmids), Dr. Pradeepa Jayachandran (mouse harvests), Uday Ganapathy (mouse harvests), and Shuang Song (mouse harvests). We thank the McKinney lab for providing the Δ*icl1*Δ*icl2* mutant *Mtb* strain, the Sacchettini lab for providing malate synthase protein and sequencing our strains, and specifically Dr. Tom Ioerger for sequencing our strains and analyzing

the data. We thank the Sassetti lab for the cholesterol media protocol. We thank Dr. Kyu Rhee and Dr. Hyungjin Eoh for metabolomics expertise and machine use, and Dr. Dirk Schnappinger and his lab for contributing to generation of the dual control *glcB* strain. Also, we thank Dr. Gang Lin and Dr. Carl Nathan for PrcB antibody.

REFERENCES

Bauzá, A., Quiñonero, D., Deyà, P.M., and Frontera, A. (2014). Long-Range Effects in Anion–π Interactions: Their Crucial Role in the Inhibition Mechanism of Mycobacterium Tuberculosis Malate Synthase. Chem. – Eur. J. *20*, 6985–6990.

Beatty, S.M., and Hamilton, G.A. (1985). Inhibition of pyruvate dehydrogenase and pyruvate dehydrogenase phosphate phosphatase by glyoxylate. Bioorganic Chem. *13*, 14–23.

Blumenthal, A., Trujillo, C., Ehrt, S., and Schnappinger, D. (2010). Simultaneous Analysis of Multiple Mycobacterium tuberculosis Knockdown Mutants In Vitro and In Vivo. PLoS ONE *5*.

De Carvalho, L.P.S., Fischer, S.M., Marrero, J., Nathan, C., Ehrt, S., and Rhee, K.Y. (2010a). Metabolomics of Mycobacterium tuberculosis reveals compartmentalized co-catabolism of carbon substrates. Chem. Biol. *17*, 1122–1131.

De Carvalho, L.P.S., Zhao, H., Dickinson, C.E., Arango, N.M., Lima, C.D., Fischer, S.M., Ouerfelli, O., Nathan, C., and Rhee, K.Y. (2010b). Activity-based metabolomic profiling of enzymatic function: Identification of Rv1248c as a mycobacterial 2-hydroxy-3-oxoadipate synthase. Chem. Biol. *17*, 323–332.

Chopra, T., Hamelin, R., Armand, F., Chiappe, D., Moniatte, M., and McKinney, J.D. (2014). Quantitative Mass Spectrometry Reveals Plasticity of Metabolic Networks in Mycobacterium smegmatis. Mol. Cell. Proteomics mcp.M113.034082.

Dangelmaier, C.A., and Holmsen, H. (2014). Glyoxylate lowers metabolic ATP in human platelets without altering adenylate energy charge or aggregation. Platelets *25*, 36–44.

Domenech, P., and Reed, M.B. (2009). Rapid and spontaneous loss of phthiocerol dimycocerosate (PDIM) from Mycobacterium tuberculosis grown in vitro: implications for virulence studies. Microbiology *155*, 3532–3543.

Dunn, M.F., Ramírez-Trujillo, J.A., and Hernández-Lucas, I. (2009). Major roles of isocitrate lyase and malate synthase in bacterial and fungal pathogenesis. Microbiology *155*, 3166–3175.

Ehrt, S., Guo, X.V., Hickey, C.M., Ryou, M., Monteleone, M., Riley, L.W., and Schnappinger, D. (2005). Controlling gene expression in mycobacteria with anhydrotetracycline and Tet repressor. Nucleic Acids Res. *33*, e21–e21.

El-Mansi, E.M.T., Nimmo, H.G., and Holms, W.H. (1986). Pyruvate Metabolism and the Phosphorylation State of Isocitrate Dehydrogenase in Escherichia coli. J. Gen. Microbiol. *132*, 797–806.

Eoh, H., and Rhee, K.Y. (2013). Multifunctional essentiality of succinate metabolism in adaptation to hypoxia in Mycobacterium tuberculosis. Proc. Natl. Acad. Sci. U. S. A. *110*, 6554–6559.

Eoh, H., and Rhee, K.Y. (2014). Methylcitrate cycle defines the bactericidal essentiality of isocitrate lyase for survival of Mycobacterium tuberculosis on fatty acids. Proc. Natl. Acad. Sci. U. S. A. *111*, 4976–4981.

Giffin, M.M., Modesti, L., Raab, R.W., Wayne, L.G., and Sohaskey, C.D. (2012). ald of Mycobacterium tuberculosis Encodes both the Alanine Dehydrogenase and the Putative Glycine Dehydrogenase. J. Bacteriol. *194*, 1045–1054.

Gould, T.A., Van De Langemheen, H., Muñoz-Elías, E.J., McKinney, J.D., and Sacchettini, J.C. (2006). Dual role of isocitrate lyase 1 in the glyoxylate and methylcitrate cycles in Mycobacterium tuberculosis. Mol. Microbiol. *61*, 940–947.

Griffin, J.E., Pandey, A.K., Gilmore, S.A., Mizrahi, V., Mckinney, J.D., Bertozzi, C.R., and Sassetti, C.M. (2012). Cholesterol Catabolism by Mycobacterium tuberculosis Requires Transcriptional and Metabolic Adaptations. Chem. Biol. *19*, 218–227.

Jiang, J., Johnson, L.C., Knight, J., Callahan, M.F., Riedel, T.J., Holmes, R.P., and Lowther, W.T. (2012). Metabolism of [13C5]hydroxyproline in vitro and in vivo: implications for primary hyperoxaluria. Am. J. Physiol. - Gastrointest. Liver Physiol. *302*, G637–G643.

Kim, J.-H., Wei, J.-R., Wallach, J.B., Robbins, R.S., Rubin, E.J., and Schnappinger, D. (2011). Protein inactivation in mycobacteria by controlled proteolysis and its application to deplete the beta subunit of RNA polymerase. Nucleic Acids Res. *39*, 2210–2220.

Kim, J.-H., O'Brien, K.M., Sharma, R., Boshoff, H.I.M., Rehren, G., Chakraborty, S., Wallach, J.B., Monteleone, M., Wilson, D.J., Aldrich, C.C., et al. (2013). A genetic strategy to identify targets for the development of drugs that prevent bacterial persistence. Proc. Natl. Acad. Sci. U. S. A. *110*, 19095–19100.

Kinhikar, A.G., Vargas, D., Li, H., Mahaffey, S.B., Hinds, L., Belisle, J.T., and Laal, S. (2006). Mycobacterium tuberculosis malate synthase is a laminin-binding adhesin. Mol. Microbiol. *60*, 999–1013.

Kondrashov, F.A., Koonin, E.V., Morgunov, I.G., Finogenova, T.V., and Kondrashova, M.N. (2006). Evolution of glyoxylate cycle enzymes in Metazoa:

evidence of multiple horizontal transfer events and pseudogene formation. Biol. Direct *1*, 31.

Koon, N., Squire, C.J., and Baker, E.N. (2004). Crystal structure of LeuA from Mycobacterium tuberculosis, a key enzyme in leucine biosynthesis. Proc. Natl. Acad. Sci. U. S. A. *101*, 8295–8300.

Krieger, I.V., Freundlich, J.S., Gawandi, V.B., Roberts, J.P., Gawandi, V.B., Sun, Q., Owen, J.L., Fraile, M.T., Huss, S.I., Lavandera, J.-L., et al. (2012). Structure-Guided Discovery of Phenyl-diketo Acids as Potent Inhibitors of M. tuberculosis Malate Synthase. Chem. Biol. *19*, 1556–1567.

Kumar, R., and Bhakuni, V. (2010). A functionally active dimer of Mycobacterium tuberculosis Malate synthase G. Eur. Biophys. J. *39*, 1557–1562.

Liu, F., Yang, M., Wang, X., Yang, S., Gu, J., Zhou, J., Zhang, X.-E., Deng, J., and Ge, F. (2014). Acetylome analysis reveals diverse functions of lysine acetylation in Mycobacterium tuberculosis. Mol. Cell. Proteomics MCP.

Lohman, J.R., Olson, A.C., and Remington, S.J. (2008). Atomic resolution structures of Escherichia coli and Bacillus anthracis malate synthase A: Comparison with isoform G and implications for structure-based drug discovery. Protein Sci. Publ. Protein Soc. *17*, 1935–1945.

McKinney, J.D., zu Bentrup, K.H., Muñoz-Elías, E.J., Miczak, A., Chen, B., Chan, W.-T., Swenson, D., Sacchettini, J.C., Jacobs, W.R., and Russell, D.G. (2000). Persistence of Mycobacterium tuberculosis in macrophages and mice requires the glyoxylate shunt enzyme isocitrate lyase. Nature *406*, 735–738.

Merkov, L.N. (2006). Glyoxylate Metabolism in Mycobacterium smegmatis. Thesis.

Michelucci, A., Cordes, T., Ghelfi, J., Pailot, A., Reiling, N., Goldmann, O., Binz, T., Wegner, A., Tallam, A., Rausell, A., et al. (2013). Immune-responsive gene 1 protein links metabolism to immunity by catalyzing itaconic acid production. Proc. Natl. Acad. Sci. U. S. A. *110*, 7820–7825.

Micklinghoff, J.C., Breitinger, K.J., Schmidt, M., Geffers, R., Eikmanns, B.J., and Bange, F.-C. (2009). Role of the Transcriptional Regulator RamB (Rv0465c) in the Control of the Glyoxylate Cycle in Mycobacterium tuberculosis. J. Bacteriol. *191*, 7260–7269.

Munoz-Elias, E.J., and McKinney, J.D. (2005). M. tuberculosis isocitrate lyases 1 and 2 are jointly required for in vivo growth and virulence. Nat. Med. *11*, 638–644.

Muñoz-Elías, E.J., Upton, A.M., Cherian, J., and McKinney, J.D. (2006). Role of the methylcitrate cycle in Mycobacterium tuberculosis metabolism, intracellular growth, and virulence. Mol. Microbiol. *60*, 1109–1122.

Nambi, S., Gupta, K., Bhattacharyya, M., Ramakrishnan, P., Ravikumar, V., Siddiqui, N., Thomas, A.T., and Visweswariah, S.S. (2013). Cyclic AMP-dependent Protein Lysine Acylation in Mycobacteria Regulates Fatty Acid and Propionate Metabolism. J. Biol. Chem. *288*, 14114–14124.

Nandakumar, M., Nathan, C., and Rhee, K.Y. (2014). Isocitrate lyase mediates broad antibiotic tolerance in Mycobacterium tuberculosis. Nat. Commun. *5*, 4306.

Quartararo, C.E., and Blanchard, J.S. (2011). Kinetic and chemical mechanism of malate synthase from Mycobacterium tuberculosis. Biochemistry (Mosc.) *50*, 6879–6887.

Quartararo, C.E., Hazra, S., Hadi, T., and Blanchard, J.S. (2013). Structure, Kinetic, and Chemical Mechanism of Isocitrate Dehydrogenase-1 from Mycobacterium tuberculosis. Biochemistry (Mosc.) *52*.

Rocco, C.J., and Escalante-Semerena, J.C. (2010). In Salmonella enterica, 2-Methylcitrate Blocks Gluconeogenesis. J. Bacteriol. *192*, 771–778.

Rohde, K.H., Veiga, D.F.T., Caldwell, S., Balazsi, G., and Russell, D.G. (2012). Linking the Transcriptional Profiles and the Physiological States of Mycobacterium tuberculosis during an Extended Intracellular Infection. PLoS Pathog. *8*.

Ruffo, A., Testa, E., Adinolfi, A., Pelizza, G., and Moratti, R. (1967). Control of the citric acid cycle by glyoxylate. Biochem. J. *103*, 19–23.

Sasikaran, J., Ziemski, M., Zadora, P.K., Fleig, A., and Berg, I.A. (2014). Bacterial itaconate degradation promotes pathogenicity. Nat. Chem. Biol. *10*, 371–377.

Savvi, S., Warner, D.F., Kana, B.D., McKinney, J.D., Mizrahi, V., and Dawes, S.S. (2008). Functional Characterization of a Vitamin B12-Dependent Methylmalonyl Pathway in Mycobacterium tuberculosis: Implications for Propionate Metabolism during Growth on Fatty Acids. J. Bacteriol. *190*, 3886–3895.

Schnappinger, D., Ehrt, S., Voskuil, M.I., Liu, Y., Mangan, J.A., Monahan, I.M., Dolganov, G., Efron, B., Butcher, P.D., Nathan, C., et al. (2003). Transcriptional Adaptation of Mycobacterium tuberculosis within Macrophages Insights into the Phagosomal Environment. J. Exp. Med. *198*, 693–704.

Shi, L., Sohaskey, C.D., Pfeiffer, C., Datta, P., Parks, M., McFadden, J., North, R.J., and Gennaro, M.L. (2010). Carbon flux rerouting during Mycobacterium tuberculosis growth arrest. Mol. Microbiol. *78*, 1199–1215.

Silva, B.D.S., Tannus-Silva, D.G.S., Rabahi, M.F., Kipnis, A., and Junqueira-Kipnis, A.P. (2014). The use of Mycobacterium tuberculosis HspX and GlcB proteins to identify latent tuberculosis in rheumatoid arthritis patients. Mem. Inst. Oswaldo Cruz *109*, 29–37.

Smith, C.V., Huang, C., Miczak, A., Russell, D.G., Sacchettini, J.C., and Bentrup, K.H. zu (2003). Biochemical and Structural Studies of Malate Synthase fromMycobacterium tuberculosis. J. Biol. Chem. *278*, 1735–1743.

Upton, A.M., and McKinney, J.D. (2007). Role of the methylcitrate cycle in propionate metabolism and detoxification in Mycobacterium smegmatis. Microbiology *153*, 3973–3982.

Vereecke, D., Cornelis, K., Temmerman, W., Jaziri, M., Van Montagu, M., Holsters, M., and Goethals, K. (2002). Chromosomal Locus That Affects Pathogenicity of Rhodococcus fascians. J. Bacteriol. *184*, 1112–1120.

Watanabe, S., Zimmermann, M., Goodwin, M.B., Sauer, U., Barry, C.E., and Boshoff, H.I. (2011). Fumarate Reductase Activity Maintains an Energized Membrane in Anaerobic Mycobacterium tuberculosis. PLoS Pathog. *7*.

Wayne, L.G., and Lin, K.Y. (1982). Glyoxylate metabolism and adaptation of Mycobacterium tuberculosis to survival under anaerobic conditions. Infect. Immun. *37*, 1042–1049.

Xu, H., Hegde, S.S., and Blanchard, J.S. (2011). The Reversible Acetylation and Inactivation of Mycobacterium tuberculosis Acetyl-CoA Synthetase is Dependent on cAMP. Biochemistry (Mosc.) *50*, 5883–5892.

Yushok, W.D. (1971). Control Mechanisms of Adenine Nucleotide Metabolism of Ascites Tumor Cells. J. Biol. Chem. *246*, 1607–1617.

Zhang, Y.J., Ioerger, T.R., Huttenhower, C., Long, J.E., Sassetti, C.M., Sacchettini, J.C., and Rubin, E.J. (2012). Global Assessment of Genomic Regions Required for Growth in Mycobacterium tuberculosis. PLoS Pathog. *8*.

CHAPTER 4

CONCLUDING REMARKS

Carbon metabolic pathways are becoming well recognized for their roles in *Mtb* pathogenesis. Here, we evaluated the importance of two enzymes in separate pathways; fructose 1,6-bisphosphate aldolase (FBA) in glycolysis and gluconeogenesis, and malate synthase (MS) in the glyoxylate shunt. We found that both were essential for growth and persistence of *Mtb* in the mouse model, supporting their further pursuit as potential drug targets. This further exemplifies the importance of *Mtb* carbon metabolic pathways during host infection.

This work would not have been possible without the development of conditional knockdown mutants. The dual control system developed by Kim and O'Brien et al. allowed us to generate *Mtb* mutants in which both gene expression and protein stability of FBA and MS were regulated by the addition of anhydrotetracycline or doxycycline. These mutants were generated in conditions in which these enzymes were essential but then used to test the effect of FBA and MS depletion in the mouse model and within a variety of *in vitro* conditions. In doing so, we found a condition in which both FBA and MS were dispensable: standard *Mtb* media containing glucose and glycerol, but lacking oleic acid. We also found that the essentiality of both enzymes was carbon source-dependent.

Why is identification of condition-specific essentiality important? First of all, this demonstrates how gene essentiality studies based on detecting transposon insertions within *Mtb* libraries can be contradictory. Both of the genes of interest, *fba* and *glcB*, were predicted to be essential and non-essential, depending on the study (Griffin et al.,

2011; Sassetti et al., 2003; Zhang et al., 2012). Our data suggested that this variability could be due to the differences in the growth media used to perform these experiments. Also, this work highlights the importance of targeted genetic studies to validate gene essentiality predictions.

Secondly, when testing enzyme inhibitors against live bacteria, it is critical to test in a condition where the enzyme is required for growth or viability. We found that growth of both *fba* and *glcB* knockouts was similar to wild type in standard liquid *Mtb* media. This was unexpected due to the inability to generate knockouts for these enzymes on standard *Mtb* plate media. We confirmed that FBA is essential in single carbon source media and that MS is essential in the presence of acetate or fatty acids, suggesting that inhibitor testing should be done in these conditions. Standard media may be a good control to identify off-target inhibitor effects.

Lastly, this carbon source-dependent essentiality provides one hypothesis for the phenotype we observe *in vivo*, and contributes to our understanding of the host environment. We found that FBA is required for growth and survival in single carbon sources, and that an *fba* knockout requires a specific balance of carbon sources for growth. In contrast, MS is required for growth and survival in acetate, regardless of the presence of glucose. If carbon source contributes to death of these mutants *in vivo*, these data are consistent with the current paradigm of an *Mtb* diet high in lipids, including fatty acids, and low in other carbon sources such as carbohydrates.

Why are both mutants killed by carbon as opposed to just inhibited for growth? We used a metabolomics LC-MS-based approach to determine the metabolic changes of the knockouts upon exposure to carbon sources that were permissive and non-permissive for survival. We observed large metabolite accumulations in both knockouts consistent with their established functions. Metabolite toxicity of

glyoxylate (for MS-deficient *Mtb*) or phosphorylated metabolites surrounding the FBA reaction (for FBA-deficient *Mtb*) could contribute to the death that we observe. However, metabolic pathways also have other roles in maintenance of redox balance, membrane potential, and cell wall synthesis, altering the lipid profile. Further studies are needed to elucidate the specific mechanisms accounting for the death we observe.

Carbon source may not be the only cause of death of strains lacking MS or FBA *in vivo*, as FBA or MS could contribute to resistance of *Mtb* to other host stresses. For example, hypoxia has been shown to trigger a reductive TCA cycle with an output of succinate, whose production contributes to *Mtb* survival (Eoh and Rhee, 2013; Watanabe et al., 2011). Also, both FBA and MS are known to be secreted and could play roles in altering the host environment in a way that favors *Mtb* survival within the host (Kinhikar et al., 2006; de la Paz Santangelo et al., 2011). Future work could involve mutation of either the active site or potential host-interacting domains within these proteins to see what effect this has on pathogenicity within the host.

How feasible would it be to develop inhibitors to target FBA and MS? The crystal structures of both enzymes are available, allowing for structure-based drug design. Development of inhibitors for both enzymes is currently ongoing in other institutions. Progress is furthest on MS inhibitors, which have been shown to reduce bacillary load *in vivo* (Krieger et al., 2012). MS may be easier to target compared to isocitrate lyase (ICL) because of its accessible active site.

FBA inhibitors have been generally ineffective at inhibiting *Mtb* growth *in vitro* against live bacteria, and one of the issues could be a lack of potency. To determine the potency required for an FBA inhibitor, we assessed the vulnerability of *Mtb* to FBA depletion and found that FBA needed to be depleted over 97% in butyrate to have an effect on growth. This mimics the findings of a study with the fungus *Candida*

albicans, in which FBA expression needed to be silenced over 95% to block growth (Rodaki et al., 2006). Interestingly, we found that vulnerability was dependent on the growth condition, as in glucose FBA needed to be depleted by only 87% to have an effect on growth. This suggests that it may be difficult to predict the level of depletion required in various environments, including the host. Also, there are examples of effective antibiotics whose targets require high levels of depletion (Wei et al., 2011). These data suggest that while FBA may need to be inhibited substantially for an effect *in vivo*, FBA should not be ruled out as a drug target.

In conclusion, we have outlined a critical role for both MS and FBA for *Mtb* pathogenesis. Depletion of either enzyme after establishment of infection in mice resulted in drastic declines in bacterial load over time in lungs and spleens. Both enzymes were also required for *in vitro* survival in specific carbon source conditions that may mimic the carbon source condition *in vivo*. Moreover, *Mtb* lacking either enzyme exhibited metabolic buildups and depletions in death-inducing carbon source conditions. It is possible that these metabolic perturbations contributed to the death that we observed *in vitro*, and potentially in the mouse model. This work justifies continued research on the importance and function of carbon metabolism enzymes in *Mtb* and the development of novel inhibitors targeting FBA and MS.

REFERENCES

Eoh, H., and Rhee, K.Y. (2013). Multifunctional essentiality of succinate metabolism in adaptation to hypoxia in Mycobacterium tuberculosis. Proc. Natl. Acad. Sci. U. S. A. *110*, 6554–6559.

Griffin, J.E., Gawronski, J.D., DeJesus, M.A., Ioerger, T.R., Akerley, B.J., and Sassetti, C.M. (2011). High-Resolution Phenotypic Profiling Defines Genes Essential for Mycobacterial Growth and Cholesterol Catabolism. PLoS Pathog. *7*.

Kim, J.-H., O'Brien, K.M., Sharma, R., Boshoff, H.I.M., Rehren, G., Chakraborty, S., Wallach, J.B., Monteleone, M., Wilson, D.J., Aldrich, C.C., et al. (2013). A genetic strategy to identify targets for the development of drugs that prevent bacterial persistence. Proc. Natl. Acad. Sci. U. S. A. *110*, 19095–19100.

Kinhikar, A.G., Vargas, D., Li, H., Mahaffey, S.B., Hinds, L., Belisle, J.T., and Laal, S. (2006). Mycobacterium tuberculosis malate synthase is a laminin-binding adhesin. Mol. Microbiol. *60*, 999–1013.

Krieger, I.V., Freundlich, J.S., Gawandi, V.B., Roberts, J.P., Gawandi, V.B., Sun, Q., Owen, J.L., Fraile, M.T., Huss, S.I., Lavandera, J.-L., et al. (2012). Structure-Guided Discovery of Phenyl-diketo Acids as Potent Inhibitors of M. tuberculosis Malate Synthase. Chem. Biol. *19*, 1556–1567.

De la Paz Santangelo, M., Gest, P.M., Guerin, M.E., Coincon, M., Pham, H., Ryan, G., Puckett, S.E., Spencer, J.S., Gonzalez-Juarrero, M., Daher, R., et al. (2011). Glycolytic and Non-glycolytic Functions of Mycobacterium tuberculosis Fructose-1,6-bisphosphate Aldolase, an Essential Enzyme Produced by Replicating and Non-replicating Bacilli. J. Biol. Chem. *286*, 40219–40231.

Rodaki, A., Young, T., and Brown, A.J.P. (2006). Effects of Depleting the Essential Central Metabolic Enzyme Fructose-1,6-Bisphosphate Aldolase on the Growth and Viability of Candida albicans: Implications for Antifungal Drug Target Discovery. Eukaryot. Cell *5*, 1371–1377.

Sassetti, C.M., Boyd, D.H., and Rubin, E.J. (2003). Genes required for mycobacterial growth defined by high density mutagenesis. Mol. Microbiol. *48*, 77–84.

Watanabe, S., Zimmermann, M., Goodwin, M.B., Sauer, U., Barry, C.E., and Boshoff, H.I. (2011). Fumarate Reductase Activity Maintains an Energized Membrane in Anaerobic Mycobacterium tuberculosis. PLoS Pathog. *7*.

Wei, J.-R., Krishnamoorthy, V., Murphy, K., Kim, J.-H., Schnappinger, D., Alber, T., Sassetti, C.M., Rhee, K.Y., and Rubin, E.J. (2011). Depletion of antibiotic targets has widely varying effects on growth. Proc. Natl. Acad. Sci. U. S. A. *108*, 4176–4181.

Zhang, Y.J., Ioerger, T.R., Huttenhower, C., Long, J.E., Sassetti, C.M., Sacchettini, J.C., and Rubin, E.J. (2012). Global Assessment of Genomic Regions Required for Growth in Mycobacterium tuberculosis. PLoS Pathog. *8*.

PUBLICATIONS

Puckett, S., Trujillo, C., Eoh, H., Marrero, J., Spencer, J., Jackson, M., Schnappinger, D., Rhee, K., Ehrt, S. (2014). Inactivation of fructose-1,6-bisphosphate aldolase prevents optimal co-catabolism of glycolytic and gluconeogenic carbon substrates in *Mycobacterium tuberculosis*. PloS Pathog 10(5): e1004144.

de la Paz Santangelo, M., Gest, P.M., Guerin, M.E., Coincon, M., Pham, H., Ryan, G., **Puckett, S.E.**, Spencer, J.S., Gonzalez-Juarrero, M., Daher, R., Lenaerts A.J., Schnappinger, D., Therisod, M., Ehrt, S., Sygusch, J. and Jackson, M. (2011). Glycolytic and non-glycolytic functions of *Mycobacterium tuberculosis* fructose-1,6-bisphosphate aldolase, an essential enzyme produced by replicating and non-replicating bacilli. J Biol Chem *286*, 40219-40231.